UVINERSITY OF CALIFORNIA, MERCED

Differences in Neural Mechanisms for Auditory and Visual Rhythm Processing

A dissertation submitted in partial satisfaction of the requirements for the degree Doctor of Philosophy

in

Cognitive and Information Sciences

by

Daniel C. Comstock

Committee in charge:

Professor Ramesh Balasubramaniam, Ph.D. Chair
Professor Michael J. Spivey, Ph.D.
Professor David C. Noelle, Ph.D.

2021

The dissertation of Daniel Charles Comstock is approved, and it is acceptable in quality and form for publication on microfilm and electronically:

Professor David C. Nolle, Ph.D.

Professor Michael J. Spivey, Ph.D.

Professor Ramesh Balasubramaniam, Ph.D., Chair

University of California, Merced

2021

This dissertation is dedicated to my family:

To my parents, Charles and Bonnie, for always supporting me, no matter what crazy fool thing I was up to.

To my sister, Janna, for always believing in me, even when she shouldn't have.

To my partner, Camila, for keeping me sane during the pandemic year we spent trapped in our apartment. We were always isolated, but I never felt alone.

Contents

List of Tables, and Figures

Tables

Figures

Acknowledgements

Work contained in this dissertation was funded in part by NSF Grant No: 1626505

I would like to thank my committee members Ramesh Balasubramaniam, Michael Spivey, and David Noelle – for their support and mentorship during my studies at UC Merced. I want to specifically thank my advisor, Ramesh Balasubramaniam for his constant encouragement, support and enthusiasm, for the always useful feedback and ideas to improve my work, and for pushing me to be the researcher I have become.

I would like to express my gratitude to my lab mates: Alex Pabst, Butovens Mede, Brandon Batzloff, Chelsea Gordon, Shannon Proksch, Jas Kaur, Jessica Ross, Sam Carey, and Tim Shea for their insights, their companionship, and for making my time at UC Merced always enjoyable. Even though I was thousands of miles from home, I always felt like I had a family in my lab mates.

I would like to also give thanks to my undergraduate mentors at the University of Wisconsin – Stout, Desiree Budd, Michael Donnelly, and Sarah Wood, for encouraging my interests and pursuits in research and academia, the many hours spent teaching me, and for being my friends.

Additional thanks go out to my amazing co-authors and collaborators during my time at Merced: Micheal Hove, Ramesh Balasubramaniam, Jessica Ross, Alex Pabst, Butovens Mede, Shannon Proksch, John Iversen, Tony Shahin, Alejandra Santoyo, Chris Kello, Adolfo Ramirez, Ali Rahimpour, Luca Pollonini, and Heather Bortfeld.

Curriculum Vita

Daniel C Comstock

Cognitive and Information Sciences Program,
University of California, Merced,
DComstock@UCMerced.edu
http://sites.google.com/view/danielccomstock

EDUCATION

Ph.D. Cognitive and Information Sciences, anticipated Summer 2021, University of California – Merced,

B.S. Cognitive Science, 2014 University of Wisconsin – Stout

PUBLICATIONS

Pabst, A., Proksch, S., Mede, B., Ross, J. R., **Comstock, D. C.,** Balasubramaniam, R. (In review). A systematic review of the efficacy of intermittent theta burst stimulation on cognitive enhancement.

Comstock, D. C., & Balasubramaniam, R. (In preparation). Comparative motor system entrainment to auditory and visual rhythms

Ross, J. M., **Comstock, D. C.**, Iversen, J. R., Makeig, S., Balasubramaniam, R. (In preparation). The EEG Mu Rhythm and Musical Beat Perception

Rahimpour, A., **Comstock, D. C.**, Pollonini, L., Padryumna, L., Balasubramaniam, R., & Bortfeld, H. (In preperation). Neural Basis of Synchronized and Syncopated Rhythmic Finger Tapping Assessed by Electroencephalography

Comstock, D. C., Ross, J. M., & Balasubramaniam, R. (2021) Modality-specific frequency band activity during neural entrainment to auditory and visual rhythms. *European Journal of Neuroscience, (in press)*

Comstock, D. C., & Balasubramaniam, R. (2018). Neural responses to perturbations in visual and auditory metronomes during sensorimotor synchronization. *Neuropsychologia*, *117*, 55-66. doi: 10.1016/j.neuropsychologia.2018.05.013

Comstock, D. C., Hove, M. J., & Balasubramaniam, R. (2018). Sensorimotor synchronization with auditory and visual modalities: Behavioral and neural differences. *Frontiers in computational neuroscience*, *12*. doi: 10.3389/fncom.2018.00053

Rahimpour, A., Pollonini, L., **Comstock, D**., Balasubramaniam, R., & Bortfeld, H. (2020). Tracking Differential Activation of Primary and Supplementary Motor Cortex Across Timing Tasks: An fNIRS Validation Study. *Journal of Neuroscience Methods*, 108790. doi: 10.1016/j.jneumeth.2020.108790

Proksch, S., **Comstock, D. C.,** Médé, B., Pabst, A., Balasubramaniam, R. (2020) Motor and predictive processes in auditory beat and rhythm perception. *Frontiers in Human Neuroscience, 14, 375*. doi: 10.3389/fnhum.2020.578546

INVITED TALKS

2019 - Neural time-frequency characteristics of auditory and visual rhythm entrainment. Biennial Conference of the Society for Music Perception and Cognition 2019

2017 - The Primacy of Error Correction of the Auditory System: Neural Correlates of Auditory and Visual Error Correction During Sensorimotor Synchronization. Biennial Conference of the Society for Music Perception and Cognition 2017

2016 - Tapping in Synch to a Perturbed Metronome: An EEG Study on the Differences in Detection and Correction of Sensorimotor Synchronization Errors Between the Visual and Auditory Senses. University of Wisconsin – Stout

POSTER PRESENTATIONS

2020 - **Comstock, D. C.**, Santoyo, A., Balasubramaniam, R. Hemispheric Specialization in Auditory Rhythm Processing. 27th Annual Cognitive Neuroscience Society Meeting, Boston, MA

2019 - **Comstock, D. C.**, Balasubramaniam, R. Time-Frequency Characteristics of Neural Responses to Perturbations During Sensorimotor Synchronization to Auditory and Visual Rhythms. 26th Annual Cognitive Neuroscience Society Meeting, San Francisco, CA

2019 - Ramirez-Aristizabal A. G., **Comstock, D. C.,** Kello, C. Complexity Matching to EEG Response of Speech and Music. 26th Annual Cognitive Neuroscience Society Meeting, San Francisco, CA

2018 - **Comstock, D. C,** Balasubramaniam, R. Synchronizing Movements to a Visual Rhythm Shifts the Neural Frequencies of Entrainment to Lower Frequency Bands Compared to Passive Perception of Visual Rhythms. 48th Annual Society for Neuroscience Meeting, San Diego, CA

2018 - Budd, D., Donnelly, P.W., Line, E., **Comstock, D. C.,** Sabinash, A., Grassman, S., Cops, M., Wrobel, N., Complex ERP Components Characterize Athletes Based on Concussion History and the Type of Sport Played. 58th Annual Society for Psychophisiolgocial Research meeting, Quebec, Canada

2017 - **Comstock, D. C.**, Balasubramaniam, R. Beta-Band Response Synchronizes and Predicts Rhythmic Flashing Visual Stimuli. 47th Annual Society for Neuroscience Meeting, Washington D. C.

2017 - **Comstock, D. C.**, Balasubramaniam, R. Differences in Neural Correlates of Error Correction in Auditory and Visual Sensorimotor Synchronization. 24th Annual Cognitive Neuroscience Society Meeting, San Francisco, CA

2016 - Ross, J., Iversen, J., Makeig, S., & Balasubramaniam, R. **Comstock, D. C**. An EEG examination of neural entrainment and action simulation during rhythm perception. 14th International Conference for Music Perception and Cognition, San Francisco, CA

2014 - **Comstock, D.**, Davis, B., Olson, K., Sulma, A., Krause, P., Domagala, L., Donnelly, M., Budd, D. Lies, Damned Lies, and the N200. 86th Annual Meeting of the Midwestern Psychological Association, Chicago, IL.

PROFESSIONAL TRAINING

2020 – Google X Online Machine Learning Bootcamp.

2020 – Neuromatch Academy: Online School for Computational Neuroscience: Interactive Track

2019 – Synchrony and Rhythmic Interaction: From Neurons to Ecology Workshop, Leiden University, The Netherlands

2017 – 5th Science Factory: TMS-EEG Workshop and Summer School, Aalto University, Helsinki, Finland

2016 - UC Music Experience Research Community Initiative (MERCI) Student Exchange, Swartz Center for Computational Neuroscience (SCCN), University of California, San Diego (Hosts: Scott Makeig and John Iversen)

2016 - Generalized Linear Model Workshop, University of California, Merced (Instructor: Bodo Winter)

2016 - Python Workshop: Using Python for Data Analysis, University of California, Merced (Instructor: Bryan Kerster)

2016 - UC Retreat Workshop on Research in Music Experience and Communication, Marconi, CA

2016 - Non-Invasive Brain Stimulation (NIBS) Methods and Practice, Division of Biokinesiology and Physical Therapy, University of Southern California, Los Angeles

2016 - Teaching Matters – Mastering the Classroom with First-Generation College Students, University of California, Merced

2016 - Teaching Matters – Developing Teaching Strategies, University of California, Merced

2015 - UC MERCI Symposium/Workshop on Research on Music Experience and Communication, University of California, Los Angeles

PEER REVIEWER

Frontiers in Human Neuroscience – ad hoc article reviewer (2021)

Brain and Behavior – ad hoc article reviewer (2021)

Timing and Time Perception – ad hoc article reviewer (2020)

Psychological Research – ad hoc article reviewer (2020)

Society for Music Perception and Cognition – conference abstract reviewer (2017, 2019)

Experimental Brain Research – ad hoc article reviewer (2018)

TEACHING EXPERIENCE

Teaching Assistant - COGS 140 - Perception and Action, UC Merced (Fall 2020)

Guest Lecturer – COGS 105 – Research Methods – Lecture on Neuroscience Methods, UC Merced (Summer 2020),

Teaching Assistant - COGS 130 - Cognitive Neuroscience, UC Merced (Spring 2020)

Teaching Assistant - COGS 101 - Mind Brain and Computation, UC Merced (Fall 2019)

Teaching Assistant - COGS 130 - Cognitive Neuroscience, UC Merced (Spring 2019)

Teaching Assistant - COGS 101 - Mind Brain and Computation, UC Merced (Fall 2018)

Teaching Assistant - COGS 130 - Cognitive Neuroscience, UC Merced (Spring 2018)

Teaching Assistant - COGS 101 - Mind Brain and Computation, UC Merced (Fall 2017)

Teaching Assistant - COGS 001 - Introduction to Cognitive Science, UC Merced (Spring 2017)

Teaching Assistant - COGS 140 - Perception and Action, UC Merced (Fall 2016)

STUDENT MENTORING

2019 – SOAR Student research mentor, UC Merced

2018 – UROC Student research mentor, UC Merced

2017 – UROC Student research mentor, UC Merced

FELLOWSHIP

2015 - Graduate Dean's Recruitment Fellowship, 2015 – 2016, University of California – Merced

GRANTS

2016 - UC MERCI Travel Grant (UC San Diego)
$1800 grant to travel to, and stay in San Diego for the second round of research collaboration related to music collaboration with Dr. John Iverson and Dr. Scott Makeig

2015 - UC MERCI Travel Grant (UC San Diego)
$1600 grant to travel to, and stay in San Diego for research collaboration related to music collaboration with Dr. John Iverson and Dr. Scott Makeig

Abstract

Only humans and a few other species of animals share the ability to reliably entrain and synchronize to rhythms. Accurately synchronizing to rhythms, as in tapping a foot to a metronome, requires the ability to precisely predict the onset of each rhythmic event. Curiously, humans have much greater difficulty synchronizing to flashing visual rhythms compared to auditory rhythms, even when both stimuli contain exactly the same timing information. While it is known that the auditory system works in conjunction with the motor system for the timing processing needed for rhythm perception, it has not been clear how the visual system processes rhythm timing. In collaboration with my co-authors, I present evidence to explain this discrepancy by showing the visual system has its own internal timing capabilities, which are separate than those utilized in auditory rhythms. I show that the visual system is able to detect perturbations of visual rhythms, but that error detection is not able to be translated into effective error correction in a synchronization task as is the case with auditory rhythms (Chapter 2). From an experiment in passive rhythm perception, I show evidence of visual timing activity arising from the visual system, as well as evidence of separate timing networks for auditory and visual rhythm processing (Chapter 3). I also show evidence that visual system timing information, in the form of neural entrainment, is present in the motor system at similar levels as auditory neural entrainment. Although visual timing information is present in the motor system, it is not able to be utilized in the same capacity as auditory rhythm timing in the motor system (Chapter 4). Taken together, these results suggest the visual system is processing rhythm timing through a visual modality specific mechanism. This mechanism is not as capable for rhythm processing as the motor system utilized in auditory rhythm processing, which results in poorer visual rhythm timing capabilities for visual rhythms compared to auditory rhythms.

This dissertation, *Differences in Neural Mechanisms for Auditory and Visual Rhythm Processing*, is submitted by Daniel C. Comstock in the summer of 2021 in partial fulfillment of the degree Doctor of Philosophy in Cognitive and Information Sciences at the University of California, Merced, under the guidance of Ramesh Balasubramaniam.

Prologue

Something common to nearly all humans is the ability to enjoy music, not just as a collection of sounds that are pleasant together, as is the case with wind-chimes, but as sounds that are connected through a consistent rhythm or meter. Further, humans can easily synchronize our movements to these sounds through dance. In fact, dancing to music can be observed in the very young and across cultures world-wide (Nettl, 2015; Savage et al., 2015). But what is so natural to humans does not appear to happen at all in most other animal species. The ability to entrain one's movements to music rhythms seems to be limited to humans, and a small group of birds and mammals (Kotz et al., 2018; Ravignani et al., 2019). All this begs the question, what is it that is special about humans and those other species that are able to synchronize their movements to rhythms?

The key to synchronizing to a rhythm is not to just move in time with that rhythm, but to predict the timing of rhythmic events. In other words, there needs to be a mechanism that can keep time internally that is flexible enough to quickly match the timing of an external rhythm. The need for this prediction is clear if you think of tapping your finger in time with a metronome: in order to tap on the beat, your finger has to begin its motion prior to the onset of that beat. But it is not just the movement that needs to start before beat occurs, as the transmission of the neural signal from your brain to your finger is not instantaneous, and can take over 100 ms (Merchant & Lafuente, 2014) Indeed, it is well established that when asked to tap in synchrony to a beat in what is called a sensorimotor synchronization task (SMS), most people will tap up to 50 ms before the beat! (Repp & Su, 2013).

Given humans ability to synchronize to auditory rhythms so closely, it can be somewhat surprising to find that the ability to synchronize to a rhythm is not consistent across the senses. This is most clear when comparing SMS capabilities between auditory and visual rhythms. Humans synchronize with greater precision to auditory rhythms, and are also capable of synchronizing to faster auditory rhythms than to visual rhythms (Repp, 2003). This difference doesn't just exist during SMS tasks either, it is also seen in perceptual tasks where people are asked to tell the difference in speed between two rhythms, where auditory rhythms are judged much more accurately than visual rhythms (Silva & Castro, 2016).

Interestingly, there is one major caveat to the differences seen between auditory and visual rhythm SMS capabilities. The studies that I have so far mentioned have all used simple rhythmic flashes of light as visual rhythms. If you ask a person to synchronize their movements with an object moving in a rhythmic pattern however, that person will be able to synchronize their movements with a level of precision that is comparable to their ability to synchronize to a similar auditory rhythm (Hove et al., 2013a). Interestingly, this effect only applies to synchronization tasks as the benefit of a moving rhythmic stimulus is lost in a purely perceptual task (Silva & Castro, 2016). Additionally, if the trajectory of the moving object being synchronized with is not compatible with trajectory of the persons finger (e.g., a bar moving horizontally back and forth while a person's finger moves vertically up and down), the precision of the SMS will be less than compared to a compatible trajectory (Hove & Keller, 2010; Hove et al., 2010). Likewise, if you ask someone to synchronize to a rhythmically frequency

modulated siren, that person will have more difficulty synchronizing accurately than if they were asked to synchronize with a rhythmically equivalent auditory metronome (Hove et al., 2013b).

Even though it is clear that there are large differences across the senses in rhythm capabilities, it is not yet understood exactly why those differences exists. What is clear is that humans and at least a few other species appear to have specialized neural systems that allow for auditory rhythm perception and synchronization. A recent paper explored this issue by discussing two hypotheses that aim to explain this capability (Proksch et al., 2020). The first hypothesis is the Action Simulation for Auditory Prediction hypothesis (ASAP), which hypothesizes that auditory beat perception is achieved by simulating the beat in the motor system, and it posits that that auditory system and motor system are tightly linked through the dorsal auditory stream due to the vocal learning abilities present in humans (Patel & Iversen, 2014). The second hypothesis is the Gradual Audio Evolution hypothesis (GAE), which suggests that human auditory rhythmic timing capability evolved out of the interval timing capability that is common in primates through a cortico-motor-basil ganglia-cortical circuit (Merchant & Honing, 2014). While these two hypotheses differ on their explanations of how human auditory rhythm perception capabilities arose, they share the idea that the motor system is heavily involved in auditory rhythm processing, which has been reported in a number of other studies (Grahn & Brett, 2007; Chen et al., 2008a,b; Gordon et al., 2018).

The auditory-motor connection put forth in the ASAP and GAE hypotheses can help explain how the enjoyment of music and dance is a near universal human trait, as they posit a specific neural mechanism that evolved for those specific tasks. Since that motor connection is specific to the auditory system and not the visual system, these hypotheses could further explain why there is such a significant difference in rhythm processing capabilities between the sense modalities. But the issue of the role of the motor system in auditory and visual timing also applies beyond just rhythm perception. It also applies to non-rhythmic timing, such as in time perception.

When most people think of time perception, they think of what is commonly known as interval timing, which is the ability to accurately perceive how much time has passed over a given duration. This can take place over range of time scales, from under a second to as long as years or even decades! But it turns out that timing is also an important aspect of many functions carried out in physiology across a wide range of time scales. For example, determining the direction of a sound one hears depends on the brain being able to determine the microsecond differences between that sound reaching one ear faster or slower than the other ear, and on longer other end of the spectrum we have rhythms that unfold over the case of a day, as in our circadian rhythms, or over the course of a month as with menstrual cycles (Merchant & Lafuente, 2014). But timing at those extremes seem to depend on specific mechanisms specialized to their specific task, while timing activity that occurs in the millisecond to second range, the range of timing important for movement and perception, may depend on a more generalized timing system, such as described by the GAE hypothesis (Merchant & Honing, 2014). Research into interval timing with monkeys strongly implicates the premotor cortex and SMA in interval timing for visual tasks (Merchant et al., 2013; Wang et al., 2018). While this finding does not guarantee that humans use the same mechanism for interval timing as

the monkeys in that study use, it does suggest that the motor system can be used in visual timing. When taken together with the evidence of the motor system involvement in auditory timing, it suggests that the motor system operates as a modality independent means of timing processing. Fitting with this idea, it has been proposed that the motor system works as prediction system across sensory modalities (Schubotz, 2007). If the motor system is able to operate as a modality independent timing center, and it is known to be involved in auditory rhythm perception, then the fact that visual rhythmic timing is not as precise as auditory rhythmic timing suggests that the auditory system is working in concert with the motor system for rhythm timing in a fashion that the visual system is not capable of.

There still are a number of remaining questions, however. If auditory rhythm perception is facilitated by the audio-motor connection, through what mechanism is visual rhythm perception processed? Is it the case that the visual system itself is performing rhythm timing, or does the visual system also utilize the motor system, but in a less effective manner? Further, why is it that the type of stimuli used in a visual rhythm perception task (flashes vs moving stimuli) have such a large effect on visual SMS precision? Since auditory SMS capability can increase with training, as is the case with trained musicians, could training improve visual SMS capability to the level of auditory SMS? This dissertation does not aim to definitively answer these questions however, its aim is to provide enough context to make answering these questions easier, especially the question of which mechanisms are involved in rhythm perception. The central question this dissertation does attempt to answer is if the mechanisms of rhythm timing and perception are modality general or modality specific. In other words, are there separate mechanisms for rhythm timing for the different senses, or is there a single mechanism that the different senses have unequal access to.

Through the work presented in this dissertation, I argue that the visual system is not utilizing the motor system for rhythmic timing the way the auditory system does, and instead is processing timing internally. This is due to the visual system and the circuits connecting it to the motor system being tuned to spatial processing for control of movements with continuous updating of spatial information. This is opposed to being tuned to discrete temporal events that need to be predicted without continuous updating, such as occurs in auditory rhythm timing. In chapter 1 my co-authors and I present a review of the differences in capabilities between auditory and visual rhythm SMS as well as the modality differences in the corresponding neural activation for such tasks (Comstock et al., 2018). In addition to the review, the chapter also includes a discussion of the how the different perceptual systems may interface with the motor system. The second chapter provides evidence of rhythm timing in the visual system that is not as tied into to the motor system as the auditory system through an experiment comparing the neural correlates of auditory and visual error correction during a SMS task (Comstock & Balasubramaniam, 2018). Chapter 3 shows further evidence of processing of visual timing by the visual system, as well as evidence of separate, but overlapping networks of timing activity for auditory and visual rhythm perception using an omission protocol during a purely perceptual task (Comstock et al., 2021). In chapter 4 we present evidence that neural entrainment within the motor cortex of visual rhythms is as strong, if not stronger, than auditory rhythms, which suggests that the differences seen between

auditory and visual SMS and rhythm perception are not due to the how the rhythms are captured as neural entrainment, but rather how the entrainment is utilized. In the final section, I discuss the findings from chapters 2-4 in relation to the existing literature on rhythm processing, and propose future directions for auditory and visual rhythm perception investigations.

Chapter 1

1 Sensorimotor Synchronization with Auditory and Visual Modalities: Behavioral and Neural Differences

This chapter is a published review in which the behavioral and neural differences of SMS across modalities are described. In addition to modality differences, the mechanisms involved in rhythm perception, and their possible evolutionary origins are discussed. The chapter ends with speculation on why we see the modality differences described earlier, along with some suggestions for future research on the topic.

Published as:
Comstock, D. C., Hove, M. J., & Balasubramaniam, R. (2018). Sensorimotor synchronization with auditory and visual modalities: behavioral and neural differences. *Frontiers in computational neuroscience*, *12*, 53.

Abstract

It has long been known that the auditory system is better suited to guide temporally precise behaviors like sensorimotor synchronization (SMS) than the visual system. Although this phenomenon has been studied for many years, the underlying neural and computational mechanisms remain unclear. Growing consensus suggests the existence of multiple, interacting, context-dependent systems, and that reduced precision in visuo-motor timing might be due to the way experimental tasks have been conceived. Indeed, the appropriateness of the stimulus for a given task greatly influences timing performance. In this review, we examine timing differences for sensorimotor synchronization and error correction with auditory and visual sequences, to inspect the underlying neural mechanisms that contribute to modality differences in timing. The disparity between auditory and visual timing likely relates to differences in the processing specialization between auditory and visual modalities (temporal vs. spatial). We propose this difference could offer potential explanation for the differing temporal abilities between modalities. We also offer suggestions as to how these sensory systems interface with motor and timing systems.

1.1 Introduction

Many behavioral studies have examined human timing ability in tasks of sensorimotor synchronization (SMS) where subjects synchronize their movements to an external rhythm. Comparisons between auditory metronomes and visual flashing metronomes reveal that movement synchronization is less variable and can occur at faster rates with auditory metronomes (Chen et al., 2002; Repp, 2003; Repp and Penel, 2004; Lorås et al., 2012). However, visuo-motor synchronization greatly improves when synchronizing with a moving periodic visual metronome (Hove et al., 2010). Adding a changing velocity profile to the moving visual metronome further reduces variability in SMS tapping (Hove et al., 2013a; Iversen et al., 2015), and Gan et al. (2015) suggests that

a more realistic velocity profile can bring visual SMS to be as temporally precise as auditory SMS, at moderate but not fast tempi. While most studies of SMS look at finger tapping, others have included synchronized circle drawing, gait, dancing, and eye movements in the context of modality-specific timing effects (e.g., Repp and Su, 2013).

Studies on auditory and visual interference also suggest auditory timing is more prominent. When concurrent auditory metronomes and visual flashing metronomes are presented out-of-phase, the auditory sequences interfere with visuomotor timing, but not vice versa (Chen et al., 2002; Repp and Penel, 2002, 2004). The interference effect is considerably reduced with moving visual metronomes and is tied to training and experience as the auditory dominance is stronger in musicians and weaker in video gamers (Hove et al., 2013a). Similarly, auditory cues can improve visual temporal discrimination (Morein-Zamir et al., 2003; Parise and Spence, 2008). This effect only holds for the temporal domain however, as the visual system dominates when auditory and visual stimuli conflict in the spatial domain; spatial dominance in the visual modality is apparent in the well-known "ventriloquist effect" (Vroomen et al., 2001).

1.2 Role of Error Correction in Timing

Error correction is a crucial component of any SMS task. By inducing perturbations and errors in SMS, we can gain insight into the underlying timing mechanisms. A common method to induce errors in a SMS task is to occasionally perturb an otherwise isochronous metronome (Repp, 2000, 2001a,b; Praamstra et al., 2003; Repp and Keller, 2004; Jang et al., 2016; Jantzen et al., 2018). Error correction in SMS can be broken down into two distinct mechanisms: a phase-correction mechanism for correcting errors in relative phase, and a period-correction mechanism that corrects changes to the internal timekeeper period (Repp, 2001b; Repp and Keller, 2004). Period corrections require conscious awareness of the error as it involves a conscious updating of the internal rhythm; while a phase correction can happen even with errors too small for conscious awareness and does not involve updating the central timekeeper period and so is considered a more peripheral process than period correction (Repp, 2001b, 2005). An error corrected under the phase-correction mechanism is typically a gradual adjustment that occurs over several beats, while an error corrected under the period-correction mechanism will be evidenced by a pronounced correction, usually followed by a more gradual phase-correction-like pattern after the initial large correction (Repp, 2001b).

While error correction has been well documented in auditory SMS, relatively little work has investigated error correction in visual SMS. In a recent study comparing error correction for auditory and flashing visual sequences, we observed error corrections for perturbations in the auditory condition that were modulated by the direction of the perturbations, but no such modulation was found for perturbations in the visual condition (Comstock and Balasubramaniam, 2017a). This suggests the visual system may not engage in the same SMS timing mechanisms as the auditory system. Additional evidence for a discrepancy in error correction for auditory and visual sequences can be gleaned from the autocorrelation structure of adjacent taps: unlike auditory SMS, tapping with visual flashes does not produce a negative lag1 autocorrelation that can indicate of the presence of a robust central timekeeping and error-correction mechanism (Hove and Keller, 2010). However, visuomotor synchronization with moving and apparent-motion

metronomes do produce a negative lag1 autocorrelation, suggesting that a moving visual metronome may engage error correction (Hove and Keller, 2010; Hove et al., 2010); note that negative lag1 autocorrelation does not necessarily stem from error correction and can arise from other timing factors (e.g., Wing and Kristofferson, 1973). It remains unclear if error correction will occur with perturbations in moving visual metronomes or with larger phase perturbations in a flashing visual metronome.

1.3 Underlying Physiology of the Auditory and Visual Timing System

1.3.1 Brain Networks Involved in Timing Activity

Investigating the neural underpinnings in auditory and visual timing is a massive undertaking due to the many different timing subprocesses and tasks, including: SMS, interval timing, rhythm perception, timing recall, time perception, etc. Excellent reviews of the brain mechanisms involved in various timing activities include: a review of neural activity in music production (Zatorre et al., 2007); a review of neural activity involved in time perception (Wiener et al., 2010); and an overview of neural activation in SMS as part of a larger review of SMS (Repp and Su, 2013). This body of work consistently demonstrates that temporal processing across tasks and sensory modalities relies heavily on the motor system. This motor network includes the supplemental motor area (SMA), primary motor cortex, lateral premotor cortex, anterior cingulate, basal ganglia, and cerebellum (Repp and Su, 2013). Auditory rhythm perception activates the motor system and is closely linked to movement (Janata et al., 2012; Iversen and Balasubramaniam, 2016; Ross et al., 2016a,b). The SMA is also strongly implicated in motor timing (Coull et al., 2016; Merchant and Yarrow, 2016), and along with the pre-SMA could be a hub of motor timing (Schwartze et al., 2012). Subcortical regions are especially active during sub-second time perception (Wiener et al., 2010), sub-second interval timing (Repp and Su, 2013), and rhythm timing (Grahn and Rowe, 2009; Wiener et al., 2010; Coull et al., 2011; Teki et al., 2011; Hove et al., 2013b). There is evidence of a dorsal auditory stream connecting the auditory cortex to the motor cortex through the posterior parietal cortex that plays a role in rhythm perception (Patel and Iversen, 2014; Ross et al., 2018). Interestingly this dorsal stream is also implicated in visual and tactile rhythm perception (Araneda et al., 2017; Rauschecker, 2017), adding to the idea of a common timing system tied to the motor system. Further evidence of the common timing system is found in a study of auditory and visual synchronization that dissociated modality and tapping stability –putamen activation was highest when synchronizing to auditory beeps, moderate with a frequency-modulated siren and with a moving visual metronome, and lowest with a flashing visual metronome, closely paralleling behavioral performance (Hove et al., 2013b).

While visual SMS activates many of the same motor regions as auditory SMS (Hove et al., 2013b; Araneda et al., 2017), some activations are specific to the visual system. The visual cortex shows activity related to interval timing that follows the expected scalar property, such that size of timing errors measured in the visual cortex scale in proportion to size of the interval being timed as predicted by Weber's law (Shuler, 2016). Additionally, Zhou et al. (2014) found evidence that visual feature processing in the early visual cortex can contribute to duration perception, furthering the notion that at least some timing information is processed independently within the visual

cortex. Additionally, in visual rhythm perception, the visual cortex plays a role predicting rhythmic onsets (Comstock and Balasubramaniam, 2017b, 2018). The additional activations with visual timing tasks, taken together with behavioral results, suggest the timing accuracy in visual processing may be compared to the auditory system due to the additional computational demands of processing the higher complexity of visual spatial information along with temporal information.

1.3.2 Role of Cortical Oscillations in Timing Encoding and Spreading Information Across the Brain

In addition to looking at the networks and regions involved in temporal processing, a growing body of work shows the role of cortical oscillations in encoding timing across multiple frequency bands. Cortical oscillations play a role in connecting regions across the brain, with higher frequencies utilized for localized interaction and lower frequencies for longer range interaction (Sarnthein et al., 1998; Von Stein and Sarnthein, 2000). This pattern of oscillations is used to connect and calibrate disparate timing systems in the brain (Gupta and Chen, 2016). Oscillations relating to timing appear to arise from multiple context-specifc timing systems in the brain (Wiener and Kanai, 2016). The question is then how these functionally and anatomically disparate systems integrate and interact. It appears that oscillations from different timing systems are coordinated within the striatum (Matell and Meck, 2004; Gu et al., 2015).

Beta band activity (~20 Hz) is tied to the motor system and several studies indicate beta's role in predicting timing of auditory rhythms (Fujioka et al., 2009, 2012, 2015). Additionally, beta activity reflects top-down imposition of metrical structure on auditory rhythms (Iversen et al., 2009). Recently, beta activity has also been linked to timing predictions within the visual system in response to visual rhythms (Comstock and Balasubramaniam, 2017b).

With rhythm perception, evidence shows that internal oscillations arise to match the fundamental frequency of the rhythm, and frequency of the meter (Nozaradan et al., 2011), as well as to the frequency of imagined rhythms (Okawa et al., 2017). These findings align with the Neural Resonance Theory that posits neural rhythms synchronize to auditory rhythms, and these neural rhythms can influence attention, expectancy, and motor planning (Large and Snyder, 2009). As of yet, it is unclear if this same neural resonance to meter would arise with visual stimuli.

1.3.3 Neural Underpinnings of Error Correction

The neural correlates of error correction reveal more evidence for multiple interacting and overlapping timing mechanisms. Error detection of timing perturbations in auditory SMS tasks modulates the P1, N1, and N2 auditory ERP components depending on both the size and direction of the perturbation (Praamstra et al., 2003; Jang et al., 2016). Jantzen et al. (2018) also found a theta response stemming from the Pre-SMA and anterior cingulate for error detection, an increase in theta coupling between the SMA and the motor cortex for late perturbations. In visual error detection, the visual P1 component is reduced in latency only for large late perturbations (Comstock and Balasubramaniam, 2017a). Each of these instances show cortical activation specific to a type of perturbation, although these effects are generally limited to larger perturbations.

Smaller perturbations that elicit a phase-correction response are believed to be driven primarily by subcortical mechanisms. Applying repetitive TMS to downregulate motor and premotor cortices produced no effect on phase correction (Doumas et al., 2005), whereas phase-correction was impaired by repetitive TMS to the cerebellum (Bijsterbosch et al., 2011). This fits with the suggestion that phase-correction is primarily subcortical based on evidence from how rapidly the movement trajectory changes after a perturbation (Hove et al., 2014). A possible network that exhibits the rapid timing required for the phase-correction response is a cortico-striatal circuit connecting the cerebellum to the SMA-striatal network via the thalamus (Kotz et al., 2016).

The data on the neural underpinnings of error correction suggest multiple timing systems, each with specific roles, yet able to coordinate for rapid response. Commensurate with this idea is work suggesting the basal ganglia integrates various timing systems through oscillation comparators (Matell and Meck, 2004; Gu et al., 2015). The limited data on visual error correction, however, leave open how well this network can interface with the visual timing systems.

1.4 Evidence the Auditory System has Privileged Access to Timing Systems

Considering the auditory system's timing advantage along with the prominence of the motor system in timing processing, we suggest that the auditory system's advantage in timing stems from its stronger coupling to the motor system. Auditory timing compared to visual timing tasks often yield more activation in motor structures, such as the SMA and premotor cortex (Jäncke et al., 2000). Even when visual SMS tasks employed the modality-appropriate moving visual metronomes, audio-motor synchronization with auditory beeps yielded greater activation in the putamen (Hove et al., 2013b). Likewise, priming a visual rhythm with a similar auditory rhythm resulted in increased putamen activation compared to a visual rhythm alone, while a visual rhythm yielded no priming effect on an auditory rhythm (Grahn et al., 2011). The finding that the increased visual synchronization ability provided by a bouncing ball does not transfer to purely perceptual rhythm perception provides further evidence of the role of motor coupling in timing tasks (Silva and Castro, 2016). Additionally, the privileged link between auditory and motor systems can be seen in Parkinson's disease, a disorder that impairs movement due to cell loss within the basal ganglia (Davie, 2008). For example, Parkinsonian gait can improve when cued by an external rhythm, and these interventions are more effective when synchronizing with auditory metronomes than with flashing visual metronomes (Rochester et al., 2005; Arias and Cudeiro, 2008).

Visual timing activities recruit timing centers within the visual system that, based on behavioral results, are less precise compared to the auditory timing system. In Jäncke et al. (2000), visual timing tasks resulted in increased activity in the right superior cerebellum, vermis, and right inferior parietal lobe compared to auditory timing tasks. Visual timing tasks also recruit areas MT, V5, and the superior parietal lobe, tying into the dorsal visual stream (Jantzen et al., 2005), and visual rhythm perception induces increased beta activity at event onsets arising from the visual cortex (Comstock and Balasubramaniam, 2017b). It is unclear if these timing activations in the visual system are the result of compensating for a weaker connection to the motor timing system. It

may be that the temporal processing in the visual system is additional processing of visual information required to interface with the motor system.

While differences in coupling strength to the motor system are crucial for modality timing differences, other factors are likely. To that end, it is clear that the visual system is able to pick out high speed temporal information, for example, V1 will phase lock its input/output to up to a 100 Hz visual flashing stimuli (Williams et al., 2004). This suggest that entrainment is not easily transferred to the systems involved in time/rhythm perception, especially at the time frame usually involved in rhythm perception, indicating that the issue may be one of translation. A likely place for that translation would be within the dorsal pathway, which has been found to have neurons with high temporal resolution in macaques, with higher temporal resolution in the auditory dorsal stream (Rauschecker, 2017). If there is a higher temporal resolution of the auditory dorsal stream than in the visual dorsal stream, then it may give explanation as to why the visual system cannot synchronize at the higher frequencies achieved by the auditory system. Of course, it cannot be ruled out that the difference in temporal resolution is due to different levels of timing precision available to the dorsal stream. Reduced timing precision in the visual stream may be caused by increased necessary processing due to richer sensory input of the visual system compared to the auditory system. Indeed, greater processing requirements and longer processing time may help to account for the inability of the visual system to allow for synchronization at the higher tempos allowed by the auditory system.

1.5 Role of the Vestibular-Tactile-Somatosensory System

Another link between auditory and motor systems is that auditory rhythm perception may be tied to the vestibular-tactile-somatosensory (VTS) system, which is important for movement and dance, and therefore closely tied to the motor system and attuned to timing (Todd and Lee, 2015). In addition to its ties for movement, the VTS system is clearly tied to the auditory system with regards to rhythm perception (Phillips-Silver and Trainor, 2005, 2007, 2008; Trainor et al., 2009), and through common neural activation (Araneda et al., 2017). These ties between the auditory and VTS system may be an additional factor in the dominance of the auditory system in the temporal domain.

Since VTS rhythms are ubiquitous in fetal life through the mother's gait, heart rate, breathing, etc., and since these networks are tied into auditory rhythm systems, it is likely that the VTS system is heavily tied into the timing systems used in auditory rhythm perception and in motor rhythm production (Provasi et al., 2014). This is further strengthened by the fact that movement and rhythms are linked and proprioception (part of the VTS system) plays a large role in perception of rhythms that is tied into auditory rhythm perception and production (Trainor et al., 2009). Interactions between the VTS system with visual rhythm perception remains mostly unexplored at this point however, so it is unclear how much this system plays a supramodal role in the timing involved in rhythm perception/production, or if it is only tied to the auditory and motor rhythm timing systems. Further research in this area is needed to answer these questions.

1.6 Evolutionary Origins of Sensorimotor Synchronization

In an evolutionary context, it makes sense that auditory and motor systems would be tightly interconnected. First, rhythms in language are critical for both perception and production and may be a driver of SMS ability (Patel, 2006). Beyond language, matching movement to sound is a necessary result of human evolution that allows for the social and cultural inclination of humanity via music (Hagen and Bryant, 2003; Brown and Jordania, 2013). Dance is also tightly connected with music and culture and can provide a further explanatory account of human SMS capability and the connection between the motor and auditory systems (Fitch, 2016; Iversen, 2016; Laland et al., 2016; Ravignani and Cook, 2016).

Beyond humans, common adaptations appear to increase SMS ability in several non-human species capable of some level of audio-motor entrainment such as parrots (Patel et al., 2009), bonobos (Large and Gray, 2015), and sea-lions (Cook et al., 2013). Although some animals can exhibit rhythmic capabilities, some remarkably well like Ronan the sea-lion (Rouse et al., 2016), they are in some ways limited compared to humans (Patel and Iversen, 2014; Merker et al., 2015). Even though there are animals that can entrain to auditory rhythms, only humans appear to be naturally inclined to do so (Wilson and Cook, 2016). Finally, there is some evidence that non-human primates are able to synchronize their movements to predictable visual stimuli (Takeya et al., 2017), yet there has been much less research on visual SMS compared to auditory SMS in non-humans.

1.7 General Synthesis and Future Directions

In looking at how the brain processes timing information, it is clear that many context sensitive mechanisms interact and coordinate to provide optimal timing output. Much of this interaction appears to happen within the motor system and likely involves the subcortical systems to coordinate the various mechanisms. Current research suggests that oscillations play a key role coordinating the interactions among various timing circuits. However, it is not clear if the various timing systems compute measures of time in the same way. When considering that auditory and visual systems take in very different kinds of information and use it in different ways, i.e., auditory has a stronger temporal precision, and visual has a strong spatial bias, it seems likely that the timing mechanisms themselves may greatly differ.

Consider the difference between extracting timing information between a moving visual rhythm and an auditory rhythm. Moving visual stimuli contain more information than auditory stimuli, such that while entraining to auditory stimuli, prediction of the onset of the next event involves encoding the interval between two events and utilizing that information to predict the onset of the next event. With a moving visual rhythmic stimulus, that interval information is present, but so is information on position/velocity/acceleration. This means predictions of the onset of the next event can be made as part of a continuous process. The fact that even with this information, visual SMS is at best equal to auditory SMS except at fast speeds, begs the question as to why visual SMS is less capable. One possible explanation for this is that the visual system has to encode much more information, and further, encoding that information into a form that is usable by the motor network may require extra processing. This may explain the timing

activity found within the visual cortex during visual SMS. Even when there is a simple flashing metronome, there is a measure of timing activity originating from the visual cortex. Considering the reduced temporal ability with visual flashing metronomes, it suggests there may be a translation issue in harnessing a system not optimized to temporal processing the way the auditory system has been, resulting in a weaker connection to the motor timing network.

Different timing systems likely employ varying mechanisms and computational principles that are appropriate to the time scale, cellular properties, and general needs of the system. Existing computational models that capture a range of these phenomena across levels include: pacemaker accumulator models, multiple oscillator models, memory trace models, random process models, ramping activity models, delay line models, and state space trajectory-based models (Addyman et al., 2016; Hass and Durstewitz, 2016). Such models help illustrate the variety of ways to process timing information within a neural network. Evidence also suggests that cells with specific timing mechanisms exist in the basal ganglia and cerebellum (Lusk et al., 2016), yet other areas with multiple functional properties also process timing, such as in the prefrontal cortex (Hyman et al., 2012) and hippocampus (MacDonald et al., 2011). The areas that have multiple functions, as in the hippocampus and prefrontal cortex, will then likely have different computational approach than more specialized timing structures.

Given that there are multiple ways to process timing, and that many forms of cognition require some form of temporal processing, it would be surprising to find that timing mechanisms are not ubiquitous in the brain. This raises an important question. If many different timing mechanisms are available for a given task, and only one output (through action), how do neural systems arrive at the best timing information to use? A strong candidate explanation for this would implicate a mechanism that helps integration through an optimal Bayesian process (Hass and Durstewitz, 2016). Evidence from multimodal sensory integration suggests that when timing information is presented from multiple modalities, the modalities are combined and weighted based on reliability in a Bayesian optimal solution (Ernst and Banks, 2002). Since most timing related activity requires motor output, we would expect that the source of timing to be utilized would be determined before, or as that timing information becomes available to the motor system. This seems to make the case that the striatal cells operating as a comparator may be the seat of the Bayesian process to determine the optimal timing source for motor timing.

Since there is some disparity in the amount of work on auditory and visual SMS error correction, there is a need to further study the error correction capabilities within visual SMS. It is currently unknown if visual error correction can be as fast as auditory error correction when dealing modality appropriate stimuli, such as a moving visual sequence or bouncing ball. Another major area of needed work is in understanding the mechanisms by which the Bayesian optimal timing source is chosen in cases where multiple sources are available. If timing mechanisms are as ubiquitous in the brain as evidence suggests, then there may be a variety of ways these mechanisms interface with the motor timing system to produce a single output. Further imaging and computational work is required to understanding this mechanism.

Chapter 2

2 Neural responses to perturbations in visual and auditory metronomes during sensorimotor synchronization

This chapter consists of a published experiment comparing auditory and visual error-correction during a SMS task. The advantage of using an error correction task is that it allowed us to measure both sensory evoked and tap-evoked responses to interruptions in timing. The sensory evoked responses inform on the role the sensory cortices are playing during error monitoring, which are necessarily modality specific. The tap-evoked responses inform on the role of the motor and somatomotor systems during error monitoring, which are modality general with regard to the auditory and visual rhythms. By comparing these responses to the behavioral outcomes, we gain a better picture of how the auditory and visual systems are interacting with the motor system to facilitate rhythm processing. The results of this experiment provide evidence of visual system specific rhythmic timing processing, as well as suggest that visual timing information is not effectively communicated to the motor system in a way that could assist with error correction.

Published as:
Comstock, D.C. & Balasubramaniam, R. (2018). Neural responses to perturbations in visual and auditory metronomes during sensorimotor synchronization. *Neuropsychologia* http://doi.org/10.1016/j.neuropsychologia.2018.05.013.

Abstract

Tapping in synchrony to an isochronous rhythm involves several key functions of the sensorimotor system including timing, prediction and error correction. While auditory sensorimotor synchronization (SMS) has been well studied, much less is known about mechanisms involved in visual SMS. By comparing error correction in auditory and visual SMS, it can be determined if the neural mechanisms for detection and correction of synchronization errors are generalized or domain specific. To study this problem, we measured EEG while subjects tapped in synchrony to separate visual and auditory metronomes that both contained small temporal perturbations to induce errors. The metronomes had inter-onset intervals of 600 ms and the perturbations where of 4 kinds: ± 66 ms to induce period corrections, and ± 16 ms to induce phase corrections. We hypothesize that given the less precise nature of visual SMS, error correction to perturbed visual flashing rhythms will be more gradual than with the equivalent auditory perturbations. Additionally, we expect this more gradual error correction will be reflected in the visual evoked potentials. Our findings indicate that the visual system is only capable of more gradual phase corrections to even the larger induced errors. This is opposed to the swifter period correction of the auditory system to large induced errors. EEG data found the peak N1 auditory evoked potential is modulated by the size and direction of an induced error in line with previous research, while the P1 visual evoked

potential was only effected by the large late-coming perturbations resulting in reduced peak latency. Looking at the error response EEG data, an Error Related Negativity (ERN) and related Error Positivity (pE) was found only in the auditory + 66 condition, while no ERN or pE were found in any of the visual perturbation conditions. In addition to the ERPs, we performed a dipole source localization and clustering analysis indicating that the anterior cingulate was active in the error detection of the perturbed stimulus for both auditory and visual conditions in addition to being involved in producing the ERN and pE induced by the auditory + 66 perturbation. Taken together, these results confirm that the visual system is less developed for synchronizing and error correction with flashing rhythms by its more gradual error correction. The reduced latency of the P1 to the visual + 66 suggests that the visual system can detect these errors, but that detection does not translate into any meaningful improvement in error correction. This indicates that the visual system is not as tightly coupled to the motor system as the auditory system is for SMS, suggesting the mechanisms of SMS are not completely domain general.

2.1 Introduction

Tapping in synchrony to a rhythmic stimulus like a metronome involves the use of several key components of the sensorimotor system including time, prediction, and error correction. Finger tapping has been widely used to study sensorimotor functions and abilities, especially with auditory sensorimotor synchronization (Repp, 2005). Behavioral studies of finger tapping have contributed to our understanding of how movement trajectories contribute to error correction in motor timing (Balasubramaniam et al., 2004, Hove et al., 2014). Recently, neuroimaging techniques have also been used to build understanding of the neural basis of error correction in sensorimotor synchronization (SMS) using EEG (Praamstra et al., 2003, Jang et al., 2016) By studying the neural processes involved in visual and auditory SMS, the two modalities can be compared, and thus tested to see to what extent the neural mechanisms of SMS are modality specific or generalized.

To understand the differences between auditory and visual SMS we must first understand the differing capabilities between the two. One of the largest differences is the greater variability of the timing of taps with visual SMS (Repp, 2005). In addition to the differences in tapping variability, there are different limits to the tempo at which a stimulus can be entrained to; an auditory metronome can be synchronized to an interonset interval (IOI) as low as 100 ms, while the lower IOI limit for accurate visual synchronization to a flashing stimulus is around 500 ms (Repp, 2005). Even though there are clear differences in synchronization ability between the visual and auditory domains, it remains to be seen exactly why those differences exist.

Another important aspect of synchronizing movements to rhythmic stimulus is error detection and correction. Monitoring of the timing of each stimulus and of the synchronized movements is necessary to ensure continued synchronization. Since any movement action takes time from initiation to completion, the timing of each stimulus must be predicted in advance (Chen et al., 1998). The prediction of the onset of each oncoming event then allows for a comparison of the predicted timing with the actual timing for error detection in the stimulus. Errors of synchronization must be monitored for in addition to errors in the stimulus before error correction can occur. To study the

nature of error correction in SMS, occasional temporal perturbations in an otherwise isochronous stimulus have been used to induce errors (Thaut et al., 1998, Repp, 2000, Repp, 2001), and a two-level system of error correction has been put forward (Vorberg and Wing, 1996). The models posit that error correction falls into two types: Period correction and Phase correction. A period correction occurs in response to a large, noticeable error in timing, and involves updating a central time keeper. A phase correction takes place in response to a small error in timing that is below the conscious threshold and is thought to involve a more peripheral adaptive process (Repp, 2001, Repp and Keller, 2004).

To understand the neural mechanisms involved in error correction in SMS, previous work on auditory error correction has shown a modulation of the auditory-evoked potentials believed to modulate attention in response to errors in the timing of an otherwise isochronous auditory rhythm (Tecchio et al., 2000; Praamstra et al., 2003). The auditory evoked potentials, in this case the auditory P1 and N1, have shown that both the direction of the induced error, and the magnitude of the error modulate the components (Praamstra et al., 2003). In addition to the sensory evoked potentials, error induced potentials have been found in response to synchronization errors caused by perturbing the timing of a metronome (Praamstra et al., 2003). The error related components, the Error Related Negativity (ERN) and associated Error Related Positivity (Pe) have been shown to be indicative of detection of response errors, allowing for another measure of the error response (Yeung et al., 2004).

This study explores the differences in auditory and visual SMS error correction, as well as the correlating neural substrates. By measuring EEG while synchronizing finger taps with separate auditory and visual flashing metronomes, both with occasional timing errors, we can measure behavioral and neural differences between the two sense modalities. We hypothesize that since the visual system does not facilitate the same temporal precision in synchronizing to a visual flashing metronomes as the auditory system facilitates with an auditory metronome that error correction in the visual system will be a more gradual phase correction, even for larger perturbations. We further expect this reduced error correction ability to be reflected in a diminished modulation of the visual evoked components compared to the auditory evoked components, as well as reduced error response components.

2.2 Materials and methods

2.2.1 Participants

Ten subjects participated in the experiment (6 females; ages 18–34). All participants were right handed. Data from 4 additional subjects were collected but not included in analysis because they were unable to synchronize with the visual stimulus. All participants had normal hearing and normal or corrected vision. Participants gave informed consent after the experimental procedures where explained. This study was approved by the Institutional review board (IRB) for research ethics and human subjects. To estimate sample size, we used power computations for an analysis of variance using G*Power (Faul et al., 2009). Sample size estimation showed a minimum sample of 8 subjects would be necessary for a large effect size (.4), as seen in previous experiments by Praamstra et al. (2003). In this study, all analyses were performed to detect a

significant effect at the $\alpha = .05$ level, thus indicating that our sample size of 10 to be more than adequate.

2.2.2 Task

Participants were asked to tap in synchrony to separate auditory and visual metronomes with an inter-onset interval (IOI) of 600 ms. The 600 ms interval (standard IOI) was chosen because a faster visual metronome is difficult for most people to synchronize to (Repp and Su, 2013). In both sequences, there were occasional perturbations of the duration of the IOI. There were four types of perturbations; increasing the standard IOI by 16 ms, or by 66 ms; and decreasing the standard IOI by 16 ms, or by 66 ms. The intervals were chosen based on the Praamstra et al. (2003) protocol and increased to scale with the larger IOI (600 ms compared to 500 ms), and due to the limitations of the 60 Hz monitor used in the study.

The experiment was split into the auditory condition and the visual condition, with a counterbalanced design so half of the subjects did the auditory condition first, and half did the visual condition first, but never on the same day. Each half of the experiment consisted of 120 blocks, with each block consisting of sequences of 50 stimuli with a minimum of 3 s between each block. Each sequence contained 4 perturbations, with the perturbation in a given sequence always of one type. The temporal location of the perturbations was varied to avoid being predictable, with a minimum of 9 non-perturbed stimuli between perturbations. Subjects were given a 10-min break at the halfway point of each condition. The experiment began with applying the EEG cap after written consent was obtained. Subjects were then given written instructions for the experiment, and performed one practice block that contained shifts of each type before starting.

The auditory stimuli consisted of 50 ms 1000-Hz pure tones with a 10 ms rise time and 30 ms fall time presented through headphones at a comfortable volume. The visual stimuli consisted of a 50 ms gray flash on a black screen. Subjects faced a monitor while seated with the screen 65 cm away from the participants' head. For both conditions, the screen was black with a gray fixation cross consisting of two lines approximately 3 mm wide and each 4 cm long arranged perpendicular to each other in a cross fashion, that remained constant. The flashes in the visual condition where a shade of gray lighter than the fixation cross and 3 cm x 3 cm square (as measured on screen) in the center of the screen. The flashes appeared behind the fixation cross so that the fixation cross was always visible. Gray was chosen instead of a brighter color to help reduce the after-image effect. Tapping was performed with the index finger of the right hand on a metal plate attached to a Makey Makey input device that records tapping by sending a small electrical signal to an output lead that the subject holds on their left hand. An input lead for the Makey Makey was then attached to a metal plate that the subject tapped. When the subject touched the metal plate, it completed a circuit in the Makey Makey which sends the signal to the computer to indicate a tap (Collective and Shaw, 2012). Subjects performed the task while seated in a comfortable chair.

2.2.3 EEG data acquisition and processing

EEG was continuously recorded with an ANT-Neuro 32 electrode cap with electrodes placed according to the 10–20 International electrode system and recorded at

1024 Hz. The EEG data were uploaded and processed with EEGLAB (Delorme and Makeig, 2004), and the ERP data processed using ERPLAB (Lopez-Calderon and Luck, 2014). ERP data was preprocessed by first down sampling to 256 Hz, then applying a high pass filter with 6db cutoff at .1 Hz, followed by a low-pass filter with a 6db cutoff at 56.25 Hz to eliminate 60 Hz line noise. Data were then examined and any bad sections removed by hand. Any bad channels were detected and removed using the probability measure within the ASR plugin for EEGLAB that compares channels with their surrounding channels (Mullen et al., 2015). The data were then re-referenced to the linked mastoids, and then ICA was performed using the infomax algorithm within EEGLAB (Bell and Senjnowski, 1995). Following ICA, the component data were examined and eye blink and eye movement components were rejected to clean the data of further artifacts. Data were epoched using ERPLAB centered around the onset of the perturbed stimulus and centered on the participants taps that corresponded to the perturbed stimuli. Each epoch was from – .5 s of the event onset to 1 s past the onset. In addition to removing blink and eye movement components, any epoch that had an eye blink during the stimulus onset was removed.

For source localization, the EEG data down sampled to 256 Hz before being filtered with a high pass filter with a 6db cutoff at .5 Hz and a low pass filter with a 6db cutoff at 56.25 Hz. As specified in the earlier section, data were then examined again and bad sections removed by hand. Any bad channels were detected and removed using the probability measure within the ASR plugin for EEGLAB that compares channels with their surrounding channels. The data were then re-referenced to the linked mastoids. Then ICA was performed using the infomax algorithm within EEGLAB. Dipole source localization was performed using the Dipfit2 plugin that performs source localization by fitting an equivalent current dipole model using a non-linear optimization technique using a 4-shell spherical model (Kavanagk et al., 1978, Scherg, 1990). Data were epoched the same as with the ERP data. All components that had dipoles located outside of the brain model were rejected, as were all components with a dipole residual variance of greater than 15%. The epoched data were then clustered using a PCA method in EEGLAB with the K-means algorithm with the clustering based solely on the location of the equivalent dipoles for each component. The data were clustered into 12 clusters for both the stimulus-locked and response-locked data as that number fits closest to achieving 1 independent component per subject per cluster.

2.3 Results

2.3.1 Behavioral data

To analyze the average tap time asynchrony induced by the perturbations, we ran the tap-time asynchronies from T-3 to T + 6 for each perturbation condition and for both auditory and visual modalities in a within-subjects, repeated measures ANOVA. To get the tap time asynchrony values we first normalized the baseline by taking the average tap time asynchrony from T-4 to T-1 and subtracting it from the T-3 to T + 6. This procedure was used by Repp (2001) and was done to reduce inter-subject variability due to differing negative mean asynchronies since we are not interested in those inter-subject differences. The Auditory and Visual conditions were first analyzed separately with 3 factors: Direction (positive vs negative), Magnitude (66 ms vs 16 ms), and Position (the 10 levels

of position: T-3 to T + 6). These data are displayed in Fig. 2.1, where a large change in the amount of asynchrony can be seen after the perturbation at point T for each condition.

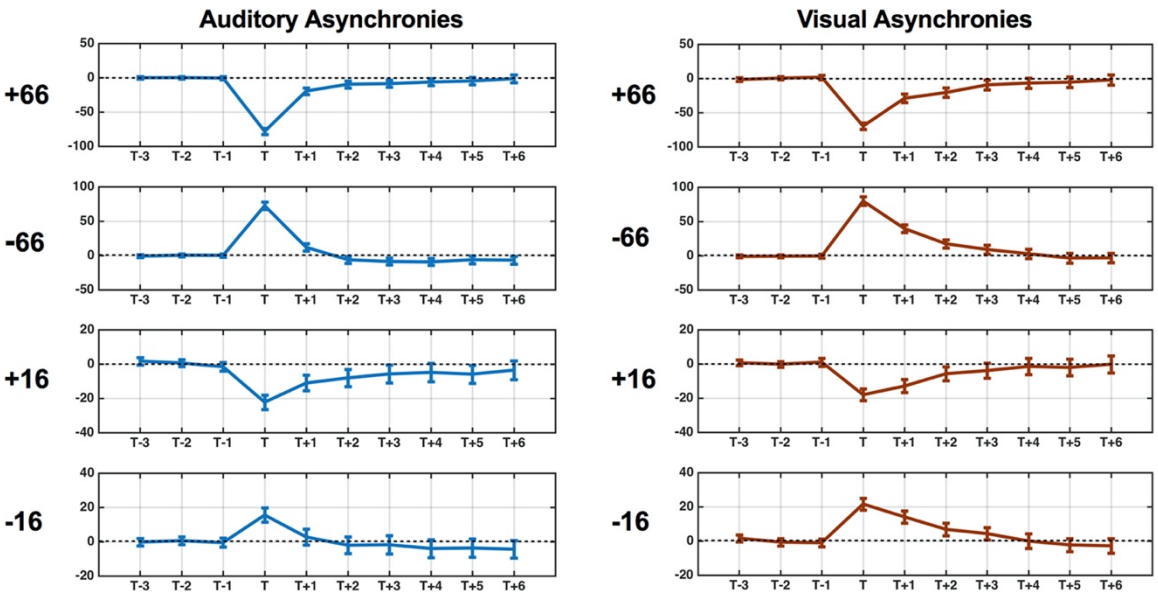

Fig. 2.1 Tap asynchronies at each stimulus position. The baseline asynchrony was normalized to 0 for all subjects and indicated by the dashed lines. Error bars show standard error. Note that the scale of the y axes are different between the 16 and 66 ms perturbations.

Similar to the results of Praamstra et al. (2003), we do not see a significant main effect of Magnitude or of Position in the Auditory condition. We do see an effect in Direction $F(1,9) = 51.11$, $P < .001$, $\eta p2 = .850$, since the direction of the asynchrony changes with the direction of the perturbation. Additionally, there is an interaction between Direction and Position $F(9,81) = 62.62$, $P < .001$, $\eta p2 = .874$ which is due to the large change in asynchrony at the position of the perturbation, T, in a direction determined by the direction of the perturbation. We also find an interaction between Direction and Magnitude $F(9,81) = 7.43$, $P < .05$, $\eta p2 = .452$. In the visual condition we find no significant main effect of either Magnitude or Position, but we do see a main effect for Direction $F(1,9) = 129.67$, $P < .0001$, $\eta p2 = .935$ as well as interactions for Direction and Position $F(9,81) = 78.94$, $P < .001$, $\eta p2 = .898$, and for Direction and Magnitude $F(9,81) = 33.89$, $P < .001$, $\eta p2 = .790$.

In order to compare the results between the auditory and visual conditions we ran a within-subjects repeated measures ANOVA on the combined auditory and visual tap-tone asynchrony data using 4 factors: Direction, Magnitude, Position, and Modality (auditory and visual). In this analysis, we found no significant main effects on Magnitude or Position. We found an effect of Direction $F(1,9) = 204.36$, $P < .001$, $\eta p2 = .958$, interactions between Direction and Position $F(9,81) = 425.71$, $P < .001$, $\eta p2 = .979$, Direction and Magnitude $F(9,81) = 55.01$, $P < .001$, $\eta p2 = .859$, and a 3 way interaction between Direction, Position, and Magnitude $F(9,81) = 159.66$, $P < .0001$, $\eta p2 = .947$.

This analysis also found a main effect of Modality F (1,9) = 11.48, P < .01, ηp2 = .561, which is a result of the more gradual corrections of the visual perturbations (interaction of Modality X Position F(9,81) = 2.03, P < .05, ηp2 = .184), and of the greater tendency for overcorrection in the Auditory negative perturbations and under-correction in the Auditory positive perturbations (interaction of Modality by Direction F(1,9) = 5.46, P < .05, ηp2 = .378, and 3 way interaction between Modality, Direction, and Position F(9,81) = 7.11, P < .0001, ηp2 = .441).

In order to check if the corrections were happening more quickly for the larger perturbations, and to check if the direction effected the speed of the correction, the tap-time asynchrony data were normalized from time points T to T + 6 for both Auditory and Visual conditions (Fig. 2.2). These data were analyzed using the same procedure and factors as the tap-time asynchrony data. The Auditory normalized asynchronies were spread out due to the amount of overcorrection in the negative perturbations and under-correction in the positive overcorrections yielding a main effect of Direction F (1,9) = 23.98, P < .001, ηp2 = .727. This under and over correction subsequently washed out any significant effects on Magnitude or Position. There was an interaction between Direction and Magnitude F (1,9) = 12.42, P < .01, ηp2 = .580, likely driven by the effect of Direction. The Visual normalized asynchronies show only a main effect of Position F(5,45) = 26.76, P < .001, ηp2 = .748 as the correction was uniformly changing and only effected by Position. The clear difference between the Auditory and Visual normalized asynchronies is shown by the main effect of Modality F (1,9) = 13.65, P < .001, ηp2 = .602 when an analysis of the two conditions combined were run. Additionally, the combined analysis shows a main effect of Direction F(1,9) = 24.23, P < .001, ηp2 = .729, and interactions between Direction and Magnitude F(1,9) = 11.08, P < .01, ηp2 = .552, Modality and Direction F(1,9) = 16.15, P < .001, ηp2 = .642, and a 3 way interaction between Direction, Magnitude, and Modality F(1,9) = 9.65, P < .05, ηp2 = .517.

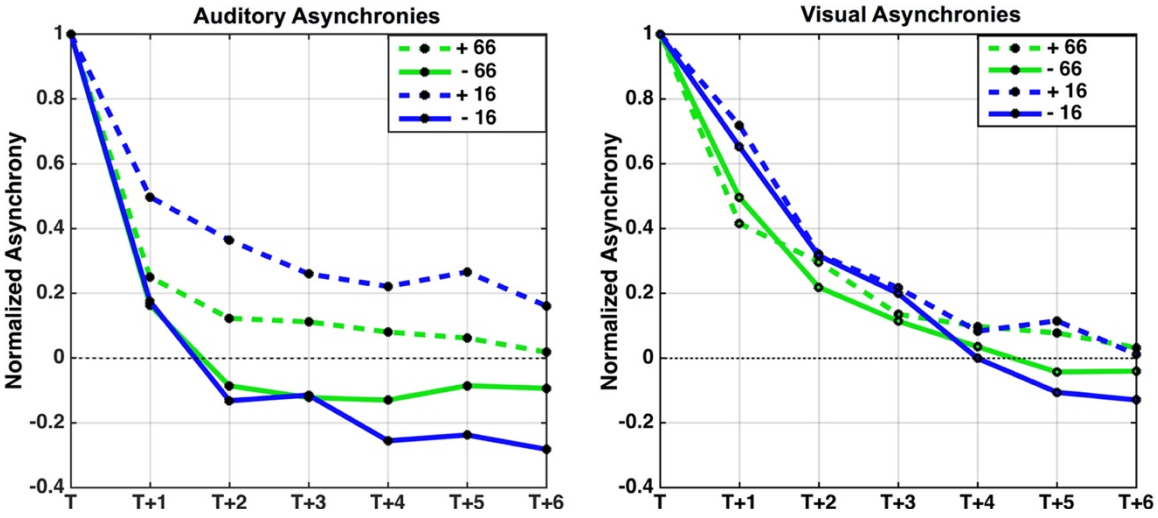

Fig. 2.2. Normalized asynchronies for both auditory and visual conditions. The visual condition induced a nearly uniform relative correction while the auditory condition shows a separation between conditions primarily due to under and overcorrections.

2.3.2 ERP waveforms

We focused on several different waveforms in studying the neural underpinnings of error correction, starting with the auditory evoked potentials shown in averaged waveforms from Fz in Fig. 2.3. The stimulus locked waveform shows a P1 component peaking around 100 ms post stimulus followed by a negative going waveform (N1) around 130 ms, and then the positive P2 component peaking near 200 ms post stimulus. Additionally, in the – 66 condition there was a second negative peak following the N1 around 170 ms which may be a mismatch negativity response (MMN). For the purposes of the current study, we focused on the auditory N1 component, which showed the strongest deviation in the + 66 condition.

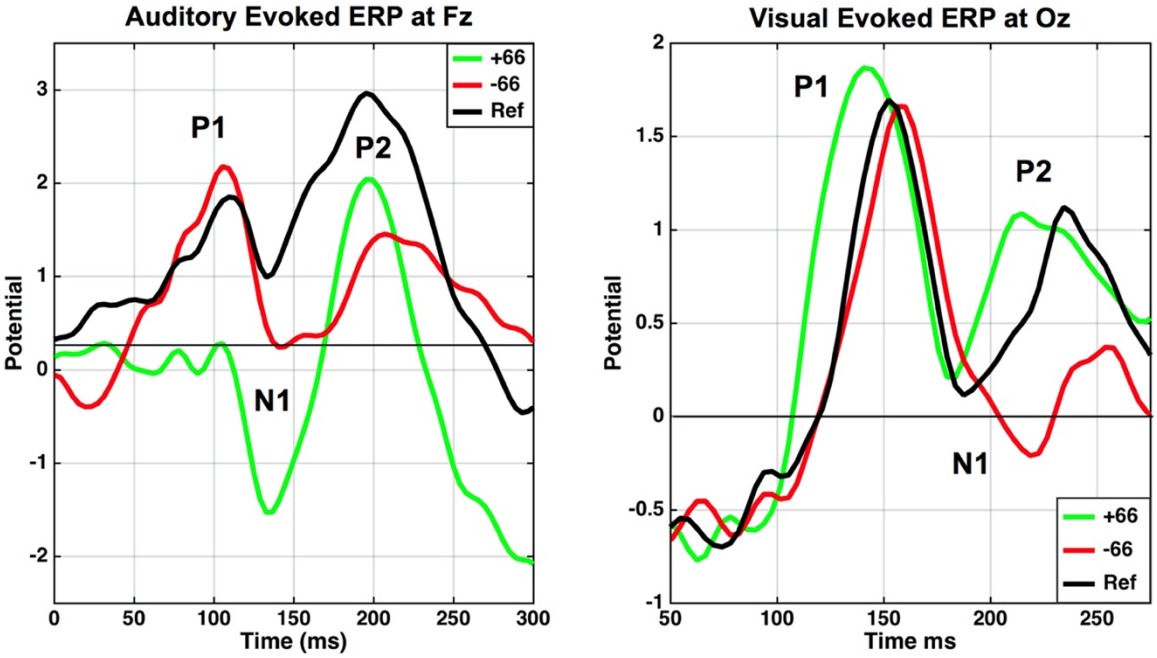

Fig. 2.3. Grand average auditory and visual evoked ERPs at Fz and Oz, respectively. The auditory evoked ERPs are stimulus locked to the onset of a tone, while the visual evoked ERPs are stimulus locked to a flash. Both plots show wave forms evoked by + 66 perturbations, the – 66 perturbations, and a non-perturbed stimulus.

To look at the visual evoked potentials seen in Fig. 2.3, we used the averaged waveform at Oz instead of at Fz, as this is the point where the primary visual attentional components can be best measured from. The wave forms consist of a large positive peak near 150 ms post stimulus (P1) followed by the negative N1 at around 180 ms. There is then a second positive waveform peaking between 200 and 250 ms labeled the P2. This

analysis focuses on the visual P1 wave, which like the auditory N1 was effected the most in the + 66 condition.

The response evoked potentials, shown in Fig. 2.4, are measured at Fz. They consist of a large negative premovement wave followed by a large positive postmovement wave near 100 ms. Following Praamstra et al. (2003), we focus on the ERN, which would occur around 200 ms, and the associated Error Positivity (Pe) near 300 ms. Since the tap time asynchrony was in the range of – 50 ms, there is some overlap with the frontal stimulus evoked components. This is especially pronounced in the visual response locked waveform as there is a large P3 component that overlaps with the expected onset of the ERN and Pe (Fig. 2.8). Since the P3 component is stimulus locked, but the response locked waves are locked to the tap time, the effect is a large positive wave in the visual response locked ERP not seen in the auditory response locked ERP. Since the expected stimulus time onset differs with the actual stimulus onset time in the perturbation conditions, the effect of the stimulus evoked waveforms on the response evoked waveforms is temporally shifted based on the size and direction of the perturbation.

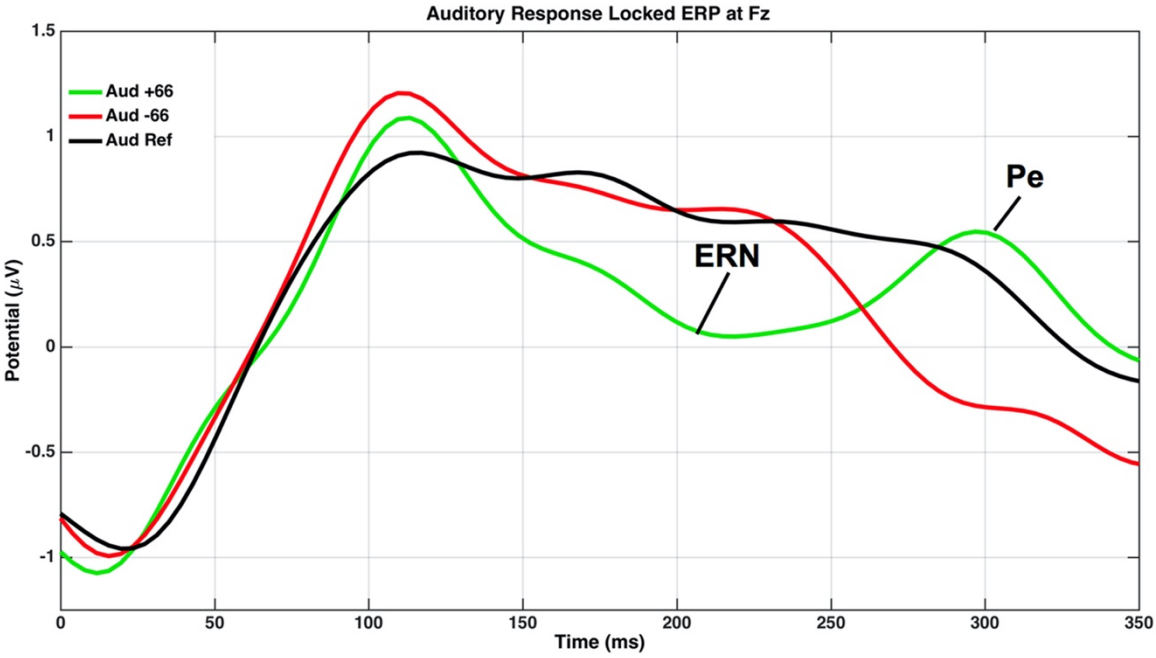

Fig. 2.4. Auditory ERP at Fz time-locked to the tap onset for ± 66 ms perturbations and a non-perturbed reference.

2.3.3 Auditory-evoked potentials

The AEPs were analyzed based on the difference in peak amplitude of the N1 wave between the perturbation conditions and the corresponding non-perturbation reference condition seen in Fig. 2.5. The perturbation condition was at T, while the reference condition was always at T-2, and taken from the same blocks as its corresponding perturbation. The peak amplitude was measured using a local peak finding procedure within ERPLAB between 110 and 160 ms post stimulus onset using a

jackknife procedure. The jackknife procedure takes as many grand averages as there are subjects, with each grand average subtracting one subjects' waveform. Applying this method has the advantage with non-linear measures, such as peak amplitude and peak latency, of reducing error variance, effectively reducing the probability of a Type II error while not increasing the likely-hood of a Type I error (Luck, 2014). These difference scores were then entered into a 2 factor within-subjects, repeated-measures ANOVA with the factors of Direction (+/- perturbations) and Magnitude (66 and 16). No comparisons were made between the auditory and visual ERPs due to the physical confound of the different stimulus types. This yielded main effects of Magnitude $(1,9) = 325.58$, $P < .001$, $\eta p2 = .973$, and Direction $(1,9) = 566.89$, $P < .001$, $\eta p2 = .984$, indicating that the N1 wave was modulated by both the direction and magnitude of the perturbations, and was concurrent with Praamstra et al. (2003). Additionally, there was an interaction between Magnitude and Direction $(1,9) = 297.37$, $P < .001$, $\eta p2 = .971$, due to the 66 ms perturbations having much larger effects than the 16 ms perturbations. These results are largely driven by the 66 ms perturbations and especially the + 66 perturbation which produced the most deviant N1.

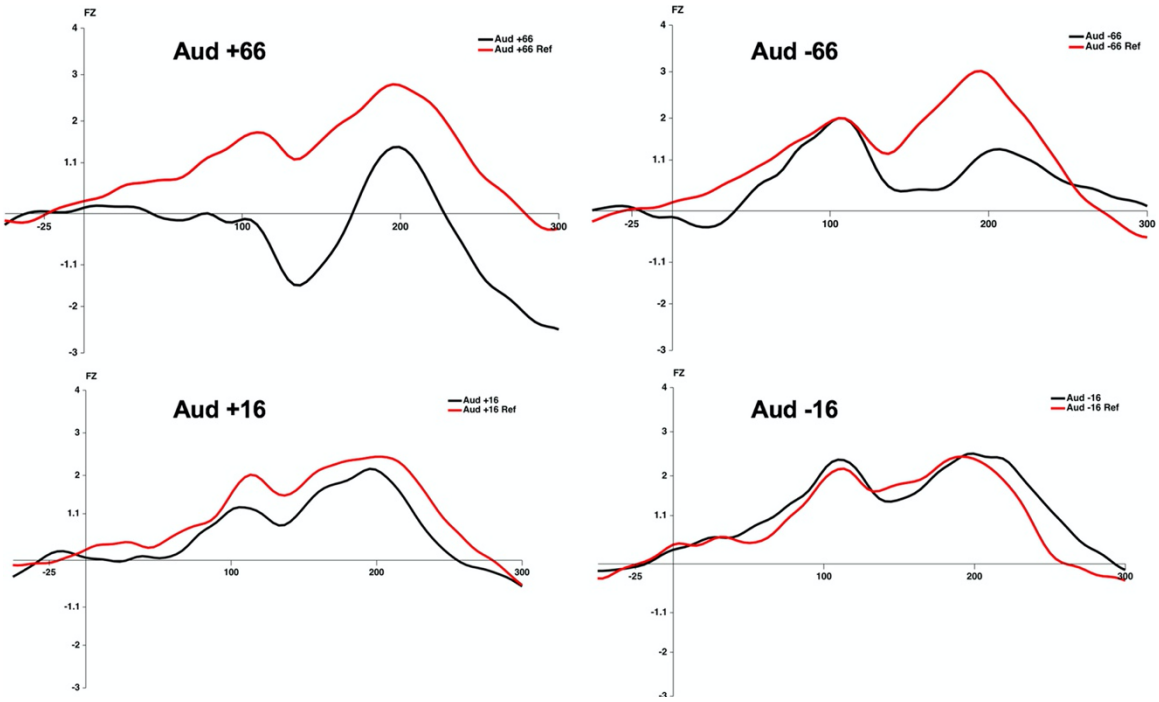

Fig. 2.5. Auditory evoked potentials at Fz for both the perturbed conditions at time T, and corresponding reference (non-perturbed) condition at T-2 for each of the 4 perturbation types.

2.3.4 Visual-evoked potentials

The VEPs were analyzed based on the difference in peak amplitude of the P1 wave between perturbation conditions and their corresponding references in the same fashion as the auditory N1 was analyzed. The peak was measured using the local peak

function in ERPLAB between 100 and 190 ms post stimulus onset as seen in Fig. 2.6. The 2-way ANOVA showed a main effect of Direction (1,9) = 107.67, P < .001, ηp2 = .923, and an interaction effect between Direction and Magnitude (1,9) = 114.49, P < .01, ηp2 = .927, but no significant main effect of Magnitude. These results are likely driven by the + 66 perturbation which resulted in a P1 wave of reduced latency. To test the differences in latency, additional analyses were performed using the differences between the local peak latency of the P1 scores of the perturbed and corresponding reference P1 waves. This analysis was done using a jackknife procedure and the 2-way ANOVA, showing significant main effects in both Magnitude (1,9) = 48.96, P < .001, ηp2 = .845, and Direction (1,9) = 36.42, P < .001, ηp2 = .802, as well as in the interaction between Magnitude and Direction (1,9) = 50.8, P < .001, ηp2 = .850. These results confirm that the P1 wave had a reduced latency in the + 66 condition.

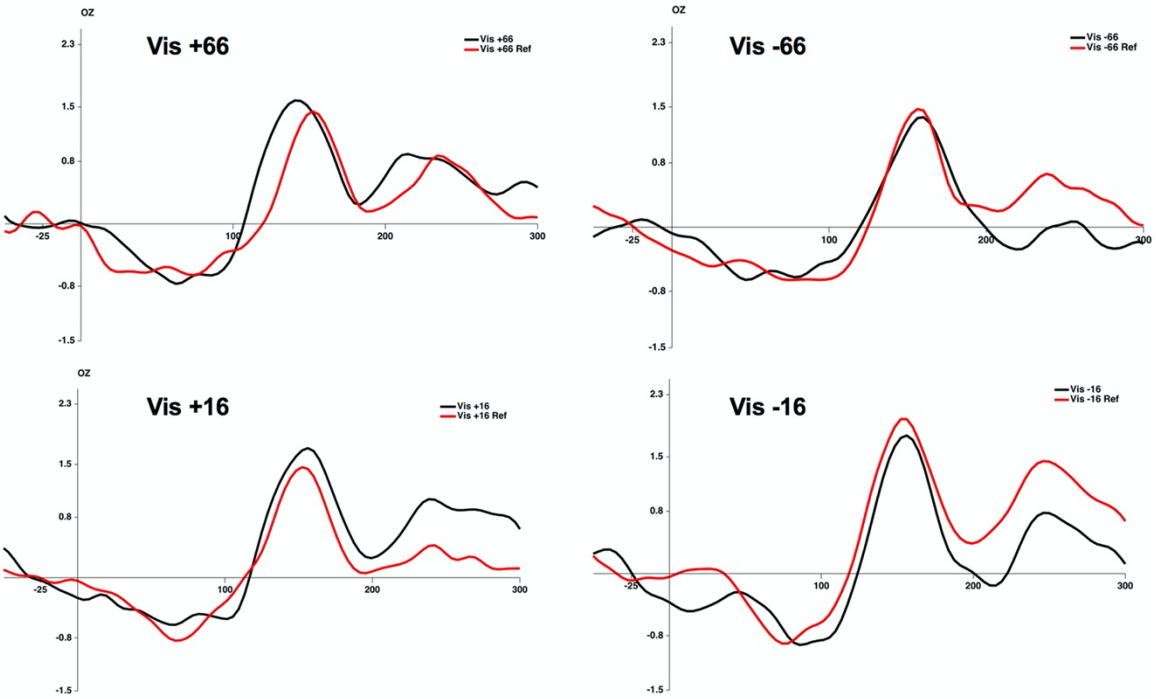

Fig. 2.6. Visual evoked potentials at Oz for both the perturbed conditions at time T, and corresponding reference (non-perturbed) condition at T-2 for each of the 4 perturbation types.

2.3.5 Response-locked potentials

The response-locked potentials from the auditory condition in Fig. 2.7 were measured at Fz. An inspection of Fig. 2.7 reveals a waveform similar to that as reported in Praamstra et al. (2003). To analyze the ERN, we measured the mean-amplitude between 180 and 220 ms of the waveforms and then took the difference of the mean-amplitude between the perturbation condition and the corresponding reference from a non-perturbed tap at T – 2. Those difference scores were entered into a within-subjects, repeated measures 2-way ANOVA with the factors of Direction and Magnitude. We found no significant effects which is in contrast to the results reported by Praamstra et al.

(2003). The Pe that usually corresponds to the ERN, and appears in the + 66 auditory condition was analyzed in the same way as the ERN, except using a mean-amplitude window of 300–400 ms. Here we find a main effect of Direction (1,9) = 10.66, P < .05, ηp2 = .542 and a significant interaction between Direction and Magnitude (1,9) = 8.44, P < .05, ηp2 = .484, but no main effect of Magnitude. Since the Pe almost always corresponds to an ERN, these results suggest that the ERN was lost due to the confound of the auditory-evoked N1 and P2 waves, while the Pe was not effected due to its later onset.

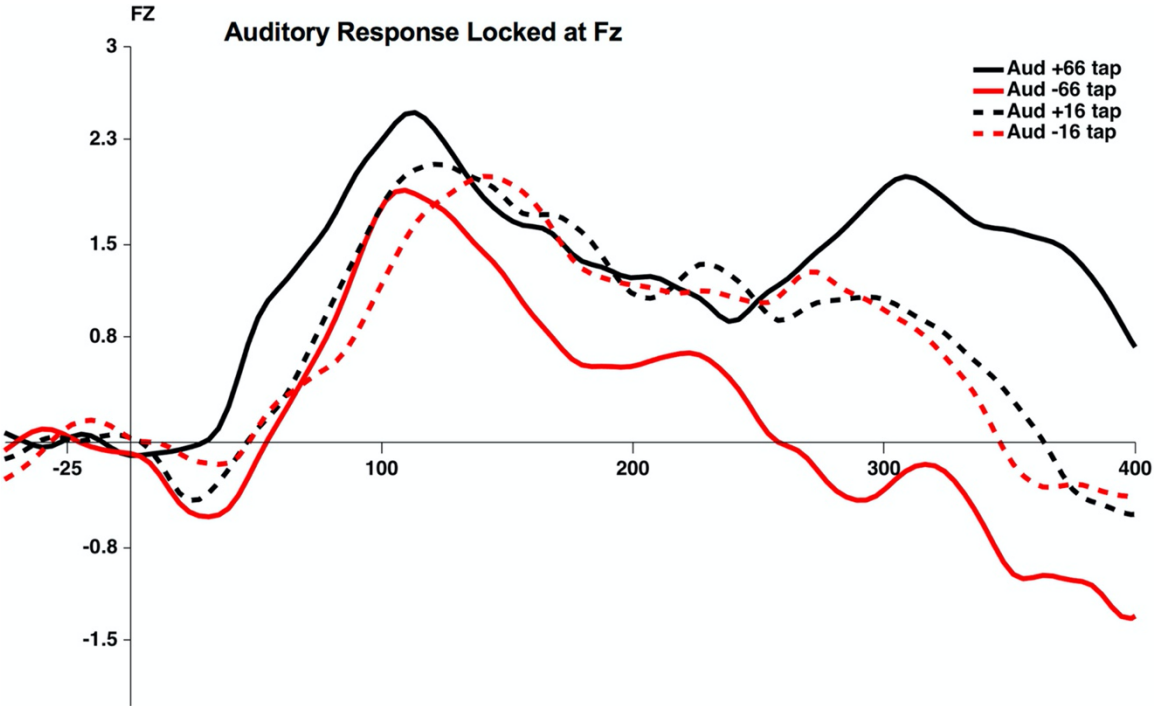

Fig. 2.7. Response locked waveforms from time T for the 4 perturbation types from the auditory condition.

The response-locked waveforms in the visual condition Fig. 2.8(A) show a somewhat different looking waveform than compared to the auditory response-locked waveforms. This difference is due to the large frontal P3 component found in the visual stimulus locked potentials at Fz shown in Fig. 2.8B. The data were analyzed in the same fashion as the auditory response locked data. Once again in terms of the ERN, no significant effects were found, just as in the auditory data. In looking at the area of the Pe, a main effect was found of Direction (1,9) = 11.21, P < .01, ηp2 = .555, but no significant effect of Magnitude was discovered. This finding corresponds to the fact that the large visual evoked frontal P3 component would show up in the response locked data shifted according to perturbation, and is not taken as an indication of any Pe or corresponding ERN.

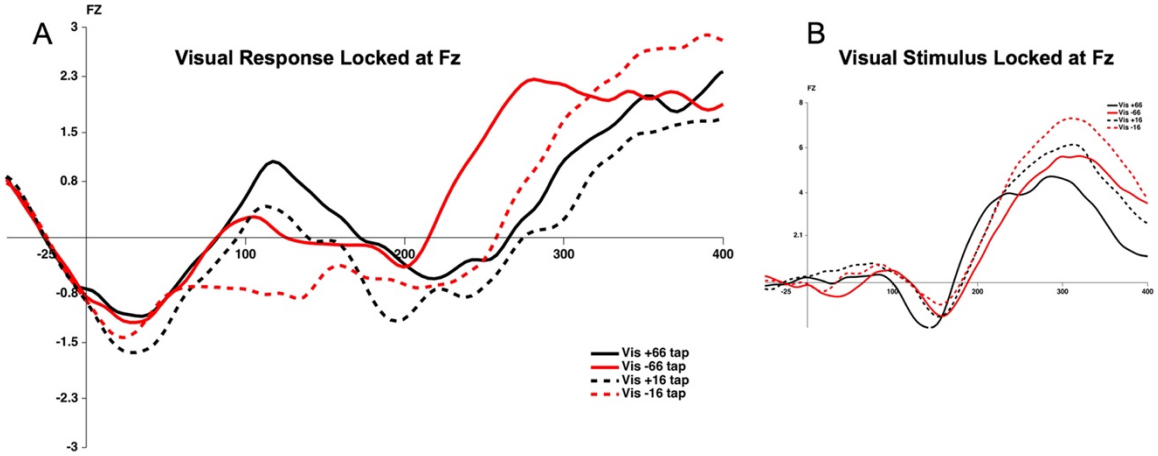

Fig. 2.8. Visual condition waveforms at time T at Fz. (A) Visual response locked with the 4 perturbation types. Note the large late positive waveforms that differentiate in latency by perturbation condition. (B) Visual stimulus locked waveforms at Fz. Note the extremely large late waveforms. These waveforms explain the large late waveforms in (A).

2.3.6 Source localization

We investigated the underlying neural components of error detection and error correction using a clustering analysis of the dipoles localized from the individual independent components. The nature of dipole source localization on EEG data means that it does not have near the spatial precision as fMRI methods, however, when it is used in conjunction with evidence from other localization methods and neuroscience research it is a useful tool to determine the sources of the neural activity measured at the electrode level. The activity of the individual independent components with each cluster was averaged, resulting in an ERP for each cluster. This is to provide insight on the function of the components in relation to the ERPs generated at the scalp level. Our clustering analysis generated 12 clusters from 223 individual independent components left after artefactual components were rejected. Artefactual components consisting of blink and eye movement components were removed manually. Additionally, any component with a dipole residual variance greater than 15%, and any component with a dipole outside of the brain were also removed from the analysis. We focus on 4 clusters here; 2 centered in the occipital lobe, one in the premotor cortex, and one focused at the anterior cingulate.

Looking at the clusters in the occipital lobe in Fig. 2.9, we see two similar components with one in the right occipital lobe and one in the left occipital lobe. The cluster in the right occipital lobe was consists of 19 independent components and the cluster in the left consists of 16 independent components. The ERPs in Fig. 9C and D are both time locked to the stimulus onset at time T for the ± 66 perturbations for both visual and auditory conditions. The ERPs generated are both consistent with the ERPs from the surface electrodes at Oz, confirming that the visual evoked P1 originates in the visual cortex.

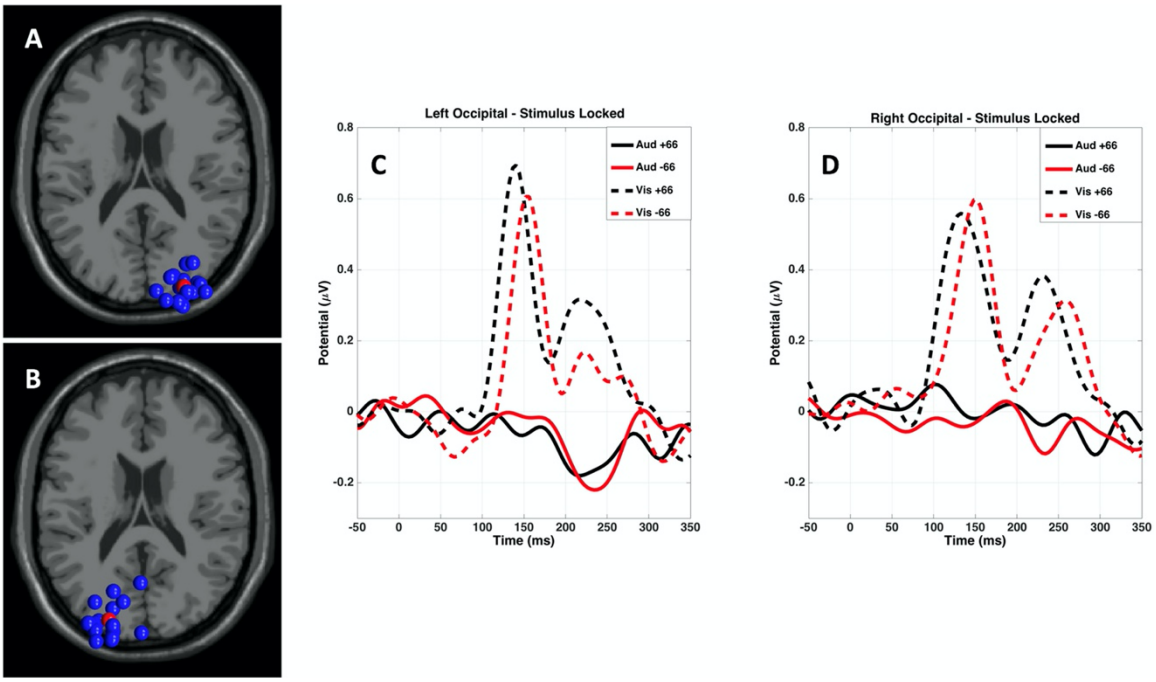

Fig. 2.9. Clusters from the occipital lobe and their associated stimulus locked ERPs. (A) Cluster in the right Occipital Lobe. (B) Cluster in the left Occipital Lobe. (C) Stimulus locked ERP from the left Occipital cluster at time T for the ± 66 ms perturbations for both Auditory and Visual conditions. (D) Stimulus locked ERP from the right Occipital cluster at time T for the ± 66 ms perturbations for both auditory and visual conditions.

The cluster centered on the premotor cortex in Fig. 1.10 consists of 19 independent components. We generated 2 ERPs from components in this cluster; one time locked to the stimulus at time T (Fig. 10B), and one time locked to the tap onset at time T (Fig. 10C). Both ERPs contain the ± 66 perturbations for both auditory and visual conditions. For the Auditory stimulus locked ERP, we find negative going waveforms peaking at approximately 130 ms post stimulus onset and a following positive waveform peaking around 190 ms in the + 66 condition and near 240 ms in the – 66 condition. These peaks correspond roughly with Auditory N1 and P2 waves found in the channel electrodes at Fz. No such waveforms are found in the visual stimulus locked ERPs, suggesting that the premotor cortex may be playing a role in auditory error detection but not in visual error detection. The response locked ERPs show a pre-movement negativity for both Auditory and Visual conditions, and large post-movement positivity around 100 ms in both Auditory conditions, with a smaller post-movement positivity in the visual conditions.

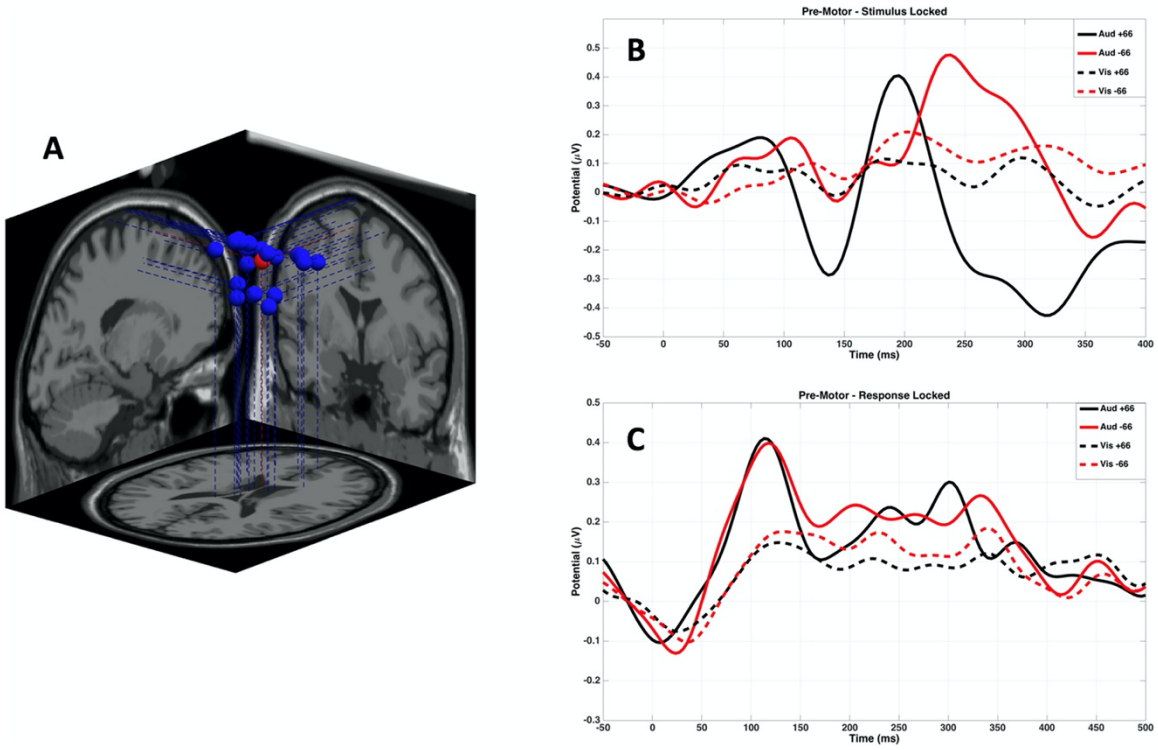

Fig. 2.10. Cluster centered around the pre-motor cortex and associated ERPs. (A) Clustered component dipoles centered approximately at the pre-motor cortex. (B) Stimulus locked ERP from pre-motor cluster at time T for the ± 66 ms perturbations for both Auditory and Visual conditions. (C) Response locked ERP from pre-motor cluster at time T for the ± 66 ms perturbations for both Auditory and Visual conditions.

The cluster centered approximately on the anterior cingulate shown in Fig. 2.11 consists of 19 independent components. We generated 2 ERPs from this cluster; one time locked to the stimulus at time T (Fig. 2.11B), and one time locked to the tap onset at time T (Fig. 2.11C). Both ERPs contain the ± 66 perturbations for both auditory and visual conditions. In the stimulus locked ERP, we see a waveform strongly resembling those detected at Fz in the auditory conditions (shown in Fig. 2.5) with similar auditory N1 and P2 peak latencies, showing a role for the anterior cingulate in auditory error detection. In the visual stimulus locked waveforms a negative wave with a peak near 150 ms post matches the anterior N1 measured at Fz for the visual stimulus shown in Fig. 8B, suggesting that there is some role for the anterior cingulate in error detection for visual stimuli. Looking at the response locked waveforms there is a pre-movement negativity followed by a post-movement positivity peaking near 100 ms post tap for both Auditory and Visual conditions. In the Auditory + 66 there is an additional peak near 330 ms, but none for the Auditory – 66 condition or for either visual condition. This peak corresponds with the Pe found in the Auditory response locked waveforms at Fz, suggesting a further role for anterior cingulate in error detection and correction.

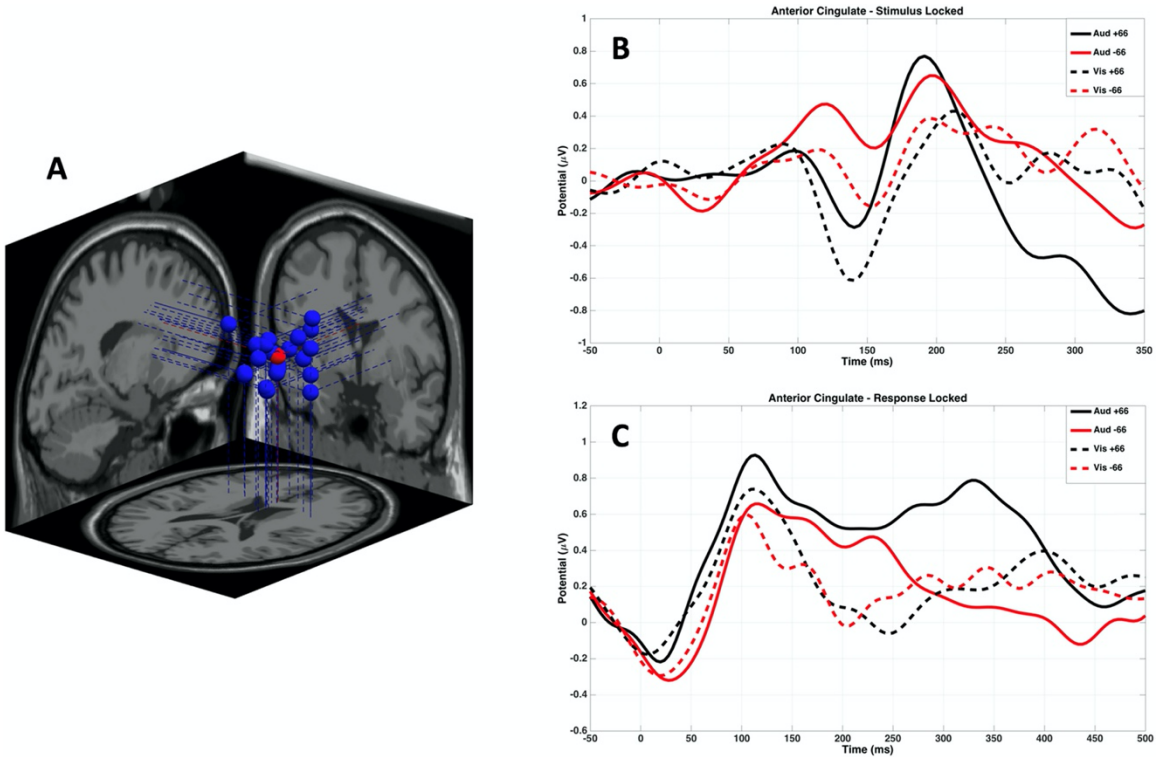

Fig. 2.11. Cluster centered around the anterior cingulate and associated ERPs. (A) Clustered component dipoles centered approximately at the anterior cingulate. (B) Stimulus locked ERP from anterior cingulate cluster at time T for the ± 66 ms perturbations for both Auditory and Visual conditions. (C) Response locked ERP from anterior cingulate cluster at time T for the ± 66 ms perturbations for both Auditory and Visual conditions.

2.4 Discussion

2.4.1 Summary of results

Our data show clear differences in error correction between auditory and visual sensorimotor synchronization. Within the tapping data, we show that changes in perturbation direction or magnitude do not affect the rate of correction in the visual condition. In the auditory condition, we find clear differences in rate of correction with the direction of the perturbations, which is largely attributed to the pronounced under- and overcorrection. Within both the AEPs and VEPs we find that the + 66 perturbations produce the largest effect. In the auditory condition we see pronounced N1 component for the + 66 condition at Fz, and in the visual condition we find a reduced latency for the visual P1 component at Oz. The – 66 condition produced what may be a MMN in the Auditory – 66 condition, while the visual – 66 condition resulted in a larger N1/attenuated P2 component. Looking at the response locked waveforms we only find evidence suggesting an ERN in the Auditory + 66 with the pronounced error positivity (Pe). The localization results suggest that the visual system is performing at least some of the timing activity of rhythm perception within the visual cortex, while the auditory timing of rhythm perception appears to be performed within the motor cortex.

Additionally, the anterior cingulate cortex is implicated in error monitoring for both the incoming stimuli and for errors made in response to perturbed stimuli.

2.4.2 Differences between auditory and visual behavioral data

The normalized asynchrony data show the visual correction is happening at the same rate regardless of the size or direction of the error. The gradual undifferentiated correction in the visual tapping data suggests that the visual system is only using a phase correction in response to the perturbations. The auditory data, on the other hand, show an effect of the direction in the normalized asynchrony of the data, which we suggest is due to the amount of undercorrection for the late coming perturbations and overcorrection for the early coming perturbations. While our data does not show a clear effect of the size of the perturbation on correction for auditory stimuli, several previous studies have shown this effect, suggesting a difference in phase correction and period correction (Repp, 2000, Repp, 2001, Praamstra et al., 2003). While our data do not clearly show the classical pattern of period correction, we suggest that the evidence from previous research shows the perturbations of ± 66 ms do induce period corrections.

2.4.3 Stimulus locked ERPs

The auditory evoked potential (AEP) of focus of this study is the N1, which is believed to signal detection of changes in the auditory environment (Hyde, 1997), and is linked to the modulation of attention such that an increase in N1 amplitude links with increased attention (Lange, 2013). The AEPs show a consistent pattern where the ± 16 ms perturbations produce no significant differences in wave forms, which suggests that the mechanisms connected to the auditory N1 are not sensitive to small phase correction inducing shifts, and therefore do not help to modulate attention in order to correct errors. Consistent with the findings in Praamstra et al. (2003), the larger magnitude errors of ± 66 ms provoke effects on the N1 by increasing the N1 amplitude and thus suggest period correction is tied to the mechanisms responsible for the N1. In addition to the effects on the N1, in the – 66 perturbation we see a wave form that may be attributed to a Mismatch Negativity (MMN), which is thought to be a pre-attentional response to an auditory change great enough to affect a pertinent behavioral activity (Näätänen, and Winkler, 1999). Previous research has shown that the MMN can be activated in response to an unexpectedly early tone in otherwise isochronous rhythms (Ford and Hillyard, 1981; Rüsseler et al., 2001). These effects suggest there may be different mechanisms of error direction depending on the direction of error.

The visual evoked potential (VEP) of focus for this study is the visual P1, which originates in the occipital lobe and is believed to be due to inhibitory processes resulting from thalamic input to the visual cortex (Kraut et al., 1985). The P1 is effected by changes in luminance, such as flashes. Additionally, the latency of the P1 peak has been shown to decrease in response to large changes in amount of luminance (Luck and Kappenman, 2011). Our data show the P1 was not responsive to any of the perturbations except for the + 66 condition, and only by way of a reduction in peak latency. The fact that the latency was reduced in the large, late coming perturbations suggests that the P1 mechanism was primed or expecting the onset of the stimulus. This indicates that a measure rhythmic timing may be occurring within the visual cortex.

2.4.5 Subcortical and cortical processes

In both the auditory and visual conditions, the evoked potentials only show responses to the large perturbations: both + and – 66 perturbations induced larger N1 amplitudes in the auditory condition, and the + 66 condition reduced the latency of P1 in the visual condition. These evoked potentials originate in the cortex since the subcortical regions of the brain do not have the geometric neural alignment necessary to evoke event related potentials. Indeed, our source localization data suggest that the anterior cingulate is directly involved in the period-correction process, as would be expected from the known error monitoring role of the anterior cingulate (Botvinick et al., 2001, Botvinick et al., 2004, Ridderinkhof et al., 2004). So, while our data show that at least some of the processing of period-correction errors is happening at the cortical level, any phase correction processing is likely happening at the subcortical level, with previous research perhaps suggesting that the basal ganglia might play a large role in this process (Cameron et al., 2016, Grahn and Brett, 2009).

2.4.6 The role of the ERN

The ERN is known to arise in the result of making an error, even when that error is not reported. (Falkenstein et al., 2000, Olvet and Hajcak, 2008) The error positivity (Pe) often follows the ERN, but only when that error is consciously detected (Overbeek et al., 2005, Endrass et al., 2007). Although our data do not show a statistically significant ERN, they are suggestive of its existence as backed up by the large Pe found in the auditory + 66 condition. This is similar to what Praamstra et al. (2003) found where only the auditory + 50 condition elicited an ERN in their study. The fact that this error monitoring activity only arose from the large, late-arriving perturbation is likely due to the fact that synchronized tapping to auditory tones usually involves tapping roughly 50 ms before the actual tone onset, or what is known as the negative mean asynchrony (Repp, 2005). Since the subjects are tapping slightly ahead of the expected onset, a late tone onset will seem slightly more deviant than it actually is, while an early tone onset will seem less deviant. In the case of the visual condition, there is a lack of evidence for the ERN which suggests there was simply not enough temporal acuity provided by the visual system to engage this error mechanism.

2.4.7 Source analysis

The clustering analysis done on the component dipoles suggest the visual system is processing the timing of the visual rhythmic flashes at some level in the visual cortex, as well as within the anterior cingulate. When looking at the timing of the evoked potentials between the visual cortex and the anterior cingulate for the large perturbations, we can see that both show large waveforms peaking at approximately the same point in time, suggesting that the two areas are tied together in the rhythmic timing and error monitoring of the visual flashes. We also find evidence that the anterior cingulate is involved in the error monitoring of the auditory stimuli as well as for monitoring response errors in tapping timing. This role of the anterior cingulate in error monitoring for both stimulus and response errors fits with the perceived role of the anterior cingulate as implicated in cognitive control functions that allow the brain to adapt behavior to

changing task demands and circumstances (Botvinick et al., 2001, Botvinick et al., 2004, Ridderinkhof et al., 2004)

2.4.8 Visual error correction mechanism

Many previous studies have shown that the auditory system is tightly coupled with the motor system for beat perception (Chen et al., 2006, Chen et al., 2008, Grahn and Brett, 2007, Grahn and Rowe, 2009). This coupling with the motor system results in strong synchronization abilities to auditory rhythms. An fMRI study by Hove et al. (2013a) showed that synchronizing to a visual flashing rhythm, as well as a moving rhythm activates basal ganglia linked to the motor network less strongly than comparable auditory rhythms, suggesting the visual system is not able to provide the necessary information to the motor system to allow for motor synchronization to flashing visual rhythms with the same level of accuracy seen with auditory rhythms. It is known that synchronization ability to a moving visual rhythm, e.g. a bouncing ball, is much closer to the ability to synchronize to an auditory rhythm (Hove et al., 2010, Hove et al., 2013b), although it is not clear that synchronizing movements to a moving stimulus is invoking a sense of rhythm in the same way as an auditory rhythm. Likewise, synchronizing to an auditory rhythm that consists of a frequency modulated siren also results in reduced synchronization ability compared to a normal rhythm (Hove et al., 2013a). Neither of these kinds of stimuli have been used in an error correction task, so the capabilities of error correction for these stimuli remain unknown. We do see evidence that the visual system can detect at least some errors with flashing stimuli based on the latency reduction of the visual P1 to the + 66 perturbations. Curiously, even though the visual system is detecting this error, it does not lead to any improvement in synchronization error correction. This suggests the visual system is simply not coupled to the motor system for rhythm entrainment in the same way that the auditory system is, and therefore explains why synchronization to flashing visual rhythms is much more difficult than synchronization to a similar auditory rhythm. It is important to underscore that we cannot conclude about other visual-motor coupling mechanisms (such as catching a ball or navigating in a cluttered environment) from the current experiment, so we are extending our findings only to predictive sensorimotor synchronization tasks of a rhythmic nature. It is also important to note that we are not making any specific comparisons between auditory and visual ERPs directly, since that would be akin to comparing two very different phenomena (Hillyard and Picton, 1987, Näätänen, 1975). Our comparisons are limited to the sensorimotor activity that is precipitated by error detection in each modality separately.

2.5 Conclusion

There are several key findings in this study. The suggestion that there is a MMN response for the – 66 auditory condition implies there may be separate mechanisms in play for detecting errors, depending on the direction of the errors. We also find that the anterior cingulate is implicated in error monitoring processes for the rhythmic timing of incoming stimuli as well as for responses in synchronization induced by perturbations in the otherwise isochronous rhythm. The lack of evidence for neural correlates of phase correction suggests that the processes involved in phase correction are subtle and likely

subcortical. Finally, the fact that it is difficult to entrain to a visual flashing rhythm is likely due to the visual system not being coupled to the motor system as strongly as the auditory system for these kinds of rhythmic entrainment tasks. It is also possible that there are separate mechanisms of visual synchronization, but this subject matter needs more study before those mechanisms may be determined.

Acknowledgments
This work was supported by an NSF grant BCS 1460633 awarded to the corresponding author (RB). DCC and RB were also supported by an award from the Office of the President, University of California (CA-15-328736) for the UC-MERCI initiative awarded to Scott Makeig (PI). We thank Scott Makeig, John Iversen, and members of the Sensorimotor Neuroscience Laboratory at UC Merced and the Swartz Center for Computational Neuroscience at UC San Diego for their thoughtful advice and guidance.

Chapter 3

3 Modality-specific frequency band activity during neural entrainment to auditory and visual rhythms

Chapter 3 is a published experiment looking at the role of beta band activity in auditory and visual rhythm perception. The previous chapter looked at the timing mechanisms involved in a SMS task, but this chapter shifts focus to investigate modality differences in rhythm perception without interference of a motor task. The benefit of this approach is that it eliminates the possibility that the act of engaging the motor system in SMS to a rhythm may effectively off-load some of the temporal processing to the motor system. It is not a coincidence that musicians often tap their feet during performances to keep time; research has shown that moving to a rhythm increases the precision with which that rhythm is perceived (Manning & Schutz, 2013; Su & Pöppel, 2012). The results of this experiment provide further evidence of visual specific rhythmic timing mechanisms.

Published as:
Comstock, D. C., Ross, J. M., & Balasubramaniam, R. (2021). Modality-specific frequency band activity during neural entrainment to auditory and visual rhythms. *European Journal of Neuroscience, (in press)*

Abstract

Rhythm perception depends on the ability to predict the onset of rhythmic events. Previous studies indicate beta band modulation is involved in predicting the onset of auditory rhythmic events (Fujioka et al., 2009, 2012; Snyder & Large, 2005). We sought to determine if similar processes are recruited for prediction of visual rhythms by investigating whether beta band activity plays a role in a modality-dependent manner for rhythm perception. We looked at electroencephalography time–frequency neural correlates of prediction using an omission paradigm with auditory and visual rhythms. By using omissions, we can separate out predictive timing activity from stimulus-driven activity. We hypothesized that there would be modality-independent markers of rhythm prediction in induced beta band oscillatory activity, and our results support this hypothesis. We find induced and evoked predictive timing in both auditory and visual modalities. Additionally, we performed an exploratory-independent components-based spatial clustering analysis, and describe all resulting clusters. This analysis reveals that there may be overlapping networks of predictive beta activity based on common activation in the parietal and right frontal regions, auditory-specific predictive beta in bilateral sensorimotor regions, and visually specific predictive beta in midline central, and bilateral temporal/parietal regions. This analysis also shows evoked predictive beta activity in the left sensorimotor region specific to auditory rhythms and implicates modality-dependent networks for auditory and visual rhythm perception.

3.1 Introduction

Perceiving a rhythm requires making predictions about the temporal onset of rhythmic events. This ability allows us to dance in time with music, play music with others, detect a musical beat, and notice when timing is off the beat. Common measures of rhythm perception are sensorimotor synchronization (SMS) tasks that involve synchronizing one's movements to rhythmic stimuli. Although most humans have little trouble synchronizing to auditory rhythms accurately, synchronizing to visual rhythms can be more variable. SMS to auditory rhythms are more reliable and adaptive (Chen et al., 2002; Lorås et al., 2012; Repp, 2003; Repp & Penel, 2004), compared with visual flashing rhythms (Comstock & Balasubramaniam, 2018; Repp & Su, 2013). However, when synchronizing movements with rhythmically moving visual stimuli such as a bouncing ball, synchronization accuracy improves, yet not to the level of auditory synchronization (Gan et al., 2015; Hove, Iversen, et al., 2013; Hove et al., 2010; Iversen et al., 2015). The reasons for the disparity in SMS accuracy across auditory and visual modalities are as of yet unclear, and a closer investigation of these mechanisms is required for a complete understanding of neural timing and synchronization processes. The present study aims to explore neurophysiological mechanisms of auditory and visual entrainment, particularly with regard to prediction of rhythmic events.

Previous functional magnetic resonance imaging (fMRI) research has shown there is overlap in the structures involved between visual and auditory rhythm perception, particularly within the premotor cortex, putamen, and cerebellum (Araneda et al., 2017; Hove, Fairhurst, et al., 2013). Although these areas appear to play a supramodal role in rhythm perception, putamen activation is stronger for auditory rhythms than for visual rhythms, suggesting the auditory system may be more tightly connected to timing networks (Araneda et al., 2017; Hove, Fairhurst, et al., 2013). There is also evidence from fMRI research suggesting the visual system has its own in-house rhythm timing mechanisms with sources in the parietal lobes (Jäncke et al., 2000; Jantzen et al., 2005), and in MT/V5 (Jantzen et al., 2005). The visual cortex has also been implicated in visual rhythm timing through ERP work (Comstock & Balasubramaniam, 2018) and through psychophysics work (Zhou et al., 2014). Taken together, we interpret this literature as support for modality-dependent rhythmic processing mechanisms, although to our knowledge this has not yet been clearly shown with a targeted electroencephalography (EEG) study.

Beyond modality-dependent rhythm processing, it has been suggested that neural timing mechanisms are task specific (Comstock et al., 2018; Wiener & Kanai, 2016). Evidence suggesting distinct aspects of rhythm timing and duration perception has been seen in the cerebellum through lesion work (Grube et al., 2010), and work using transcranial magnetic stimulation (TMS) (Grube et al., 2010), additional evidence is seen through TMS work involving the posterior parietal lobes (Ross et al., 2018) suggesting a specific role for duration timing in the cerebellum, whereas the posterior parietal cortex is involved in rhythm timing. Much of the evidence supporting predictive processing for rhythm comes through measures of neural oscillation within different frequency bands. This oscillatory modulation is believed to indicate communication between different regions of the brain, with lower frequency oscillations involved more in communication between regions that are farther away from each other, and higher frequencies involved

more in localized communication (Sarnthein et al., 1998; Von Stein & Sarnthein, 2000). Furthermore, Bastos et al. (2015) have shown in non-human primates using electrocorticography (ECoG) that activity in the gamma and theta bands are involved in feedforward, or bottom-up visual processing, whereas the beta band is involved in feedback, or top-down visual processing. Michalareas et al. (2016) have shown similar results in human visual cortical areas with gamma involved in bottom-up processing and alpha and beta involved in top-down processing by correlating human magnetoencephalography (MEG) data with corresponding macaque neural anatomy. Interestingly, Michalareas et al. (2016) also found that alpha and beta top-down processing affects the ventral and dorsal visual stream areas differently, by shifting dorsal stream activity higher in the functional hierarchy of visual processing, whereas ventral stream downward. If frequency band activity relates to specific top-down or bottom-up processing networks, then by measuring frequency band activity during different rhythm timing tasks we can find markers of the networks involved, supporting different networks for different tasks. Neural oscillations within different frequency bands are therefore a rich source of information for investigating timing networks.

Neural mechanisms of auditory rhythm perception have been suggested to rely on strong interactions between motor systems and auditory cortices (Iversen & Balasubramaniam, 2016; Janata et al., 2012; Repp & Su, 2013; Ross, Iversen, et al., 2016; Ross, Warlaumont, et al., 2016), possibly mediated through projections in parietal cortex (Patel & Iversen, 2014; Ross et al., 2018). Communication across these networks could be carried out through frequency band-specific oscillatory activity. Activity in the beta band (14–30 Hz) is of primary interest as it has been shown to play a role in prediction and timing for auditory rhythms using EEG (Snyder & Large, 2005) and MEG (Fujioka et al., 2009, 2012, 2015), as well as being implicated in the onset of movements (Kilavik et al., 2013).

Snyder and Large (2005) found differentiation between induced and evoked activity in EEG high beta and low gamma bands (20–60 Hz), where induced activity was defined as not phase locked to a stimulus onset and evoked activity was defined as phase locked to the stimulus onset. By presenting subjects with a sequence of tones with occasional tones omitted, Snyder and Large found induced activity was similar in tone trials and omitted tone trials, indicating expectation for the tones in the sequence, whereas evoked activity was greatly reduced when there was no tone. Fujioka et al. (2009) used a similar omission paradigm with MEG and found induced beta from auditory cortices decreased after tone onset and increased in anticipation of the expected tone onset. A later MEG study showed the rate of beta increase in anticipation of tone onset is dependent on the tempo of the stimulus, whereas beta decrease following tone onset is consistent across multiple tempi (Fujioka et al., 2012). Fujioka et al. (2012) additionally found cortico-cortical coherence that followed the tempo of the rhythms between auditory cortices and sensorimotor cortex, supplementary motor area (SMA), inferior-frontal gyrus, and cerebellum.

The role of beta activity in visual rhythm perception is less studied. However, beta band amplitude modulation arising from the motor cortex has also been implicated in visually mediated temporal cues indicating expectation in a study using an implanted multielectrode array in the primary motor cortex (Saleh et al., 2010). More recently,

Varlet et al. (2020), showed cortico-muscular coupling of beta-band activity induced by audio-visual rhythms between EEG recorded over motor areas and EMG recorded from finger muscles pressing down on a force sensor. Significantly, the coupling appeared to be modulated by the tempo of the rhythm and peaked roughly 100 ms prior to each tone in the sequence. Interestingly, the study did not find significant cortico-muscular coupling in response to separate auditory or separate visual rhythms. Although Saleh et al. (2010) and Varlet et al. (2020) suggest involvement of beta band modulation in visual rhythm perception, the role of beta band activity in visual rhythm perception remains unclear.

To investigate predictive mechanisms of rhythm perception across modalities, we used EEG to record beta band modulation during auditory and visual rhythms. To separate out the stimulus response activity from activity related to temporal prediction of the stimulus we used an omission paradigm similar to that used by Snyder and Large (2005) and Fujioka et al. (2009). Given that previous studies have indicated involvement of sensory and motor-related beta in rhythm perception (Fujioka et al., 2012, 2015; Varlet et al., 2020) we describe all Beta band activity. Because EEG activity smears at the scalp it can be difficult to separate out concurrent sources of activity. We used independent component analysis (ICA) as a blind source separation method in an attempt to distinguish sensory and motor related activity.

Based on the assumption that beta oscillations play a general role in top-down processing, we hypothesized that we would find induced beta power modulation for both auditory and visual modalities following the same pattern seen in Fujioka et al. (2009). Specifically, we hypothesized we would find an induced increase in beta in anticipation of the onset of each rhythmic stimulus event, and also prior to the expected onset of an omitted event (omission onset), followed by a sharp decrease in beta power after event onset, but not after omission onset. Furthermore, we expected that evoked beta power would increase only in response to stimulus onset and not in anticipation of omission onset based on the findings of Snyder and Large (2005). Because the motor system has been implicated in both auditory and visual rhythm perception, and evidence of motor related beta for rhythm perception has been seen for auditory rhythms (Fujioka et al., 2012, 2015), and implicated in visual rhythms (Varlet et al., 2020), we expected to find motor related predictive beta activity for both auditory and visual modalities. To explore modality-specific characteristics of predictive beta without prior assumptions about visual and auditory mechanism or network contributions to predictive beta, we performed an exploratory ICA-based clustering technique using component spatial information (dipole locations and scalp topographies) to group similar sources that were shared across subjects. To avoid bias in cluster interpretation, we present and describe in detail all clusters.

3.2 Materials and Methods

3.2.1 Participants

A total of 18 subjects participated in the experiment (11 female, average age of 23.6 (20–34)) with one being rejected after data collection for poor signal to noise ratio. All participants were right-handed and had typical hearing and typical or corrected vision. The experimental protocol was carried out in accordance with the Declaration of

Helsinki. This study was approved by the UC Merced Institutional Review Board for research ethics and human subjects, and all participants gave informed consent prior to testing.

3.2.2 Task

After subjects gave written consent, they were seated and fitted with a 32 electrode EEG cap. Subjects were then tasked with watching isochronous flashing visual rhythms or listening to isochronous auditory rhythms. Both kinds of rhythms had an interonset interval (IOI) of 600 ms, and both had occasional omissions of single tones or single flashes. The rhythms were broken into stimulus trains with each train consisting of 100 tones or flashes with 7 omitted tones or flashes placed randomly within the train. The location of the omitted tones or flashes in the stimulus trains were constrained such that there must be at least 8 tones or flashes between each omission. There were 20 stimulus trains per condition for a total of 140 omissions in each condition. Subjects completed all of the stimulus trains in one modality, followed by all of the stimulus trains in the other modality, in design counterbalanced across subjects. Before the omission conditions, subjects were presented with a condition with no omissions consisting of 140 tones or flashes. The non-omission stimulus trains were of the same modality as the omission stimulus trains that would follow. This design resulted in 140 trials for each of the four conditions (tone non-omission, tone omission, flash non-omission, flash omission; Figure 3.1).

To ensure that subjects were attending to the rhythms, after each train a shorter sequence of 5 tones or flashes was presented at a slightly slower or faster tempo than the experimental train, and subjects were asked to determine if the shorter rhythm was slower or faster than the preceding rhythm. The number of correct responses and response times were recorded and used to determine if subjects were adequately attending to the stimulus trains.

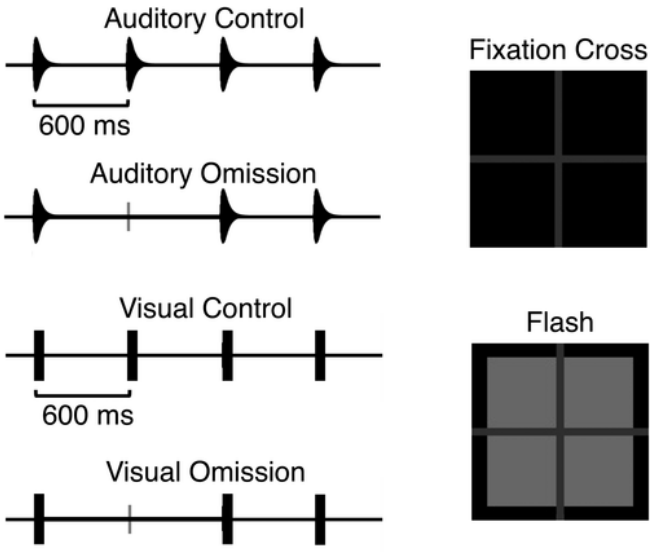

Fig. 3.1. Schematic of control and omission conditions for both auditory and visual metronomes, and depiction of the visual flash metronome stimuli. The fixation cross was

always visible for both auditory and visual conditions, even when the flash appeared in the visual condition

The auditory metronome consisted of 1,000 Hz tones lasting 50 ms with a 10 ms rise and 40 ms fall time, generated using Audacity digital audio software. The visual metronome consisted of light gray square flashes 3 × 3 cm lasting 50 ms each. In both cases, there was a black screen with a dark gray fixation cross in the center of the screen where the lines were approximately 3 mm wide and 4 cm long. The visual flashes always appeared behind the fixation cross so that the cross never disappeared when the flash appeared behind it.

The stimuli were presented using Paradigm experimental stimulus presentation software (Perception Research Systems, 2007) on a 60 Hz monitor, which was approximately 65 cm from the subject's head. Subjects responded to any prompts using a keyboard placed on a desk in front of the chair they were seated in.

3.2.3 EEG data acquisition and processing

Electroencephalography was continuously recorded using an ANT-Neuro 32 channel amplifier with the ANT-Neuro 32 electrode Waveguard cap. The electrodes were situated according to the 10–20 International system and EEG was recorded with a sampling rate of 1,024 Hz. The data were then processed using the EEGLAB v14.1.1 toolbox (Delorme & Makeig, 2004) within MATLAB 2019. Channel locations were added using the standard location montage for the Wavegaurd cap. EEG data were first pruned by hand to remove sections between stimulus train blocks. This was done to remove any break periods between trains. Following pruning, the data were down-sampled to 256 Hz and then a high-pass filter with a 2 Hz passband edge and 6 dB cutoff at 1 Hz was applied. A low-pass filter with a 50 Hz passband edge and 6 dB cutoff at 56.25 Hz was applied to remove 60 Hz line noise. Bad channels were rejected that had activity with lower than 0.8 correlation with their surrounding channels with the maximum channels rejected for any one subject being 5 (M = 2.71, MAD = 1.31). Rejected channels were then interpolated using spherical interpolation. We then removed single-channel artifacts using artifact source reconstruction (ASR), which has been shown to effectively remove large-amplitude or transient artifacts in the data (Chang et al., 2018; Mullen et al., 2015). ASR was performed using a conservative burst criterion parameter of 50 SDs. After ASR was run, we then re-referenced the data to average. To separate out non-brain artifacts and for the source-level analysis, we ran ICA using the AMICA ICA algorithm (Palmer et al., 2012). Dipole source localization was performed on the resulting components using the MNI head model, and two dipoles were fit where appropriate instead of one using the FitTwoDipoles plug in (Piazza et al., 2016). ICA components were checked to find eye blink and cardiac components, which were marked for later rejection. The remaining independent components were used for source analysis.

We then segmented the continuous data into four long epochs for the experimental conditions: Non-omission visual flashes, non-omission auditory tones, visual omissions, and auditory omissions. The non-omission conditions came from the non-omission stimulus train block that preceded the omission block. Each condition was epoched from −1.67 s prior to each tone/flash to 1.67 s following the tone/flash. Epoch

length was determined by calculating the window size needed for the later time/frequency calculations, so the resulting time/frequency data would span ±1.5 s from the tone or flash onset of interest. The omission groups were epoched in the same way in relation to omission events. Following epoching, epochs were checked for blinks that occurred during either event onset (for the non-omission conditions) or expected onset (for the omission conditions) as defined as a 50 μV or larger spike in frontal electrodes within ±100 ms of onset or expected onset. After epochs with eye blinks at event onset, or expected onset, were rejected, eye blink components determined by AMICA marked earlier were then rejected. Remaining epochs with amplitude spikes greater than ±500 μV were then rejected. Finally, epochs that were deemed improbable were rejected by computing the probability distribution of values across the epochs for individual channels and across all channels. Any epoch that contains data values >6 SDs for the channel or 2 SDs for all electrodes was rejected. One subject was rejected due to having more than 50% of their total epochs being rejected. For the remaining 17 subjects there were 140 possible epochs per condition per subject for the four conditions: visual non-omission (M = 123.24, max = 136, min = 96, MAD = 13.27), visual omission (M = 116.59, max = 132, min = 74, MAD = 18.19), auditory non-omission (M = 118.29, max = 136, min = 92, MAD = 14.24), auditory omission (M = 109.06, max = 129, min = 66, MAD = 20.12).

3.2.4 Clustering procedure

Electroencephalography activity measured at the electrode level is smeared across the scalp making it difficult to separate out signals from different sources. Because we are interested in time-sensitive neural activity from both sensory and motor areas that occur simultaneously, we focus our analysis on the source-level activity of components. To compare independent components across subjects, we performed a cluster analysis using k-means clustering based on the component dipole locations and component scalp topographies using EEGLAB's clustering tools (Delorme & Makeig, 2004). Using both dipole locations and scalp topographies allows for clusters that are more consistent across subjects than can be computed using a single measure (Onton et al., 2006). This clustering approach avoids statistical double dipping by excluding the measures of interest (event-related spectral perturbation [ERSP] and intertrial coherence [ITC]), and focusing only on the spatial features of the components. Dipole location and scalp topography were weighted equally, and PCA was applied to the component scalp topography data reducing the number of dimensions to 3, matching the number of dimensions in the dipole locations and therefore reducing the overall number of dimensions to cluster. To ensure non-brain sources, including muscle activity and channel noise, were excluded from clustering, only components with dipoles located within the head and with a residual variance of less than 15% were used resulting in a total of 289 total brain components across 17 subjects. The group of all 289 components prior to clustering constitute the parent cluster, which we used to look at global-level activity. To determine the appropriate number of clusters, we applied three measures for cluster number optimization (Calinski-Harabasz, Silhouette, and Davies-Bouldin) for between 5 and 30 clusters. The Calinski-Harabasz and Silhouette methods indicated the optimal number of clusters was 9, whereas the Davies–Bouldin method indicated an

optimum number of 13. We used nine clusters to maximize the number of unique subjects per cluster, plus one outlier cluster with components with positions of more than 3 SDs from any of the cluster centers. The resulting nine clusters (Figure 3.2; Table 3.1) averaged 31.88 components per cluster with a standard deviation of 7.17, which were made up from 15.78 subjects on average, standard deviation 0.97. The outlier cluster consisted of three components from two subjects. No cluster had more than five components from any one subject. Table 3.1 shows the individual makeup of each cluster.

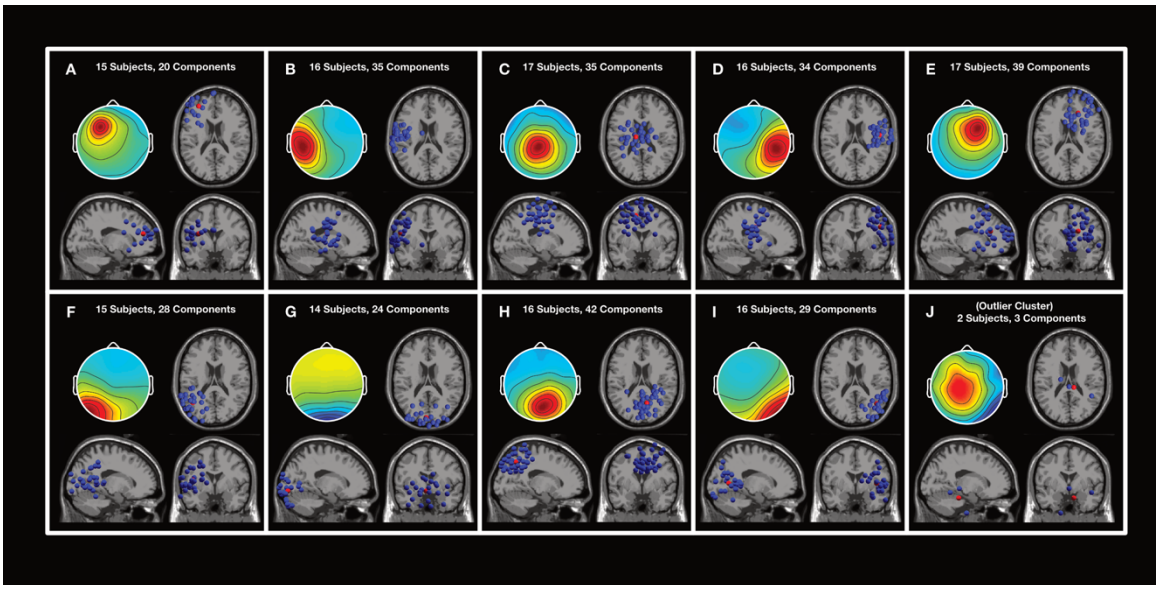

Fig 3.2. Scalp topography and dipole locations of components for the nine clusters and the outlier cluster. Scalp topography includes activity from all four conditions. Blue dots indicate individual component dipole locations. Red dots indicate the average position

Table 3.1

Cluster Information

Cluster	Subjects	Components	Components per Subject	Mean R.V. %	Mean Tal Coordinates	Corresponding Brodmann Area of Mean Coordinates
1 - Left Frontal	15	20	Avg = 1.33 Max = 3	5.88%	X: -31 Y: 45 Z: 14	Left Area 10
2 - Left Sensorimotor	16	36	Avg = 2.19 Max = 4	5.86%	X: -53 Y: -12 Z: 19	Left BA 1 / 4 (Primary Sensory / Primary Motor)
3 - Midline Central	17	35	Avg = 2.06 Max = 3	6.54%	X: -12 Y: -12 Z: 51	Left BA 6
4 - Right Sensorimotor	16	34	Avg = 2.13 Max = 4	5.21%	X: 49 Y: -9 Z: 30	Right BA 4 (Primary Motor)
5 - Right Frontal	17	39	Avg = 2.29 Max = 4	7.07%	X: 18 Y: 32 Z: 20	Right BA 8 / 9
6 - Left Temporal / Parietal	15	28	Avg = 1.87 Max = 4	4.49%	X: -42 Y: -58 Z: 13	Left BA 39 (Angular Gyrus)
7 - Occipital	14	24	Avg = 1.71 Max = 3	4.52%	X: -4 Y: -87 Z: -5	Left BA 18 (Visual Assoc)
8 - Parietal	16	42	Avg = 2.63 Max = 5	4.42%	X: 10 Y: -58 Z: 45	Right BA 7
9 - Right Temporal / Parietal	16	29	Avg = 1.81 Max = 3	3.42%	X: 41 Y: -61 Z: 7	Right BA 19 / 37 (Peristriate Area / Fusiform Gyrus
10 - (Outlier)	2	3	Avg = 1.5 Max = 2	7.03%	X: 10 Y: -31 Z: -19	Null

Table 3.1. Information containing the component make-up of the nine clusters and outlier cluster. Although the corresponding Brodmann area for each cluster is determined based on the average Talaiarch coordinates of the component dipoles, the dipole locations for the individual components for each cluster are not all contained within the indicated Brodmann area. Individual dipoles for each component are shown in Figure 3.2. Components per subject column indicates both the average number of components per subject in the cluster, and the maximum components any single subject had in the cluster

3.2.5 Time–frequency analysis

Time–frequency analysis was completed for each subject at each channel and for each component used in the clustering analysis. The resulting time–frequency representations were then averaged across subjects for the individual channels in each condition and averaged across the components for each cluster for each condition.

Induced and evoked time–frequency representations were calculated to determine the different roles they play during the rhythm perception task as they have been found to play different roles in auditory rhythm perception (Snyder & Large, 2005). Induced activity was calculated for each trial by first removing the mean of activity (ERP) from each trial so only non-phase locked activity remains, and then averaging the resulting time–frequency computations across trials. Evoked activity was calculated on the mean of the activity (ERP) to focus on the phase locked activity. All three time–frequency calculations were performed using the same parameters. The time–frequency calculations were computed with the newtimef function in EEGLAB (Delorme & Makeig, 2004) using 85 linear spaced Morlet wavelets between 8 and 50 Hz with a fixed window size of 300 ms resulting in 2.4 cycles at 8 Hz and scaling up to 15 cycles at 50 Hz. The 300 ms window size was chosen to ensure the time–frequency representation from each individual stimulus was not contaminated by either surrounding stimuli, which were 600 ms apart. The convolution used the minimum step size for the sample rate of 256 Hz resulting in 772 evenly spaced steps with a step length of 3.9 ms. Baselines were computed separately for each condition using a relative to the mean baseline with a period of −1,200 to −600 ms from the stimulus or omitted stimulus onset, dependent on condition. This baseline period consisted of one complete 600 ms stimulus cycle for both the omission and control conditions, allowing us to focus on the oscillatory dynamics between stimulus events. Separate baselines for each condition were used to minimize effects of individual variation and of differences that might arise between omission and non-omission conditions due to habituation to stimuli in the unvarying and longer blocks in the non-omission conditions. Although a common baseline would allow us to determine overall power differences between conditions in the frequency bands, our focus is on the changes in power that occur within condition within the timeframe of each stimulus train as described later in the slope analyses description. These computations were used to determine the ERSP values in terms of dB, such that the ERSP plots show shift in power from baseline at each time point.

To ensure changes in evoked activity were due to stimulus-driven phase shifts, we additionally calculated phase coherence across trials using the ITC measure in the newtimef function of EEGLAB (Delorme & Makeig, 2004). ITC is calculated by extracting the phase angle at each time–frequency point for each trial and comparing the phase angles across trials for coherence providing a coherence measure between 1 and 0, where 1 indicates complete coherence across trials for a given time–frequency point, and 0 indicates no coherence across trials. The ITC calculation required an additional time–frequency computation of the data using the same parameters as was done for induced activity except there was no subtraction of the ERP.

Beta activity was extracted from the ERSP values by averaging the power at each step between 14 and 30 Hz. Beta ITC was extracted using the same procedure except applied to ITC values instead of ERSP values.

3.3 Analysis

3.3.1 Attention behavioral task

To assess if attention was maintained evenly between the two modalities, we analyzed the behavioral data from the attention task for the two omission conditions.

Both auditory (94.72%) and visual (88.61%) conditions showed a correct response rate well above chance. To assess the differences between the auditory and visual conditions, the number of correct responses and response times were assessed using paired t tests. There was a significant difference in number of correct attention trials between the auditory (M = 18.94, SD = 1.09) and visual (M = 17.65, SD = 1.69) conditions; $t(16) = -2.72$, $p = 0.015$ which we ascribe to the visual rhythm task being more difficult than the auditory rhythm task. There was no significant difference in response time measured in ms between auditory (M = 1,405.04, SD = 572.09) and visual (M = 1,495.99, SD = 585.94) conditions; $t(16) = 0.66$, $p = 0.52$.

3.3.2 Event-related spectral perturbations

To determine if ERSP power was being significantly modulated by the stimuli and omissions, permutation statistics comparing ERSP power values to baseline values using unpaired t tests with 2,000 permutations testing for significance were performed. False discovery rate (FDR) correction was used to correct for multiple comparisons with alpha values being the computed p-value for each time–frequency point using a parametric FDR algorithm (Benjamini & Hochberg, 1995).

3.3.3 Beta band slope analysis

Although significance testing in ERSP power can indicate significant power modulations in response to stimuli, we are interested in the dynamics of beta band activity following findings that indicate beta power rises to peak at the expected onset of an auditory tone followed by a trough after a tone, where the rate of the rise beta power, yet not the fall, is dependent on the tempo of the stimuli (Fujioka et al., 2012). Since we hypothesized that rise in beta activity is related to the timing of the rhythmic stimuli, we would see beta power rise prior to the expected onset of the omitted stimuli at the same rate as beta would rise prior to the non-omitted stimuli. Furthermore, by investigating the slope of activity prior to the omission onset, we have a measure that is less likely to be affected by activity due to a response to the omission. To test this hypothesis, two slopes were fitted in the averaged beta activity for each subject for each condition based on a least squares measure in a procedure similar to that performed by Meijer et al. (2016). The first slope started at –300 ms prior to stimulus or omission onset and ended at stimulus or omission onset (0 ms). Using –300 ms as the starting point was chosen as the halfway point between stimuli. Because there is considerable variation across subjects in slope activity, a second slope was fitted starting at the lowest measured activity between –300 and –100 ms and ending at stimulus or omission onset. Although comparing the slopes of the omission and non-omission condition could tell us if the two slopes are significantly different, our goal is to show that the two slopes are not significantly different and in fact are very similar. One way to show this is to compare against a third condition. To provide the third condition for comparison, we shuffled the ERSP data used to find slopes in the control condition for each subject at each channel, and for each component for each cluster, and then extracted beta band power and fitted slopes. Fitting a slope to the beta band extracted from the shuffled ERSP power results in an effective slope of 0, which we use to compare the other slopes to. For the shuffled condition, ERSP power values along the entire time axis of each epoch of each frequency step were

randomly shuffled 1,000 times using the randperm function in Matlab. Beta band power for each time point was then extracted from resulting shuffled ERSPs, the same as done with the non-shuffled ERSPs. Slopes were then fitted in the same way as with the non-shuffled data, except that instead of finding the minimum beta power between –300 and –100 ms for the shuffled condition, we used the same starting point used in the non-shuffled control condition for the corresponding subject or component. Figure 3.3 depicts slope fitting to beta band from the trough to 0 ms.

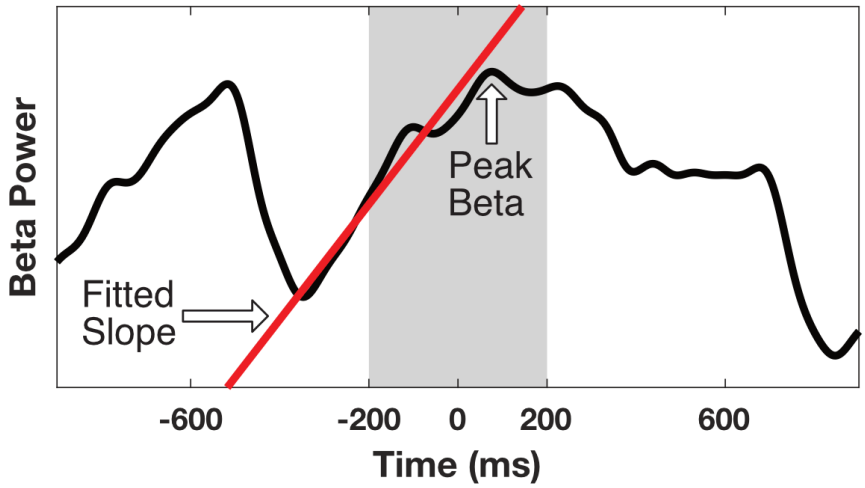

Fig 3.3. Schematic for slope fitting and peak finding for beta activity. Slopes were fitted between the trough (between –300 and –100 ms) and 0. Peak beta was determined between –200 and 200 ms (range depicted in shaded area). Slopes were fitted for evoked and induced beta power, whereas peaks were found in evoked and induced beta power as well as in intertrial coherence in the beta range

Four sets of t tests were used to determine if the fitted slope of beta activity prior to the onset of a tone or flash was equivalent to the fitted slope of beta activity prior to the expected but omitted onset of a tone or flash for both induced and evoked activity and for both the slopes fitted from –300 ms to onset and for the slopes fitted to the trough between –300 and –100 ms and onset. FDR correction was used to correct for multiple comparisons for all t tests using the method described in Benjamini and Hochberg (1995) with alpha set to 0.05. The first three analyses were performed using paired t tests comparing: the slopes of the omission conditions to the slopes of the non-omission conditions, the slopes of the non-omission conditions to the slopes of the shuffled conditions, and the slopes of the omission conditions to the slopes of the shuffled conditions. If beta power is being modulated such that it shows anticipation of the stimulus we would expect both the omission and control fitted slopes to indicate beta power is rising prior to stimulus onset, and therefore be significantly different from the shuffled fitted slopes, which are effectively flat. Additionally, we would expect the omission and non-omission fitted slopes to not be significantly different from each other

as they both rise in anticipation of the incoming event regardless if that event is omitted or not.

Showing that a fitted slope in the omission condition is not significantly different than a fitted slope in the non-omission condition, and that both omission and non-omission-fitted slopes are significantly different than the shuffled slopes is not sufficient to claim that the slopes in the omission and non-omission conditions are equivalent. This is because a comparison between significant results and non-significant results is not necessarily significant (Gelman and Stern, 2006), and therefore, an additional test is required. To assess the viability of the comparison between the two results, we applied a post hoc comparison test as used in Abbott and Shahin (2018). The test calculated if the slope of the non-omission condition + the slope of the shuffled condition – 2 × the slope of the omission condition was significantly different from zero using a t test with the same FDR correction as used for the other t tests at each channel and each cluster. With these four tests, we show the beta slope is showing anticipation of the next event and that the slope of the omission condition is equivalent to the slope of the non-omission condition if: (a) the omission and non-omission slopes are not significantly different, (b) both the omission and non-omission slopes are significantly different from the shuffled (flat) slope, (c) the post hoc comparison test of the three slopes is significant showing omission and non-omission slopes are equivalent.

3.3.4 Evoked and induced comparison

To further understand the different roles evoked and induced beta play in the temporal aspects of auditory and visual rhythm processing, we applied an additional exploratory analysis that measured peak power and peak time in response to both present and omitted tones and flashes similar to performed by Snyder and Large (2005). To make the comparison, ERSP power P was converted from dB to μV2 and normalized using the formula: Pnorm = (P – Pmin)/(Pmax – Pmin). This normalization conversion resulted in values between 0 and 1 and was applied to ERSP values for both evoked and induced activity for each individual component for each cluster, after which beta power was extracted in the same manner as done for the slope analyses. Peak power and peak time were determined by finding the time and normalized power of the peak power between ±200 ms of the expected event onset. Paired t tests were then run on each cluster as well as the parent cluster to determine the roles evoked and induced activity within each cluster. All t tests used FDR correction to account for multiple comparisons (Benjamini & Hochberg, 1995).

3.3.5 Intertrial coherence

While measuring induced and evoked activity allow us to contrast our results to the work from Snyder and Large (2005), neither measure provides a direct measure of the changes in phase coherence in relationship to the omission and non-omission onsets. We use ITC to confirm that the evoked activity we measure is due to phase coherence by comparing peak times of beta ITC with peak times of beta induced and evoked activity. The same procedure was used to extract beta coherence and find peaks as was used to find the peaks in induced and evoked beta activity. Paired t tests comparing ITC beta peak times with induced and evoked peak times were then run on each cluster including

the parent cluster. All t tests used FDR correction to account for multiple comparisons (Benjamini & Hochberg, 1995).

3.3.6 Baseline comparison

To assess potential differences in habituation to the stimuli, an analysis was performed on the computed baseline levels across non-omission and omission conditions within each modality. Although differences in baselines would not provide direct evidence to invalidate results from the slope, beta peak time, or ITC analyses, differences in baselines between conditions could account for reported differences in beta peak power between omission and non-omission conditions. Separate paired t tests comparing the baseline spectrum in the beta band were computed for each cluster for both induced and evoked activity. All t tests used FDR correction to account for multiple comparisons (Benjamini & Hochberg, 1995). Baseline power for the comparisons was taken directly from the time–frequency calculations used in the previous analyses and averaged across the beta band (14–30 Hz) to match the other beta band analyses we report.

3.4 Results

3.4.1 Channel-level beta slope analysis

Figure 3.4 depicts the results of these tests at the electrode level show that only channel P8 meets the criteria for the four tests for visual beta: $p > 0.05$ for the omission to non-omission slopes comparison, $p < 0.05$ for the comparisons of the non-omission to shuffled and omission to shuffled slopes, and $p < 0.05$ for the post hoc comparison test as applied to the slopes fitted to the between the trough of beta power and onset for induced beta. Additional channels met the first three criteria but did not reach significance in the post hoc test for the induced trough-fitted slope for both visual and auditory conditions. No channels met these criteria for the slopes fitted at the fixed values between –300 ms and onset for the visual condition for induced or evoked beta. No auditory channels met the four criteria for any of the conditions.

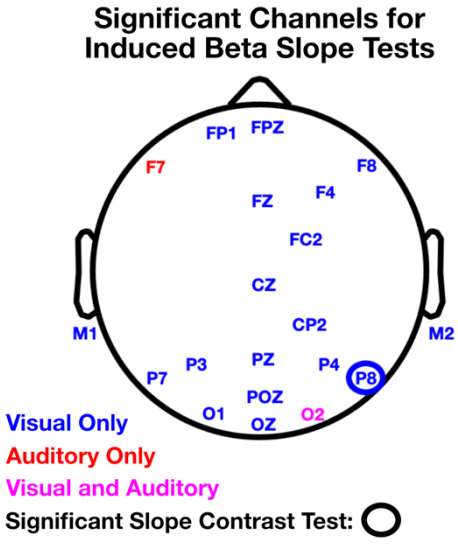

Fig 3.4. Significant channels for the induced beta tests to slopes fitted from the trough of beta power between −300 and −100 ms to the event onset at 0 ms. Channels labeled had $p > 0.05$ for the omission to control slopes comparison, and $p < 0.05$ for the comparisons of the control to shuffled and omission to shuffled slopes. The circled channel indicates $p < 0.05$ for the post hoc comparison test as applied to the slopes fitted to the between the trough of beta power and onset for induced beta

3.4.2 Cluster-level analyses

To better separate sensory and timing related activity and to investigate the sources of timing-related activity, we performed the remaining analyses at the cluster level. Due to the large number of tests results from our analyses at the cluster level, we focus on four clusters of interest: the parietal and occipital clusters for the visual condition, and the left and right sensorimotor clusters for the auditory condition. In the visual condition, we focus on the parietal cluster as it shows the strongest visual predictive beta results while producing a beta time course very similar to two of the other posterior clusters: the left and right temporal/parietal clusters. We focus on the occipital cluster for the visual condition as its activity is mostly likely to arise from the visual cortex, yet its markers of predictive activity are not as pronounced as with the other posterior clusters. The left and right sensorimotor clusters are of interest as they are the only clusters that show predictive beta activity exclusively in the auditory modality, and additionally suggest hemispheric differences in auditory rhythm processing. In addition to these clusters, we also present results from the parent cluster for both sensory modalities to provide a global-level view of the beta activity. The test results from all clusters for both modalities, along with figures, are available in Supporting Information.

3.4.3 Event-related spectral perturbations

In the parent cluster containing all components, we find increased evoked power following both visual and auditory stimulus onset, but not in response to visual or auditory omission onsets (Figure 3.5). Induced activity from the visual condition in the parent cluster not only increases significantly and peaks roughly at stimulus onset but also increases at omission onset, particularly in the low beta range. This pattern is also seen in the posterior clusters for visual activity, especially in the parietal cluster (Figure 3.6a). In the occipital cluster, visual induced beta peaks much closer to the stimulus onset and prior to the omission onset (Figure 3.6b). Visual-evoked activity for the parietal and occipital clusters follows the same pattern seen in the parent cluster. ERSP power modulation is less pronounced in response to auditory rhythms compared with visual rhythms in the parent cluster with both induced (Figure 3.5c) and evoked (Figure 3.5d) measures. Modulation of induced activity appears stronger in response to auditory rhythms in the right sensorimotor cluster (Figure 3.6d) than the left sensorimotor cluster (Figure 3.6c). Evoked beta modulation in response to auditory rhythms is relatively weak but appears less affected by an auditory omitted event than seen with the visual clusters, especially in the left sensorimotor cluster (Figure 3.6c).

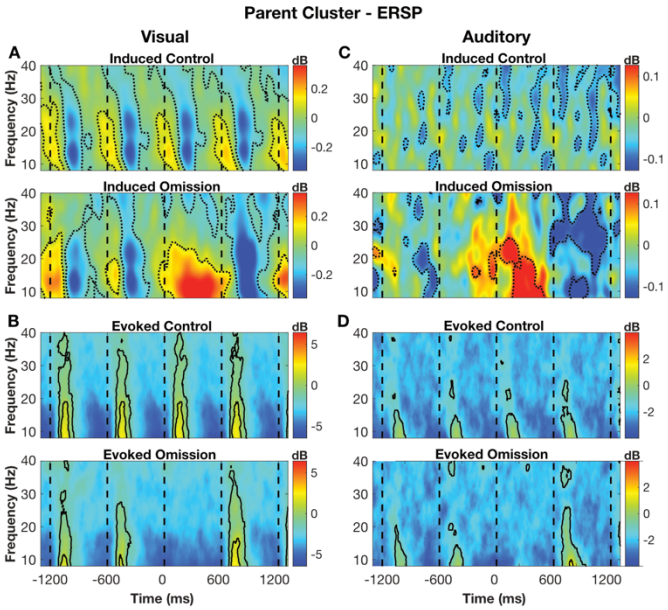

Fig 3.5. Time–frequency dynamics in the parent cluster for visual (a,b) and auditory (c,d) conditions. Data shown are grand averages across all components in the parent cluster, which is made up of all components prior to clustering to present global-level activity. Dotted lines in induced activity (a,c) indicate time–frequency values significantly different from baseline $p < 0.01$. Solid lines in evoked activity (b,d) indicate time–frequency values significantly different from baseline $p < 0.001$. ERSP, event-related spectral perturbation

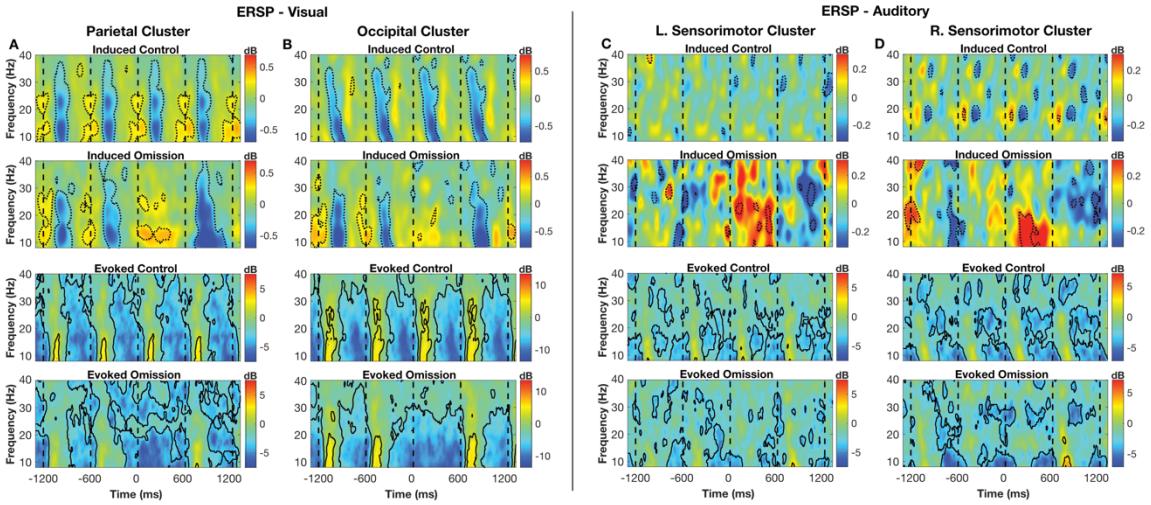

Fig. 3.6. Time–frequency dynamics in selected clusters for visual (a,b) and auditory (c,d) conditions. Data shown are grand averages across all components in the indicated cluster. Dotted lines in induced activity indicate time–frequency values significantly different from baseline $p < 0.01$. Solid lines in evoked activity indicate time–frequency values significantly different from baseline $p < 0.001$. Induced and evoked ERSP values in response to visual rhythms from the parietal (a) and occipital (b) clusters, and ERSP

values in response to auditory rhythms from the left sensorimotor (c) and right sensorimotor (d) clusters are depicted. ERSP, event-related spectral perturbation

3.4.4 Beta slope analysis

Slopes were fitted to the cluster-level beta activity with the four previously described tests applied. Figure 3.7 shows the time course of visual beta activity in the parietal (a) and occipital (b) clusters and auditory beta activity for the left (c) and right (d) sensorimotor clusters for both induced and evoked activity. At the cluster level in the visual modality two clusters plus the parent cluster met the criteria in induced activity for the slopes fitted to –300 to 0 ms: right temporal/parietal and parietal clusters. The left temporal/parietal cluster met the criteria for three of the slope tests but not for the contrast. No auditory clusters met the criteria for induced activity with a fixed slope. Slopes fitted to the trough (between –300 and –100 ms) and 0 ms for induced beta activity in the visual condition resulted in five clusters plus the parent cluster meeting the criteria for the four slope tests: midline central area, right frontal, left temporal/parietal, parietal region, and right temporal/parietal clusters. The occipital cluster met the first three slope criteria in the visual modality for the trough-fitted slope in induced activity. The parietal and the parent cluster met all four criteria for the auditory condition for trough-fitted slopes to induced beta. All other clusters except the midline central area cluster met the first three slope criteria for auditory-induced beta trough-fitted slopes.

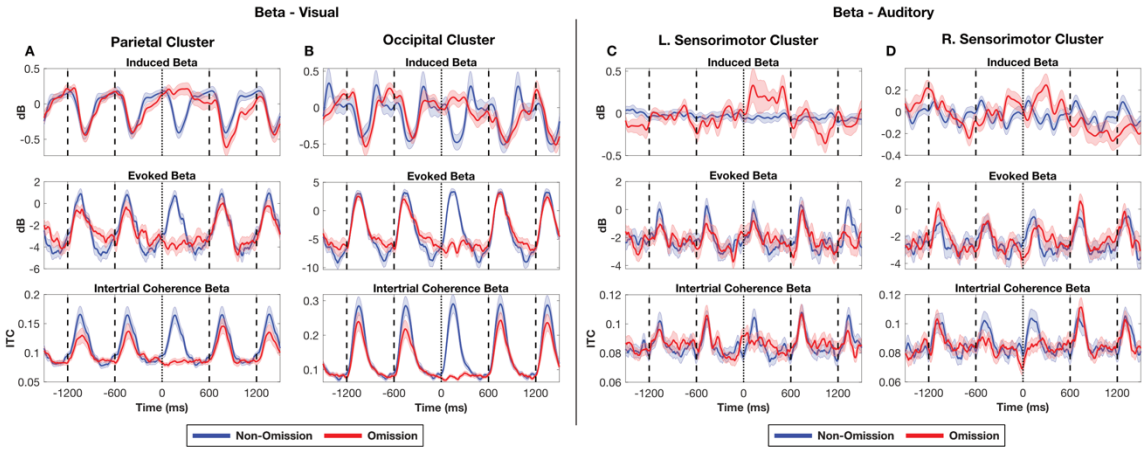

Fig. 3.7. Time course of induced and evoked beta activity, and intertrial coherence (ITC) in the beta band for selected clusters in response to visual (a,b) and auditory (c,d) rhythms. Standard error is indicated with shaded bars. Values in response to visual rhythms from the parietal (a) and occipital (b) clusters, and values in response to auditory rhythms from the left sensorimotor (c) and right sensorimotor (d) clusters are depicted. Note that evoked beta and ITC increase in anticipation of an event only in the left sensorimotor cluster (c).

Slopes fitted to evoked beta at the cluster level resulted in the parent cluster for both auditory and visual modalities, and the left sensorimotor cluster for the auditory

modality meeting all four slope criteria for the trough-fitted slopes. The midline central area cluster, right sensorimotor, and parietal cluster met the first three criteria for the trough-fitted slope tests in both modalities. the left temporal/parietal and left frontal cluster in the auditory and visual modalities, respectively, met the first three slope criteria for the trough-fitted slopes. No cluster met any of the necessary criteria in the slopes fitted between −300 and 0 ms to evoked beta activity. All slope measures and tests for the visual and auditory slopes can be found in the Tables S1 (visual) and S2 (auditory).

3.4.5 Induced and evoked beta peaks

Test values presented here are for the parent cluster containing all components unless otherwise indicated. For a full listing of all test values and statistics for each cluster, refer to Tables S3 (visual peak times), S4 (visual peak power), S5 (auditory peak times), and S6 (auditory peak power). Figure 3.8 shows the distribution of visual beta peak times and power for the parietal and occipital clusters. Figure 3.9 shows the distribution of auditory beta peak times and power for the left and right sensorimotor clusters. In the visual modality, evoked peak times for the control condition were generally after flash onset (M = 68.49 ms, SD = 122.18) and later than omission peak times (M = 11.04 ms, SD = 133.51); $t(288) = 5.43$, $p = <0.001$. Visual-induced peak times for the control condition tended to fall prior to onset (M = −12.95 ms, SD = 120.03), whereas omission peak times fell after expected onset (M = 28.74 ms, SD = 129.27); $t(288) = -4.47$, $p = <0.001$. Both tests were also significant for the midline central area and parietal cluster, with the left temporal/parietal cluster significant in induced activity and the right temporal/parietal cluster significant for evoked. The evoked control peak was significantly later than the induced control peak; $t(288) = 8.06$, $p = <0.001$. This difference was also reflected in the midline central area, right frontal, left temporal/parietal, occipital, parietal, and right temporal/parietal clusters. Evoked and induced omission peak times were not significantly different in the parent cluster ($t(288) = -1.67$, $p = 0.164$) or any other cluster. To determine if the differences in control and omission peak times across induced and evoked activity were relative for each kind of activity, a further test compared the difference in evoked control and omission peak times (M = 57.44 ms, SD = 178) to the difference in induced control and omission peak times (M = −41.68 ms, SD = 158.43), revealing the relative shifts were significantly different; $t(288) = 7.03$, $p = <0.001$. A significant relative difference was also seen in the midline central area, left temporal/parietal, occipital, and parietal clusters.

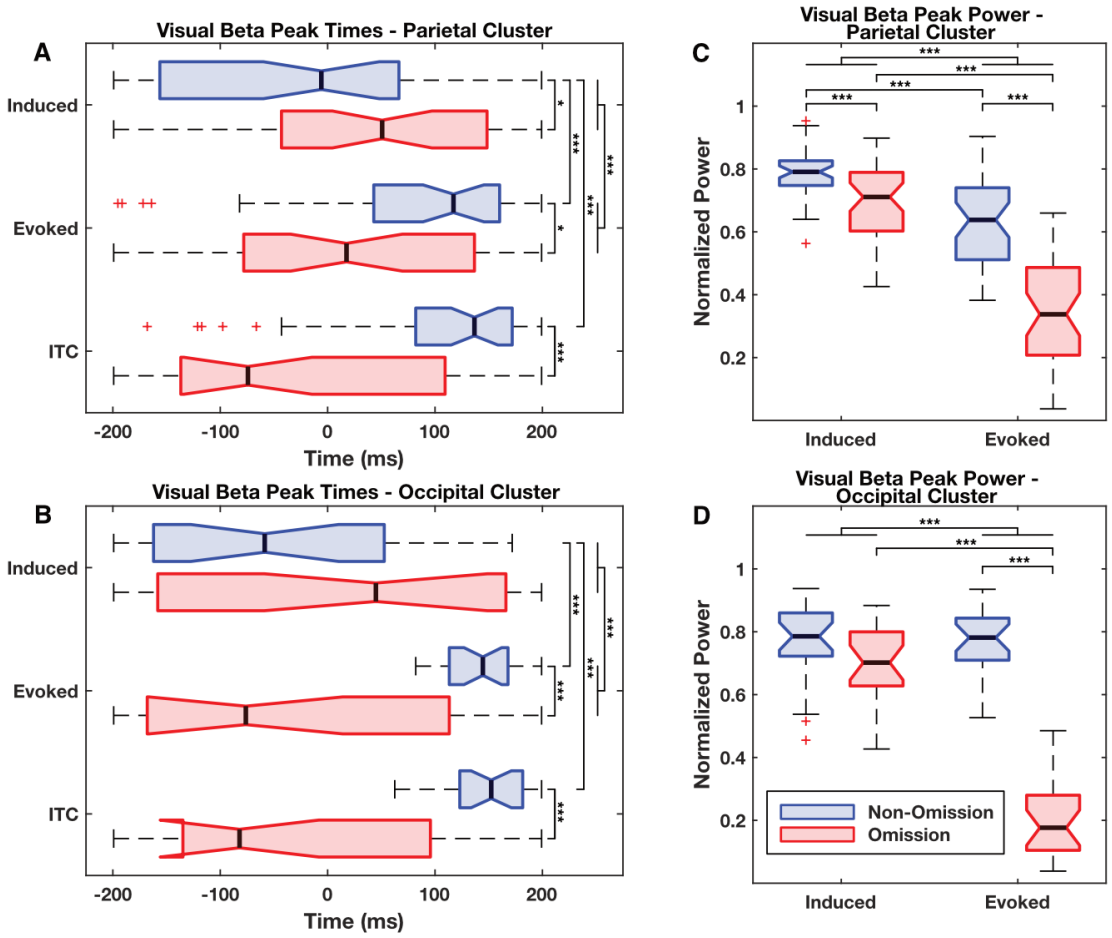

Fig. 3.8. Mean beta peak times (a,b) and normalized beta peak power (c,d) for components in the parietal (a,c) and occipital clusters (b,d) in the visual condition. Induced activity for both clusters tended to peak prior to non-omitted flash onset and after omitted flash onsets, whereas the opposite pattern is seen in evoked activity and in intertrial coherence (ITC) (a,b). Normalized induced and evoked beta power peaks were higher in non-omission trials compared with omission trials in the parietal cluster (c), whereas only evoked beta power peaks were higher in non-omission trials than omission trials in the occipital cluster (d). Box plots depict interquartile range with median values indicated by black bars and 95% confidence intervals indicated with notches. Significance differences are shown through bars where *$p < 0.05$, ***$p < 0.001$

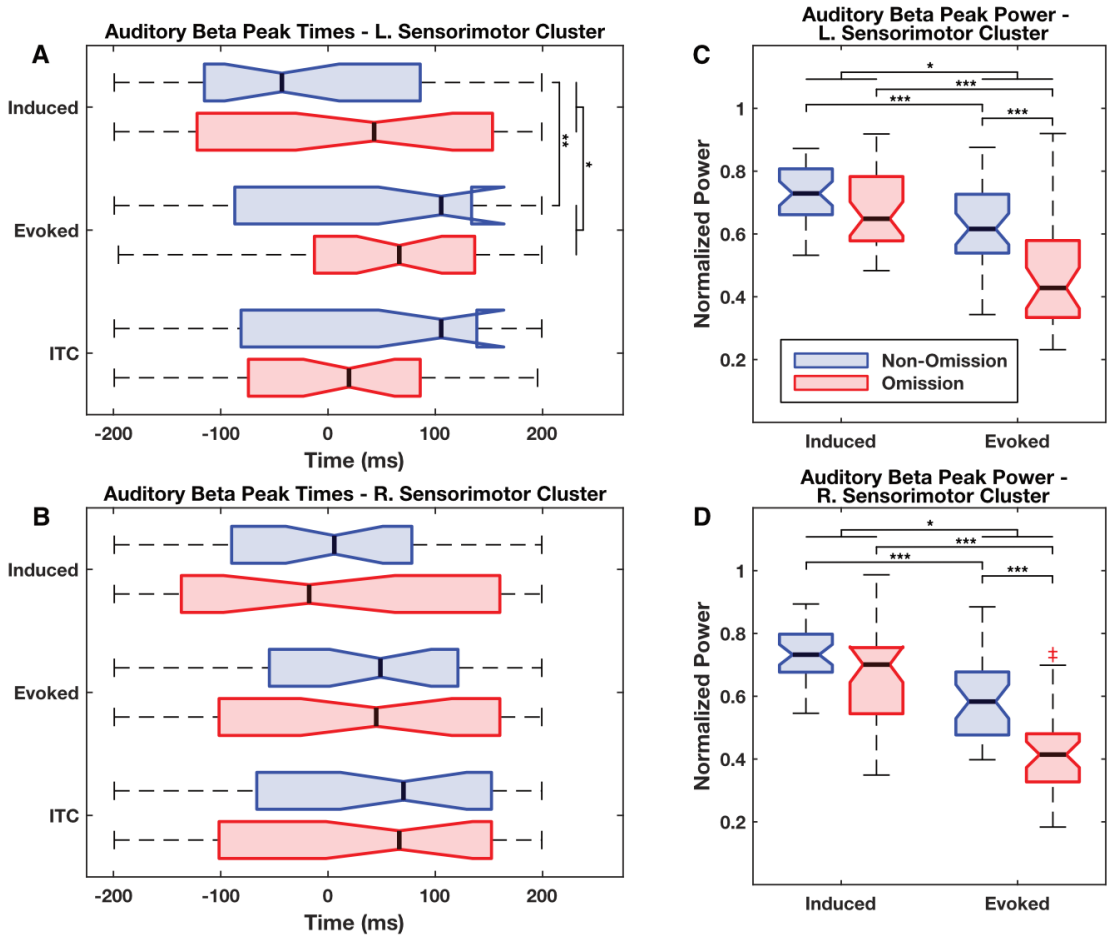

Fig. 3.9. Mean beta peak times (a,b) and mean normalized beta peak power (c,d) for components in the left sensorimotor (a,c) and right sensorimotor clusters (b,d) in the auditory condition. In the left sensorimotor cluster (a) induced beta peaked prior to tone onset in the non-omission trials, but after expected onset in omission trials. Note that evoked and intertrial coherence (ITC) beta peak times appear less variable in response to omitted tone than to non-omitted tones in the left sensorimotor cluster (a), whereas beta peak times were especially variabile in the right sensorimotor cluster (b). Normalized beta peak power shows the same pattern in both left (c) and right (d) sensorimotor clusters with power lower in the evoked omission trials compared with the evoked non-omission trials and overall lower evoked power than induced power. Box plots depict interquartile range with median values indicated by black bars and 95% confidence intervals indicated with notches. Significance differences are shown through bars where *$p < 0.05$, **$p < 0.01$, ***$p < 0.001$

The same tests were run on the auditory beta peak times, revealing that evoked auditory peak times for control (M = 10.64 ms, SD = 122.49) and omission (M = –2.23 ms, SD = 131.29) and induced auditory peak times for control (M = 0.35 ms, SD = 129.6) and omission (M = 6.7 ms, SD = 135.51) conditions were generally close to onset time and not significantly different from each other across all clusters and all tests except for

the left sensorimotor cluster, where evoked control peak time (M = 64.96, SD = 124.59) was significantly later than induced control peak time (M = –23.44, SD = 122.23); t(34) = 3.27, p = 0.006 (Figure 3.9a). The difference between evoked control and omission peak times (M = 35.38, SD = 167.02) and the difference between induced control and omission peak times (M = –45.42, SD = 151.1) was also found to be significant in the left sensorimotor cluster; t(34) = 2.39, p = 0.047 (Figure 3.9a).

Visual modality-evoked control peak values (M = 0.631, SD = 0.141) were greater than evoked omission peak values (M = 0.366, SD = 0.163); t(288) = 20.04, p = <0.001. Similarly, visual modality-induced control peak values (M = 0.753, SD = 0.117) were greater than induced omission peak values (M = 0.664, SD = 0.136), although to a lesser degree; t(288) = 9.58, p = <0.001. The comparison tests across visual omission and non-omission peak values within evoked and induced activity were significant for all clusters. Comparisons across evoked and induced peak values for visual beta indicated induced non-omission peaks were generally larger than evoked non-omission peaks; t(288) = –13, p = <0.001. This comparison was found to be significant for all clusters except the occipital cluster (Figure 8d). Comparisons across visual beta evoked and induced omission-fitted peak values indicate induced omission peak values are greater than evoked omission peak values for the parent cluster; t(288) = –23.99, p = <0.001, and all other clusters. A comparison between the difference in evoked non-omission and omission peak power (M = 0.264, SD = 0.224) and the difference between induced non-omission and omission peak power (M = 0.089, SD = 0.157) indicated a greater relative difference was seen in evoked activity for the parent cluster (t(288) = 11.24, p = <0.001), as well as for clusters 3 (mid central), 5 (right frontal), 8 (parietal), and 9 (right temporal/parietal).

Running the same tests on auditory peak values show auditory evoked non-omission peak power (M = 0.592, SD = 0.125) was significantly greater than auditory evoked omission peak power (M = 0.442, SD = 0.146) for the parent cluster (t(288) = 13.24, p = <0.001), and all other clusters except for the midline central area cluster. Auditory-induced non-omission peak power (M = 0.73, SD = 0.099) was slightly larger than auditory-induced omission peak power (M = 0.677, SD = 0.124), and significantly so for the parent cluster (t(288) = 5.72, p = <0.001), as well as for the midline central area, occipital, and right temporal/parietal clusters. A comparison across auditory-evoked and auditory-induced non-omission peak power reveals induced non-omission peak power is significantly greater in the parent cluster (t(288) = –15.65, p = <0.001), as well as in all other clusters except the left frontal cluster. Auditory-induced omission peak power was found significantly larger in the parent cluster (t(288) = –20.27, p = <0.001), as well as all other clusters. Comparing the difference in evoked non-omission and omission peak power (M = 0.15, SD = 0.193) and the difference between induced non-omission and omission peak power (M = 0.053, SD = 0.156) revealed a greater relative difference in evoked activity that was significant in parent cluster (t(288) = 6.51, p = <0.001), as well as for the left sensorimotor, right sensorimotor, right frontal, and parietal clusters.

3.4.6 Intertrial coherence

The time course of ITC in the beta band for the parietal and occipital clusters in the visual condition, and in the left and right sensorimotor clusters in the auditory condition is depicted in the bottom row of plots in Figure 3.7, where ITC can be compared against evoked and induced beta activity. The distribution of ITC peak times for the aforementioned clusters are depicted in Figures 3.8a,b (visual) and 3.9a,b allowing for a comparison against evoked and induced peak times. No significant differences were found between ITC beta peak times and evoked beta peak times for either auditory or visual conditions in any cluster. Comparisons between ITC beta peak times and induced beta peak times showed induced beta peaked prior to the peak in ITC beta in the non-omission condition in the visual modality in the parent cluster ($t(288) = 8.5$, $p = <0.001$), left temporal–parietal cluster ($t(27) = 3.7$, $p = 0.012$), right temporal–parietal cluster ($t(28) = 5.28$, $p = <0.001$), parietal cluster ($t(41) = 5.59$, $p = <0.001$), occipital cluster ($t(23) = 9.83$, $p = <0.001$), and right frontal cluster ($t(38) = 3.46$, $p = 0.015$). Additionally, ITC beta peaked earlier than induced beta in the visual omission condition in the parent cluster ($t(288) = –2.83$, $p = 0.042$). There were no significant differences between induced beta peak times and ITC beata peak times in the auditory conditions. Non-omission ITC beta peaked later than omission ITC beta in the visual modality in the parent cluster ($t(288) = 7.7$, $p = <0.001$), left temporal–parietal cluster ($t(27) = 3.17$, $p = 0.035$), right temporal–parietal cluster ($t(28) = 4.79$, $p = <0.001$), parietal cluster ($t(41) = 4.81$ $p = <0.001$), occipital cluster ($t(23) = 5.72$, $p = <0.001$). In the auditory condition, non-omission ITC beta peaked later than omission ITC beta in the parent cluster ($t(288) = 3.16$, $p = 0.017$).

3.4.7 Baseline activity

The comparison of baseline power revealed no significant differences in the majority of the tests. The comparisons that do show differences are predominantly relegated to the parent cluster, and the left and right frontal clusters for both modalities. Additional differences were seen in the visual modality in induced beta in the parietal cluster and evoked beta for the occipital cluster. All instances of significant differences between baselines show reduced power in the non-omission baseline compared with the omission baseline with the exception of the occipital cluster. All test values and statistical results of the baseline analysis are listed in the supplemental Tables S7 and S8.

3.5 Discussion

3.5.1 Summary of results

Using an IC cluster-based approach for isolating network-level beta band activity, we describe predictive timing in a modality-specific way. Analyses on the slopes of beta activity from the parent clusters reveal evidence for both induced and evoked predictive timing in auditory and visual modalities at the global level. The slopes of beta activity from individual clusters indicates evidence of induced predictive timing in the visual modality in posterior regions: left and right temporal/parietal clusters, and parietal cluster; the midline central cluster, and from the right frontal cluster. Slope-based evidence for induced predictive timing in the auditory modality was found in the parietal

cluster. Cluster-specific evidence of evoked predictive timing in slope measures was seen only in the auditory modality, in the left sensorimotor cluster.

It would be expected, based on Snyder and Large (2005), that evoked beta peak power would be significantly lower for omission events compared with tone or flash events and that there would be no significant difference in induced beta peak power between omission events and tone or flash events. This pattern was seen much more prominently in the auditory modality, specifically in the parietal, left and right sensorimotor, left and right frontal, and left temporal/parietal clusters. A significant difference would additionally be expected between how much evoked beta peak power shifted between non-omission and omission conditions and how much induced beta power shifted between non-omissions and omissions. This significant difference was replicated in several clusters: the parietal cluster, left and right sensorimotor clusters, and the right frontal cluster, thus providing strong evidence for auditory-induced beta playing a predictive role in networks of those regions. There were a few differences in the peak times in auditory beta across both induced and evoked activity and conditions. The significant shift in peak time from tone to omitted tone trials between induced and evoked beta for the right sensorimotor cluster follows the expected pattern of induced beta peaking later in response to an omitted tone than in response to a non-omitted tone. The evoked beta peaked earlier in response to an omitted tone than in response to a non-omitted tone. Although not significant, we find it interesting that the opposite pattern with beta peak time appears in the left sensorimotor cluster: induced beta peaked slightly earlier in response to omitted tones than in response to tones, yet evoked beta peaked slightly later in response to the omitted tones than in response to the tones. This is in concordance with what would be expected if evoked beta was playing a predictive role, and when taken in conjunction with the slope evidence of predictive evoked activity in the left sensorimotor cluster suggests the existence of significant hemispheric differences in auditory rhythm processing mechanisms. The findings indicating no significant difference between auditory evoked beta peak times and ITC beta peak times suggests the hemispheric differences seen in the sensorimotor clusters are a result of phase resetting in the beta band anticipating the onset of the auditory event. The baseline analyses showing no significant differences for the sensorimotor and parietal clusters indicate the beta peak power differences are not due to any habituation effect. Although we do see a baseline difference in the right frontal cluster, the baseline differences only directly affect the non-omission to omission comparisons, and not the within condition comparisons, for example, non-omission-induced beta peak power compared with non-omission-evoked beta peak power. Furthermore, when taking into account that the beta peak power results of the right frontal cluster closely match those reported by Snyder and Large (2005), they are likely to represent a genuine effect, indicating auditory beta timing in a left frontal region.

Differences in evoked and induced beta power in response to visual non-omissions and omissions did not provide clear evidence of predictive beta as seen in the auditory case, except for in the shift of peak power between evoked and induced activity from flash-to-flash omission in the parent, parietal, midline central, right frontal, and right temporal/parietal clusters. Interestingly, a look at differences in peak times does provide stronger evidence suggesting separate roles for evoked and induced beta for the

parietal, right and left temporal/parietal, and occipital clusters. In these clusters, the evoked beta peak came earlier in response to omitted flashes than to non-omitted flashes, whereas induced beta peaked later in response to omitted flashes than to non-omitted flashes, which is what would be expected if induced beta activity was playing a predictive role, whereas evoked beta was only responsive to stimuli. The significant differences between ITC beta peak times and induced beta peak times in the left and right temporal-parietal clusters, parietal cluster, and occipital cluster combined with the no significant differences between ITC and evoked beta peak times add further evidence for the role of predictive beta activity. Although we do see baseline differences in the visual modality for the parietal, occipital, and right frontal clusters, those differences do not provide evidence to invalidate our findings because the slope-based and beta peak time evidence from those clusters would not be directly affected by baseline differences. Taken together with the slope results, we interpret these findings as evidence of induced beta playing a predictive role in visual rhythm perception similar to that reported in previous studies for auditory-induced beta (Fujioka et al., 2009, 2012, 2015; Snyder & Large, 2005). The overall pattern indicates induced beta power rising in anticipation of an incoming tone or flash. In response to the flash onset, we see phase resetting in the beta band as indicated by increased ITC, resulting in increased evoked activity. This increase in evoked activity appears to act as a marker to reset the anticipatory timing seen in induced beta such that induced beta power drops before beginning its rise in anticipation of the next event. When an event is omitted, there is little to no phase resetting seen and so induced beta continues to rise and plateau before eventually falling until the next event causes the induced beta power to drop further and thus restarting the cycle.

If we take together the findings from the beta slope tests and the beta peak power and time tests, we find evidence of predictive visual beta in the left and right temporal/parietal clusters, the occipital cluster, the midline cluster, the parietal cluster, and the right frontal cluster. These tests show evidence of predictive auditory beta in the left and right sensorimotor clusters, the right frontal cluster, and parietal cluster. The results taken all together suggest the existence of modality independent, but possibly overlapping networks for rhythm timing (Figure 3.10).

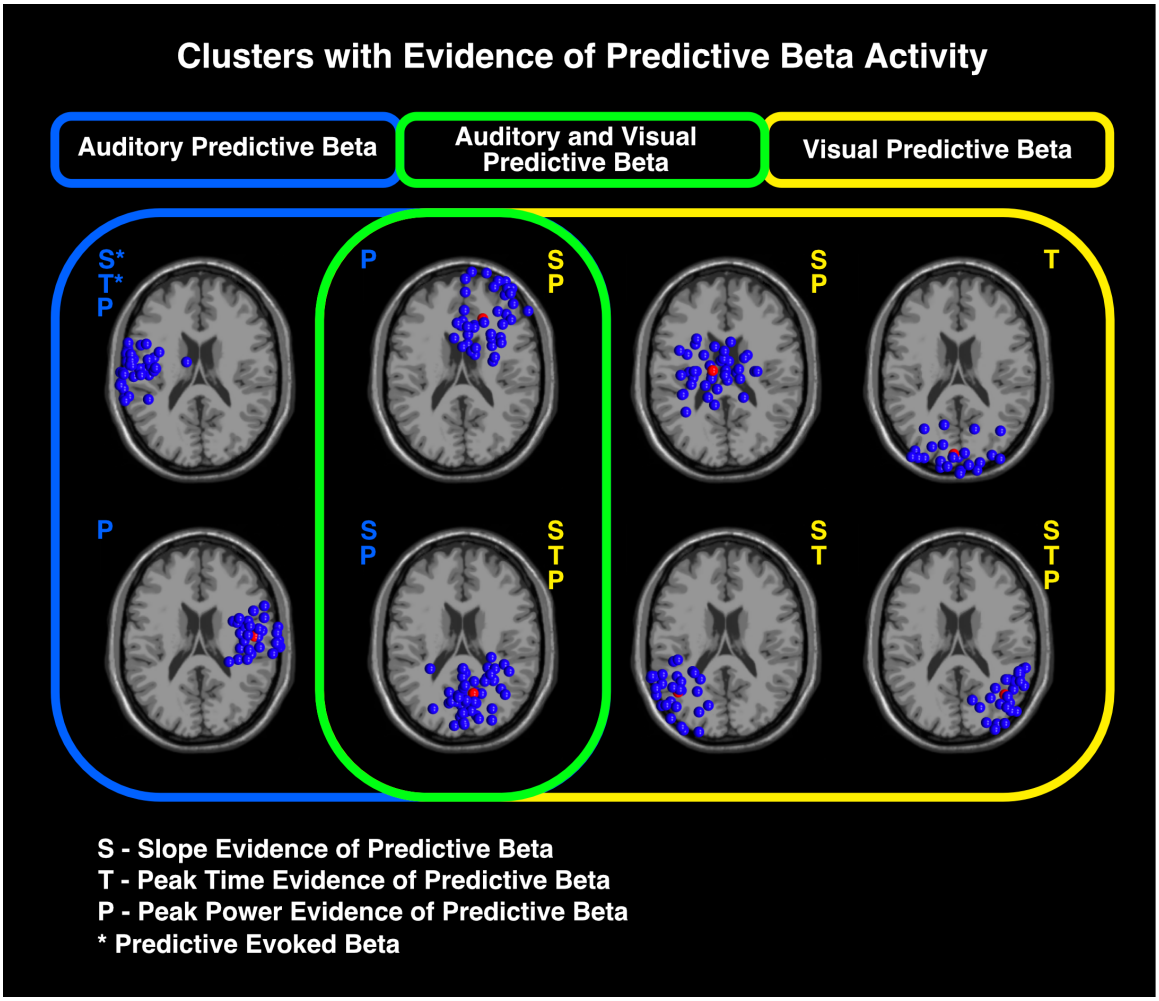

Fig. 3.10. Overview of clusters with evidence of predictive beta activity for auditory and visual rhythm processing indicated. Clusters within the blue area show predictive activity for only auditory rhythms, clusters within the yellow for only visual rhythms, and clusters within the green areas for both auditory and visual rhythms. The type of predictive evidence is listed for each cluster with evidence for visual rhythms in yellow and auditory rhythms in blue. All predictive evidence was in induced beta activity except for auditory rhythms in the left sensorimotor cluster where evidence of predictive evoked beta activity was found. P, peak power evidence of predictive beta; S, slope evidence of predictive beta; T, peak time evidence of predictive beta. *Predictive evoked beta

3.5.2 Predictive beta band activity

Beta modulation has been shown to play a role in a wide range of activities including top-down control on sensorimotor systems (Arnal et al., 2011; Engel & Fries, 2010; Haegens & Golumbic, 2018; Picazio et al., 2014), facilitating long-range communication between cortical regions (Kilavik et al., 2013; Kopell et al., 2000) such as between sensorimotor and peripheral areas (Fujioka et al., 2015), and is suggested to play a role in encoding temporal intervals (Wiener & Kanai, 2016). Beta band activity also correlates with motor behavior, with power attenuation just before and during movements

(see Kilavik et al., 2013 for review). Considering the suggested role, the motor cortex has in timing and predictive processing (Patel & Iversen, 2014; Schubotz et al., 2000), the role of beta in imposing general top-down control, and its role in facilitating communication with sensorimotor peripheral systems, it is not surprising that beta activity appears to play a role in rhythm perception and prediction.

Beyond the link to sensorimotor behavior, beta activity is known to play a role in auditory rhythm perception. Frontocentral-induced beta and gamma modulation occurs with the onset of rhythmic events and can be seen at the expected onset of an omitted event (Snyder & Large, 2005). Fujioka et al. (2012) found that beta power arising from the auditory cortices increases before tone onset in an isochronous rhythm at a rate dependent on the tempo of the rhythm and attenuates following the tone at a constant rate not dependent on the tempo of the rhythm. Beta activity has also been seen to play a role in maintaining beat and meter (Fujioka et al., 2015). Consistent with these findings, we find evidence of auditory-induced beta power peaking in anticipation of both tones and omitted tones, with the strongest evidence coming from the parietal, left and right sensorimotor, and right frontal clusters. Because the source of neural activations are more difficult to localize using EEG than MEG, some caution is needed in interpreting the location of these sources. However, given other findings suggesting predictive induced beta arising from frontocentral regions using EEG (Snyder & Large, 2005), and from the auditory cortices, sensorimotor cortices, and parietal cortices using MEG (Fujioka et al., 2012, 2015), we believe the regions indicated by the cluster locations are reasonable interpretations of the source of the predictive beta we measured. It is of note that we did not find evidence of predictive beta that we could tie clearly to the auditory cortex. This may be a limitation of the EEG IC cluster approach we used; it has been put forth that signals arising from the auditory cortex are more suited to being measured by MEG than EEG (Destoky et al., 2019).

When looking at beta modulation in the visual domain, we see a beta power increase at the expected onset of an omitted flash in multiple clusters. Comparing beta modulation in anticipation of the visual onset between the omission and non-omission conditions shows induced beta power increasing prior to onset, followed by a sharp power drop-off, but only after flash onset, and not following omission onset. Although we expected to find predictive beta activity in the visual domain, it was surprising to see evidence of predictive induced beta modulated more clearly and across more clusters in the visual domain than in the auditory domain because the timing aspects of rhythm perception in the auditory domain are thought to be more precise as evinced by less variability in auditory SMS compared to visual SMS (Repp, 2005, Repp & Su, 2013). The discrepancy between auditory and visual beta modulation may be due to auditory signals being more suited to measurement from MEG than from EEG (Destoky et al., 2019), resulting in a comparatively reduced measurement of beta modulated by auditory rhythms. The apparent size difference between the auditory and visual cortex may play an additional role.

The clusters that show evidence of predictive beta activity for the visual modality do not perfectly overlap with what is seen in the auditory modality. In the sensorimotor clusters, we only find evidence of auditory predictive beta in bilateral sensorimotor clusters, and not visual predictive beta. There is evidence of visual predictive beta in the

midline cluster, which contains dipoles localized to the premotor regions. This may indicate motor system involvement and would be in line with research suggesting the medial premotor region plays a role in predictive timing in primates across sensory modalities (Merchant et al., 2013). However, this begs the question of why the same activity was not seen in the auditory modality if premotor timing activity is not modality specific. A possible explanation is given by work reporting that a greater number of cells in the primate SMA respond to visual timing cues than to auditory timing cues (Merchant et al., 2015), although it is not clear if this finding extends to humans or if it is specific to the primates involved in that study. It is also of interest that we find predictive visual-induced beta activity from the slope analysis in left and right temporal/parietal junction and parietal clusters, but not in the occipital cluster. Given the difficulty in localizing sources with EEG, and the component distribution of the four posterior clusters, it is likely the left and right temporal/parietal and parietal clusters contain activity arising from cortical patches within the occipital cortex. Considering the distribution of components, and the faster rebound in induced beta power in the occipital cluster (Figure 3.5b), we consider it likely that activity from early processing areas of the visual cortex (e.g., V1) are more strongly represented in the occipital cluster than the surrounding posterior clusters. This, however, cannot be confirmed with the spatial limitations of EEG and will require a methodology with greater spatial precision to test.

Although beta power modulation in response to visual rhythmic flashes has been seen before (Meijer et al., 2016; Saleh et al., 2010), to our knowledge this is the first time it has been shown predicting the onset of an omitted event. However, it has been questioned whether beta modulation is even related to temporal prediction at all (Meijer et al., 2016). Meijer et al. (2016) investigated beta activity with a rhythmic visual task and found beta power modulation in response to isochronous visual rhythms of different tempi (IOI's of 1,050, 1,350, 1,650 ms), yet the rate of beta power modulation was the same regardless of the tempo used. This is different from what was found by Fujioka et al. (2012) in their study of auditory beta modulation, where the rate of beta power prior to tone onset was modulated by the tempo of the rhythm. Meijer et al. (2016) interpreted their result as evidence that beta activity is not playing an entraining role in the visual system, suggesting instead that the beta peaks seen may be caused by rebounding activity in response to the flash, peaking roughly 900 ms after event onsets. The current study provides the contrary evidence and suggests that beta modulation may be playing a role in prediction of the onset of visual events because the beta modulation during the omission could not be in response to any event and instead must be responding to the timing of the expected onset of the flash. Induced beta peaks <50 ms after the omission onset, or 650 ms after the onset of the prior stimulus (Figure 3.4), which is much earlier than would be expected for beta power rebound in response to the flash event, as described by Meijer et al. (2016). We suggest the reason for the discrepancy between Meijer et al.'s (2016) findings and those findings reported here may be due to their use of relatively slow tempi compared with the 600 ms IOI of this study. Additionally, the task used in the Meijer et al. (2016) study was much more complicated than simply attending to the timing of the rhythms as in our task and demanded more attention and possibly competing resources. There is evidence that sub-second timing and supra-second timing

use different networks (see Wiener et al., 2010 for a review). We, therefore, suggest beta synchronization may only be playing a predictive role in the sub-second time scale.

3.5.3 Contribution of the motor system

Previous studies have described induced beta modulation to auditory rhythms arising from sensorimotor cortices (Fujioka et al., 2012, 2015). There is also evidence that auditory timing appears to rely on motor cortex (Iversen & Balasubramaniam, 2016; Janata et al., 2012; Repp & Su, 2013; Ross, Iversen, et al., 2016; Ross, Warlaumont, et al., 2016) and motor networks with nodes in the parietal lobes, cerebellum, and basal ganglia (Levitin et al., 2018; Patel & Iversen, 2014; Repp & Su, 2013). This motor network activity could indicate that the motor system is playing an important role in predicting the timing of events in auditory rhythms, often discussed in the context of evolution of social activities such as dance and language (Fitch, 2016; Iversen, 2016; Patel, 2006). The auditory beta modulation from the sensorimotor clusters we present here is consistent with the narratives of the previous literature on the involvement of the motor system for auditory timing. This can be contrasted with our findings from the visual system where there is no evidence of predictive beta timing in the bilateral sensorimotor clusters and instead evidence in the mid-central cluster that may be related to activity arising from the SMA.

In the auditory modality, we found evoked predictive beta timing activity in the left sensorimotor cluster (Figure 3.6a), yet we found evidence of induced predictive timing activity in the right sensorimotor cluster (Figure 3.7a). The asymmetrical beta activity seen in the two sensorimotor clusters specific to the auditory conditions suggests hemispheric specialization specific to auditory processing. A recent meta-analysis on neural activation during music listening shows consistent MRI activation in the right but not left primary motor cortex during music listening tasks (Gordon et al., 2018). Interestingly, they found that studies that asked the subjects to move a body part while listening elicited stronger activity in the right primary motor cortex than studies using passive listening tasks. Others describe a left hemisphere role (Pollok et al., 2008) or non-motor-dominant hemisphere role (Kaulmann et al., 2017; Yadav & Sainburg, 2014) for motor timing. Similarly, for language perception there appears to be hemispheric specialization in the auditory cortices, with the left hemisphere specialized in temporal changes and the right hemisphere in spectral changes (Zatorre & Belin, 2001; Zatorre et al., 1992). Specifically, it has been shown that activity in the left anterolateral superior temporal sulcus (STS) corresponds to processing of temporal aspects of speech perception, whereas perception of spectral features of speech are associated with the same structure in the right hemisphere (Obleser et al., 2008). Our results support bilateral motor contributions to auditory timing, although the mechanism that results in predictive evoked activity in the left hemisphere and induced beta activity in the right hemisphere may be distinct. In particular, the predictive evoked activity seen in the left sensorimotor cluster suggests a timing mechanism driving phase resetting at the expected tone onset not seen in the right sensorimotor cluster or any other cluster.

3.5.4 Limitations and future directions

The current study reveals that timing and prediction for visual rhythm perception could use non-motor networks. We cannot say what role, if any, the motor system plays in visual timing. A closer look at the connections between visual and motor systems is needed to elucidate the issue. Using moving visual rhythms as opposed to flashing visual rhythms may elicit a different picture of activation as the visual system is better tuned to discerning temporal information when movement is present (Hove, Iversen, et al., 2013).

Another limitation of the current study is that we did not use multiple tempi. Having only one tempo makes it unclear how much the change in time course of neural activations is related to the tempo. Using multiple rhythms with different tempi would allow for a clearer differentiation between tempo-dependent aspects of timing. If those tempi spanned both sub-second and supra-second interstimulus intervals, this would also provide insight to the temporal limits to the mechanisms in visual rhythm perception.

Although we see frequency band-specific oscillatory modulation during rhythm perception, caution should be used in assuming this is the brain's mechanism of timing. There is evidence for multiple mechanisms for timing (for review see Comstock et al., 2018; Wiener & Kanai, 2016; Wiener et al., 2010), and here we describe one reflection of these processes. Oscillatory dynamics likely reflect more broadly the mechanism for spreading information between or across networks, and timing perception is only a subset of neural communication happening during these tasks.

Additional investigation is needed into the differences seen between left and right motor contributions to auditory timing. Although the differences suggest possible functional lateralization in auditory rhythm perception, it is unclear if those differences are driven by handedness (Kaulmann et al., 2017; Yadav & Sainburg, 2014) or other factors (Pollok et al., 2008). Future studies are needed to look more closely at specific hemispheric contributions.

The inherent low spatial resolution of EEG limits how confidently we can draw conclusions about neural sources. We describe broad cortical source regions/networks in lieu of more focal sources with respect to this methodological limitation but argue that the ICA-based cluster analysis leads to reasonable spatial and functional grouping of neural activity likely from common sources. That being said, we cannot speak with certainty about the exact cortical sources of the activity we describe. A method with better spatial resolution that retains fine temporal resolution, such as MEG or ECoG, would provide better source resolution for predictive rhythm perception networks.

The baseline differences we find in some clusters suggest habituation to the non-omission condition not seen in the omission condition. Although these baseline differences do not directly impact many of the analyses used, nor impact our main findings, they do suggest that future studies should be designed in such a way to avoid unequal habituation to the signal. We also cannot rule out the possibility that unequal baselines could reflect differences in neural activation that may have indirect effects on neural dynamics. We think it unlikely that such differences would impact neural activity in such a way to impact our findings; however, study designs that avoid this possible confound would produce stronger results.

Finally, the nature of this work was primarily to investigate and explore predictive timing markers across auditory and visual modalities in beta activity. Although the

exploratory work is often a necessary step in surveying the landscape of a given problem, it can be prone to interpretive biases. For this reason, the exploratory portions of our work should be taken primarily as a guide for further experiments to understand predictive beta activity and differences between the mechanisms of auditory and visual rhythm perception.

3.6 Conclusions

We investigated the mechanisms of prediction for auditory and visual rhythms using an omission paradigm. In confirmation of our hypotheses, the results described here support theories of predictive timing in both visual and auditory modalities, that can be observed in beta band oscillatory activity. Using an exploratory ICA spatial cluster-based approach, our results also support that visual and auditory prediction for rhythmic events may be subserved by modality-specific cortical networks, although we cannot rule out the possibility that both auditory and visual networks are subserved by a common subcortical network. We describe all clusters resulting from the blind source separation technique in detail, and these results suggest induced beta activity predicting the expected onset of visual rhythmic events bilaterally in temporal/parietal clusters, in a dorsal medial cluster, a parietal cluster, and a right hemisphere frontal cluster. We also show evidence for induced beta activity predicting the expected onset of rhythmic auditory events bilaterally in sensorimotor clusters, in a parietal cluster, and in a right hemisphere frontal cluster, and evidence for evoked auditory predictive timing in a left motor cluster. These findings suggest that auditory timing may involve hemisphere-specific activity, and reliance on motor networks not seen in visual timing.

ACKNOWLEDGMENT
The work was supported by NSF grant BCS 1626505.

CONFLICT OF INTEREST
The authors do not have any conflicts of interest to declare.

AUTHOR CONTRIBUTIONS
DCC and RB conceived and designed this study together. DCC ran all participants and conducted the original analyses. DCC and JMR conducted follow-up analysis. DCC, JMR, and RB co-wrote the paper.

Chapter 4

4 Comparative Motor System Entrainment to Auditory and Visual Rhythms

This chapter consists of an experiment designed to determine the role of the motor system in auditory and visual rhythm perception during both SMS and purely perceptual rhythm perception. While the previous experiments provided evidence of visual system specific timing processing in ERP activity (chapter 2), and in beta-band oscillations (chapter 3), this experiment focuses on measuring the frequency of a rhythm (i.e., a rhythm with a beat every 1 second would have a frequency of 1 Hz) in the neural activity arising from the motor cortex. This focus is based on the idea that synchronization to, and perception of, a rhythm of a given frequency should induce neural entrainment at that frequency. Since the motor system is known to be involved in rhythm processing and is suggested to be more strongly connected to the auditory system for rhythm perception than for visual rhythm perception, we expected to find evidence of stronger entrainment from auditory rhythms in the motor system than from visual rhythms, yet we found the opposite instead. Given that rhythm perception is generally worse for visual rhythms than auditory rhythms, we take this finding to suggest that how entrainment is utilized to perceive or synchronize to a given rhythm is just as important as the entrainment itself.

Abstract

Perception of, and synchronization to, auditory rhythms is known to be more accurate than with visual rhythms. The motor system is known to play a role in the processing of timing information for auditory rhythm perception, but it is unclear if the motor system plays the same role for visual rhythm perception. One demonstrated component of auditory rhythm perception is neural entrainment at the frequency of the auditory rhythm. In this study we use EEG to measure entrainment of both auditory and visual rhythms from motor cortex while subjects either tapped in synchrony with, or passively attended the presented rhythms. In order to isolate activity from motor cortex, we used independent components analysis to first separate out neural sources, then selected components using a combination of component topography, dipole location, mu activation, and beta modulation. This process took advantage of the fact that tapping activity will result in reduced mu power, and characteristic beta modulation that helped select motor components. Our findings indicate neural entrainment in the motor system was stronger for visual rhythms than auditory rhythms, and strongest during for the tapping conditions for both modalities. We also find no difference in mu power across modalities. These findings indicate that the generally greater rhythm perception capabilities of the auditory system over the visual system do not depend entirely on neural entrainment in the motor system.

4.1 Introduction

Human capability for sensorimotor synchronization (SMS) to auditory rhythms has been shown to be more precise than SMS to visual rhythms (Repp, 2003), but the exact reasons why are yet to be uncovered. It has been shown through fMRI work that

activation of motor structures are more pronounced for auditory rhythms than for visual rhythms during SMS tasks as (Hove et al., 2013b). This has led to the suggestion that the auditory system is more tightly tied to the motor system for temporal processing, such as needed for rhythm perception, than the visual system. In previous works, we have suggested that a corollary to this is that the visual system performs some rhythm processing in house (Comstock & Balasubramaniam, 2018; Comstock et al; 2018; Comstock et al 2021). Based on that suggestion, we would expect to see differences in electrophysiological measures of rhythm processing in the motor system between auditory and visual rhythms that match those seen in fMRI data.

It has been demonstrated using EEG that listening to auditory rhythms elicits an increase in power and phase coherence at the frequency of the beat of the rhythm (f0), that is measured most strongly over frontal-central regions (Nozaradan et al., 2011, 2012a, 2012b), and this signal is increased during an SMS task (Nozaradan et al., 2015). Likewise, it has long been known that the visual system can elicit power at the rhythm of visual flashes in what are dubbed steady-state visually evoked potentials (SSVEPs) (for review see Vialatte et al., 2010). It is unclear to what extent actvitiy at f0 induced for auditory rhythms and visual rhythms would both be present in the motor system. If the auditory system is more tightly tied to the motor system than the visual system however, we would expect measures of power and phase coherence in the motor system to be stronger for auditory rhythms than visual rhythms.

Many previous EEG studies investigating activity from the motor system have attempted to isolate motor system activity by selectively measuring activity from channels that lie over motor regions (Pfurtscheller & Neuper, 1994; Pfurtscheller et al., 1997; McFarland et al., 2000). One downside of this approach is that EEG activity arriving at the scalp level is a mix of all sources of activity in the brain (Makeig et al., 2004). Independent components analysis (ICA) has been shown to be an effective method of separating out sources of neural activity in the brain (Delorme et al., 2012). While the blind source separation of ICA allows for separating out sources, a method of selecting appropriate sources for each study is needed. Since this study aims to determine the role of the motor cortex in rhythm processing, a clear marker of motor system activity will be needed.

Mu rhythms are a well-known marker of motor system activity, which are rhythms originating from the motor cortex in the range 8-13 Hz (Pfurtscheller & Lopes da Silva 1999). Mu rhythms are known to play a role in inhibition of movement and have been shown to increase in power, or what is termed event-related synchronization (ERS), during movement suppression, and decrease power, or event-related desynchronization (ERD), during movements (Pfurtscheller & Neuper, 1994; Pfurtscheller et al., 1997; McFarland et al., 2000) as well as during movement imagery (McFarland et al., 2000). A study designed with a sufficient motor task, and a non-motor task could be expected induce modulation of mu rhythms that would likely be isolated as independent components.

A further benefit of looking at mu rhythms for a study designed to investigate the role of the motor system in auditory and visual rhythm processing is that it is speculated that mu rhythms may additionally serve as markers of rhythm perception. In preliminary work, we showed that listening to music while remaining still results mu ERS relative to

silence (Ross et al., 2016). That study was motivated by the premise in the ASAP hypothesis that the motor system is simulating the beat in music (Patel & Iversen, 2014). If the motor system is simulating the beat, then one could expect corresponding mu ERS to inhibit any movement that might arise from the beat simulation. Although there has been at least one study showing mu ERD during music listening, there is reason to doubt the results are purely due to listening music (Wu et al., 2016). The effect in that study may be due to motor imagery, as the ERD was seen in trained pianists while they listened to piano pieces they were familiar with, and therefore may have been imagining the movements required to play the pieces. As the study did not test non-musicians, nor musicians with music they were not familiar with, it cannot be confirmed that the mu ERD was a result of simply attending or processing of music.

In this study we used EEG to measure changes in mu rhythms and activity at the beat frequency (f0) induced by attending to isochronous auditory or visual rhythms. Based on the idea that the auditory system is more tightly connected to the motor system than the visual system for temporal processing, and that listening to music induces mu ERS as an inhibitory effect against beat simulation, we hypothesized that mu ERS would be greater for auditory rhythms than visual rhythms during non-tapping conditions. Additionally, we hypothesized that activity at f0, as measured by power and phase coherence, would reflect auditory rhythms more strongly than visual rhythms in the motor cortex. Since previous work has shown that music training can increase neural responses to music (Bangert & Altenmüller 2003), including measures of activity at f0 (Doelling & Poeppel, 2015), we recorded each subjects music training experience to check if differences in music training play a role in measured differences in rhythm perception. Therefore, we hypothesized that subjects with music training will show stronger Mu and f0 measures for rhythms compared to subjects without music training.

4.2 Materials and Methods

4.2.1 Participants

21 subjects participated in the experiment (11 female, $M = 21.62$ years, $SD = 3.58$). Data from 3 subjects were not used, 2 for computer error and 1 due to poor signal to noise ratio resulting in no discernable motor components. 10 subjects reported have some musical training ($M = 6.6$ years training, $SD = 3.21$). All subjects had typical hearing and typical or corrected vision, and reported being right handed. This study was approved by the UC Merced Institutional Review Board for Research Ethics and Human subjects, and was carried out in accordance with the Declaration of Helsinki. All participants gave informed consent prior to testing.

4.2.2 Task

Subjects were seated and fitted with a 32 electrode EEG cap, and were presented with 16 stimulus trains with each train consisting of 40 events. 8 of the trains were of auditory tones (1000 Hz sine wave, 50 ms duration with 10 ms rise and 30 ms fall), and the other 8 being visual flashes (light grey flash with 50 ms duration). For both tones and flashes the subjects faced a black computer screen with a grey fixation cross at the center that remained visible during both flashes and tones. All stimuli were presented with an interonset interval of 600 ms, resulting in beat frequency (f0) of 1.667 Hz. Subjects were

either instructed to tap in synchrony to the tones or flashes using their right index finger, or to attend the stimuli while remaining motionless. Tap times were not recorded. The resulting four groups of stimulus trains (auditory tapping, auditory no tapping, visual tapping, visual no tapping) were presented as separate blocks, with each block having stimuli from only one condition. The order of the groups was randomized with the exception that the 2 groups from each modality were always presented one after the other, and the tapping order was preserved across modalities, e.g., visual no tapping, visual tapping, auditory no tapping, auditory tapping. In order to ensure subjects were actively attending the stimuli, subjects were presented with an additional short test-stimulus train immediately following each stimulus train, and were asked to compare the tempos of the stimulus train with the short test stimulus train. The test-stimulus train was always of the same modality as the stimulus train it followed, with tempo that was either slightly slower or faster than the preceding train was presented. After the test-stimulus train was presented, subjects were tasked with reporting if the later train was faster or slower than the previous train.

4.2.3 EEG Processing

EEG data were processed using EEGLAB 2021 (Delorme & Makeig, 2004) and Matlab 2020b. Data were first downsampled from 1024 to 256 Hz, then high pass filtered with passband edge at 1 Hz and -6 dB cutoff at .5 Hz. Data were then pruned to remove all sections of data that did not contain stimuli events, after which the data were inspected and bad channels were removed. Spherical interpolation was used to fill the removed channels, after which ASR correction was used to fix noisy bursts in single channels. Data were then referenced to average and ICA was applied using the AMICA algorithm (Palmer et al., 2012). After ICA Dipoles were fitted to the resulting components. Eye blink, eye movement, and heart artifact components were selected by hand for each subject and removed from the data.

The independent components from each subject were then inspected using the IC Label toolbox (Pion-Tonachini et al., 2019) to visualize and help determine which component corresponded to the left hemisphere primary motor cortex for each subject based on the following criteria: Scalp topography and dipole location indication that the component source was in the left motor cortex, evidence of mu ERS in the spectral power, evidence of mu ERS in the time series based on the distinctive mu wave shape, mu modulation based on condition (mu ERD during tapping conditions). Left primary motor cortex components were found for all but 1 subject, resulting in 18 subjects. An example of a motor component can be seen in figure 4.1, along with the scalp topography of all selected motor components. Further confirmation of the veracity of the motor components was made by inspecting and comparing beta power modulation between the tapping and no tapping conditions, as beta band power attenuation from the motor cortex is known to occur during movement onset (Pfurtscheller & Lopes da Silva, 1999).

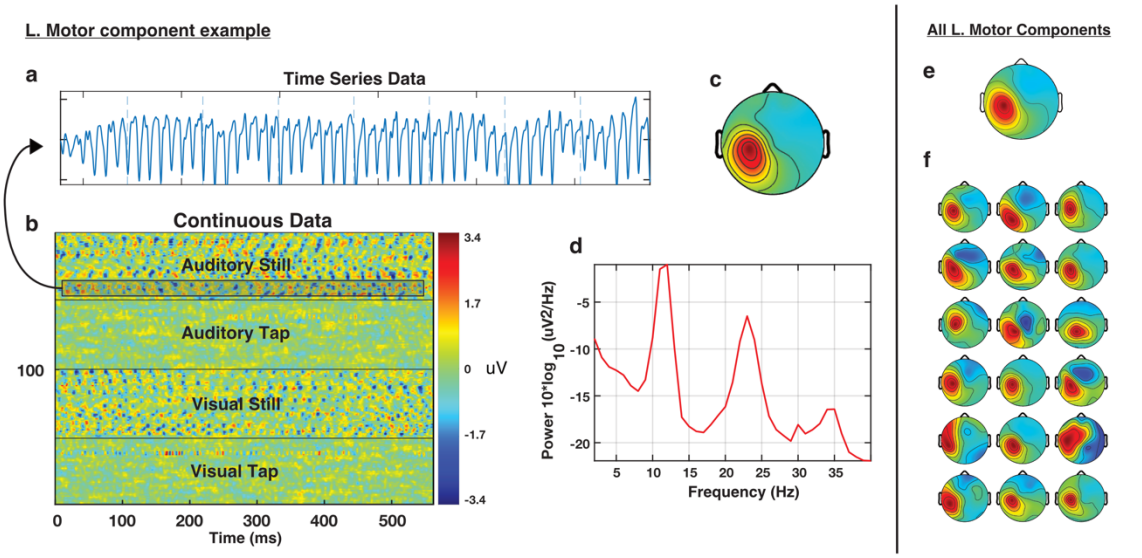

Fig. 4.1. Example of left motor component from a single subject. Characteristic mu wave shape can be seen in the time-series data (a), which is present only during the non-tapping conditions (b). The topography of the component suggests its source is from the left-motor cortex (c), while the spectral power shows the characteristic 10 Hz power with a beta harmonic resultant from mu activity (d). Topographic plots of activity from the selected left motor components with activity of all components averaged together can be seen in the top topographic plot (e). All individual left-motor component plots are shown (f).

Two separate time-frequency calculations were performed on the processed component data: an analysis to inspect beta power modulation, and an analysis to calculate phase coherence in the lower frequencies. To calculate beta power modulation, the data were epoched into 3 second epochs centered on the stimulus. Single-trial time-frequency analysis was performed on the resulting epochs using Morlet wavelets between 8 and 35 Hz with a constant wavelet length of 500 ms achieved using 4 cycles at 8 Hz and scaling up to 17.5 cycles at 35 Hz. A divisive baseline consisting of the entire epoch length for each condition was used to highlight power modulation of each frequency. The resulting time-frequency activity was used solely to confirm that the selected motor components did indeed correspond to motor activity.

A second time-frequency calculation was performed on the un-epoched trials using Morlet wavelets between 1.066 and 14.066 Hz with a constant wavelet length of 6563 ms seconds achieved using 7 cycles at 1.066 Hz and 92.31 cycles at 14.066 Hz. The frequencies used were linearly spaced at 0.1 Hz intervals so that the beat frequency of 1.666 Hz could be captured. No baseline was used so that power could be compared across all 4 conditions. Using the un-epoched data allowed for a wider window, removing potential edge artifacts that can arise from using a narrow window, and additionally allowed for better bandwidth resolution with a resulting constant bandwidth for each frequency of .3 Hz. Intertrial Phase Coherence (ITC) was calculated by extracting the phase angles from the time-frequency calculations and epoching them centered on each stimulus (+/- 300 ms), in a similar manner as implemented by Doelling & Poeppel

(2015). ITC was then calculated as phase coherence across epochs for each condition at each time-frequency point for each component. Average ITC at each frequency was then calculated by averaging across time. To extract power, a discrete Fourier transform was applied to the un-epoched data between 1 and 40 Hz with a frequency resolution of 0.0439 Hz. Mu power was extracted as the averaged power between 8 and 13 Hz. To extract power induced by the beat frequency, signal power for the individual frequencies were noise corrected by subtracting the average power of the neighboring frequencies (+ 0.088 to 0.132 Hz and – 0.088 and 0.132 Hz) in a similar fashion as used by Nozaradan et al (2011).

4.2.4 Statistical Analysis

Analyses were carried out on the selected motor components as well as on grand average activity to assess overall activity without location bias. The grand averages were calculated for each subject for each condition, and consisted of the averages of the measures of all components. To investigate if the rhythms induced a significate neural response at f0, one sample t-tests were used for both noise-corrected f0 power and f0 ITC for each condition and for both the grand averaged data and motor component data. If there were no induced effect, it would be expected that the noise corrected f0 power and f0 ITC would be expected to be zero.

To compare changes in mu power, noise corrected f0 power and f0 ITC across the four conditions, separate 3 by 2 repeated measures ANOVAs were used with within-subject factors being modality (audition and vision), and tap condition (no tapping and tapping), and a between subject factor of music training (No musical training, some musical training). Post-hoc pairwise comparisons were made where appropriate based on ANOVA results using Bonferroni adjustments.

4.3 Results

4.3.1 Mu Power

Analysis of power in the mu frequency range (8 to 13 Hz) for grand averaged data revealed a main effect only of modality $F(1,16) = 15.428$, $p = 0.004$, $n_p^2 = 0.409$. Post-hoc comparisons revealed power in the mu frequencies for auditory control ($M = 53.405$, $SD = 4.691$) was greater than visual control ($M = 52.625$, $SD = 3.794$), $p = 0.028$, and power for auditory taps ($M = 53.38$, $SD = 4.677$) was greater than visual taps ($M = 52.302$, $SD = 53.904$), $p = 0.004$ (Figure 4.2a). Power in the auditory modality ($M = 54.019$, $SD = 4.757$) was also greater than power in the visual modality ($M = 52.846$ $SD = 43.937$), $p = 0.013$ for musicians, but not for non-musicians.

Analysis of power in the mu frequency range for the left motor component data revealed opposite results, with a main effect only of tap condition $F(1,16) = 13.973$, $p = 0.002$, $n_p^2 = 0.466$. Post-hoc comparisons revealed mu power for auditory control ($M = 40.162$, $SD = 5.26$) was greater than auditory taps ($M = 37.457$, $SD = 4.415$), $p = 0.003$, and power for visual control ($M = 39.696$, $SD = 4.945$) was greater than visual taps ($M = 37.372$, $SD = 4.736$), $p = 0.006$ (Figure 4.2a). Reduction of power in the mu frequency range over the left motor region in the scalp topography in the tapping conditions compared to non-tapping corroborates the findings of the left motor components (Figure 4.2b).

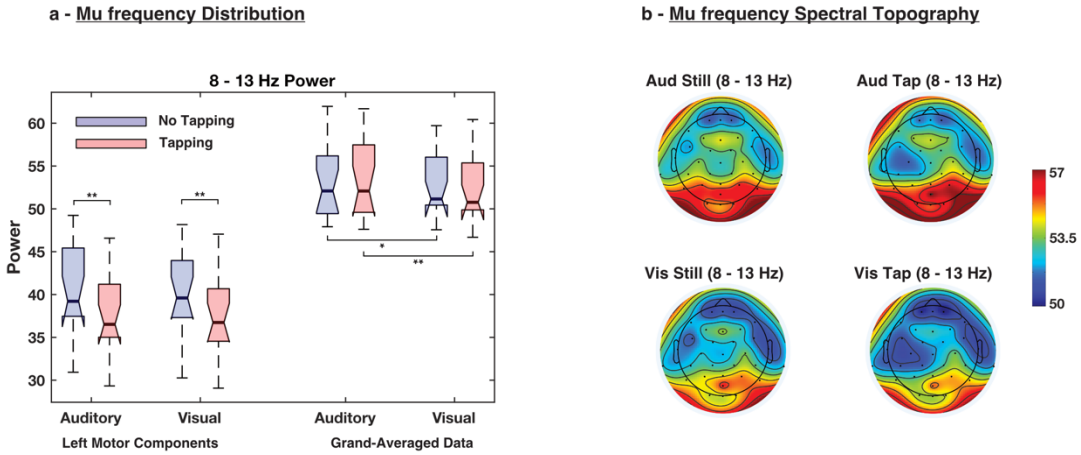

Fig 4.2. (a) Box pots depicting the distribution of power in the mu range across conditions for both the grand-averaged and left-motor component activity. The center line of each box depicts the median and the notches reflect the 95% confidence interval. (b) Scalp topographic maps of the spectral power in the mu range (8 – 13 Hz) from channel data. Both auditory tap and visual tap conditions show a reduction in power over the left motor region compared to the non-tapping conditions.

4.3.2 Beat induction at f0

One-sample t-tests of ITC at f0 indicated all conditions induced significant phase-coherence for both grand averaged and left motor component data (table 4.1, figures 4.3c & 4.3d). Tests of noise corrected power at f0 also indicated significance activity for all conditions (table 4.1, figures 4.3a & 4.3b).

Table 4.1

One-way t-test rests of activity at f0

	f0 ITC						f0 Noise Corrected Power					
Condition	Mean	Std. Dev.	t	df	p	Condition	Mean	Std. Dev.	t	df	p
Avg Aud Control	0.291	0.027	45.307	17	<.001	Avg Aud Control	2.1918	1.599502	5.814	17	<.001
Avg Aud Tap	0.340	0.060	24.152	17	<.001	Avg Aud Tap	3.2596	1.909764	7.241	17	<.001
Avg Vis Control	0.329	0.045	31.092	17	<.001	Avg Vis Control	3.2377	1.621868	8.47	17	<.001
Avg Vis Tap	0.375	0.083	19.188	17	<.001	Avg Vis Tap	4.4779	1.858721	10.221	17	<.001
L.Motor Aud Control	0.246	0.136	7.689	17	<.001	L.Motor Aud Control	1.525	2.588459	2.5	17	0.011
L.Motor Aud Tap	0.486	0.255	8.085	17	<.001	L.Motor Aud Tap	4.8233	4.077813	5.018	17	<.001
L.Motor Vis Control	0.398	0.152	11.107	17	<.001	L.Motor Vis Control	1.9961	3.433352	2.467	17	0.012
L.Motor Vis Tap	0.539	0.216	10.601	17	<.001	L.Motor Vis Tap	5.5586	3.366981	7.004	17	<.001

Table 4.1. Results of one-way t-tests to assess if f0 ITC and f0 noise corrected power is significantly different from zero. Both f0 ITC and f0 noise corrected power would be expected to be greater than zero if the rhythms are inducing activity at f0.

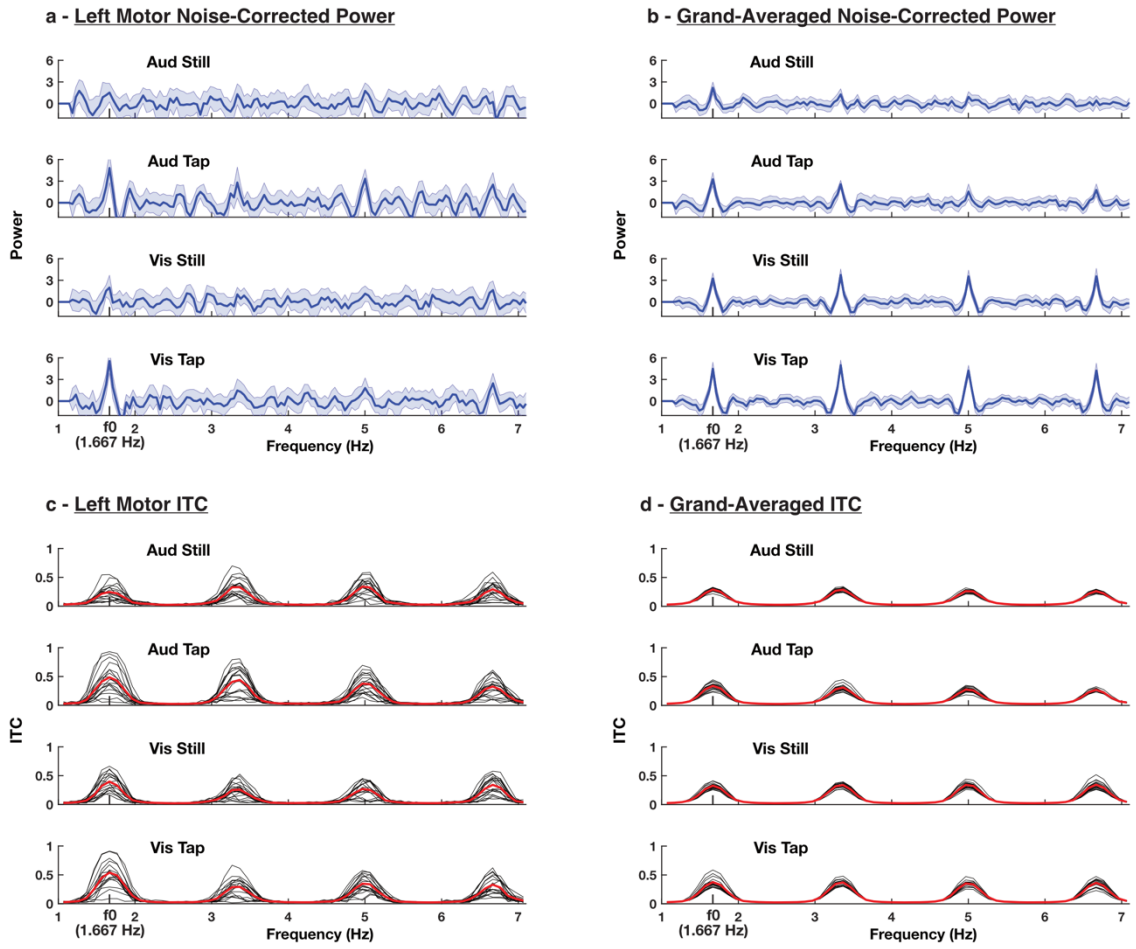

Fig. 4.3. Frequency domain representation of noise-corrected power (a & b) and ITC (c & d) across conditions for both left motor components and grand-averaged data. Average f0 noise-corrected power is represented with the dark blue line, and shaded areas represent 95% confidence intervals for both left motor power (a) and grand-averaged power (b). Individual ITC is shown with thin black lines and average ITC is shown in red for both the grand average data (c) and left motor component data (d).

4.3.3 Power

Analysis of power at f0 for the grand averaged data show main effects for both modality $F(1,16) = 5.434$, $p = 0.033$, $n_p^2 = 0.254$, and for the tap condition $F(1,16) = 14.627$, $p = 0.001$, $n_p^2 = 0.478$, and a three-way interaction between modality, tap condition, and music training $F(1,16) = 4.751$, $p = 0.045$, $n_p^2 = 0.229$. Post-hoc comparisons across modalities show f0 power from the auditory non-tapping condition ($M = 2.192$, $SD = 1.6$) was lower than for the auditory tapping condition ($M = 3.26$, $SD = 1.91$), $p = 0.026$, while f0 power for the visual non-tapping condition ($M = 3.238$, $SD = 1.622$) was also lower than f0 power for visual tapping ($M = 4.478$, $SD = 1.859$) $p =$

0.009. Comparisons of noise-corrected f0 power across modalities suggest that auditory induced f0 power was lower than visual induced f0 power for both non-tapping and tapping conditions, but neither difference reached significance ($p < 0.094$, $p < 0.052$, respectively) (figure 4.4a),

Post-hoc tests to explain the three-way interaction showed that only non-musicians had significant effects of modality on f0 power (Auditory: $M = 2.485$, $SD = 1.385$; Visual: $M = 4.1$, $SD = 1.55$; $p = 0.018$), and only in the tapping condition power (Auditory Tapping: $M = 2.574$, $SD = 1.793$; Visual Tapping: $M = 4.884$, $SD = 1.853$; $p = 0.004$). Further tests showed that f0 power induced by tapping was greater than not tapping for musicians (Tapping: $M = 4.043$, $SD = 1.47$; Non-Tapping: $M = 2.539$, $SD = 1.07.$; $p = 0.005$), but only in the auditory modality (Auditory Tapping: $M = 4.116.$, $SD = 1.793$; Auditory Non-Tapping: $M = 1.938$, $SD = 1.632$; $p = 0.008$). Non-musicians showed a similar, but just above significant, result across tapping conditions (Tapping: $M = 3.729$, $SD = 1.467$; Non-Tapping: $M = 2.855$, $SD = 1.069$; $p = 0.051$). Different from the musician group, the non-musicians showed a significant effect across tapping only for the visual modality (Visual Tapping: $M = 4.884.$, $SD = 1.853$; Visual Non-Tapping: $M = 3.315$, $SD = 1.67$; $p = 0.01$) (figure 4.5b).

Analysis of power at f0 for the left motor component data shows a main effect only for the tapping conditions $F(1,16) = 20.315$, $p < 0.001$, $n_p^2 = 0.559$. Post-hoc comparisons across tapping conditions show f0 power from the auditory non-tapping condition ($M = 1.525$, $SD = 2.588$) was lower than for the auditory tapping condition ($M = 4.823$, $SD = 4.078$) $p = 0.014$, and f0 power for the visual non-tapping condition ($M = 1.996$, $SD = 3.433$) was also lower than f0 power for visual tapping ($M = 5.559$, $SD = 3.367$) $p < 0.001$ (figure 4.4a).

Examination of the scalp topography of f0 power indicates power peaking in the frontal-central region for auditory conditions, with stronger activity for the auditory tapping condition than the auditory not-tapping condition. Similar activity in the topography is seen in the visual conditions except there is additional stronger activity peaking over the posterior regions that does not appear to change between tapping conditions. (figure 4.4c)

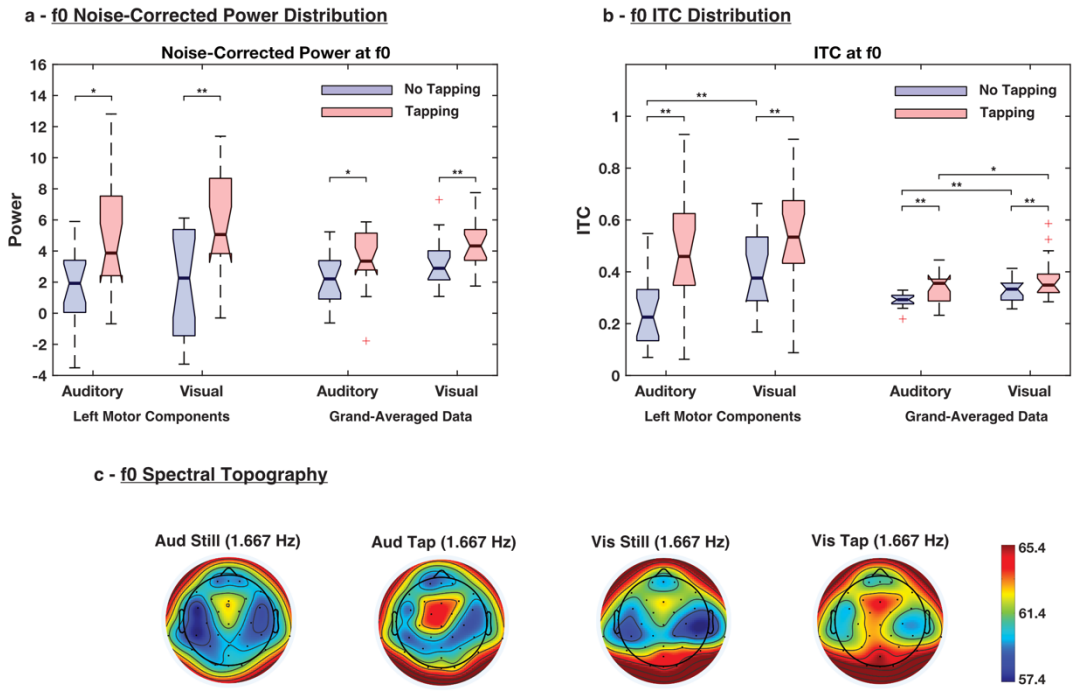

Fig 4.4. Distribution of noise-corrected power at f0 (a) and f0 ITC (b). Scalp topography is shown of spectral power at f0 across conditions from channel data (c). The center line of each box depicts the median and the notches reflect the 95% confidence interval (a & b). * = $p < 0.05$. ** = $p < 0.01$. In the spectral topography plot (c), both auditory and visual modalities show fontal-central activity that is strongest in the tapping conditions, with relatively weak power over the left and right motor regions.

4.3.4 ITC

Analysis of ITC for grand averaged data revealed main effects for modality $F(1,16) = 8.835$, $p = 0.009$, $n_p^2 = 0.356$, and for the tap condition $F(1,16) = 15.702$, $p = 0.001$, $n_p^2 = 0.495$. There was no significant effect of music training. Post-hoc comparisons across modalities revealed that non-tapping auditory ITC ($M = 0.291$, $SD = .027$) was lower than non-tapping visual ITC ($M = 0.329$, $SD = 0.045$), $p = 0.007$, and tapping auditory ITC ($M = 0.34$, $SD = 0.06$) was also lower than tapping visual ITC ($M = 0.375$, $SD = 0.083$), $p = 0.048$. Comparisons across tapping conditions revealed that tapping resulted in higher ITC than non-tapping for both auditory ($p = 0.004$), and visual ($p = 0.005$) modalities (figure 4.4b)

Analysis of ITC for the left motor components data revealed main effects for modality $F(1,16) = 5.366$, $p = 0.034$, $n_p^2 = 0.251$, and for the tap condition $F(1,16) = 17.659$, $p < 0.001$, $n_p^2 = 0.525$. Post-hoc comparisons across modalities revealed that non-tapping auditory ITC ($M = 0.246$, $SD = .136$) was lower than non-tapping visual ITC ($M = 0.398$, $SD = 0.152$), $p = 0.005$, but only for non-musicians (Auditory Non-Tapping: $M = 0.255$, $SD = 0.136$; Visual Non-Tapping: $M = 0.431$, $SD = 0.15$; $p = 0.01$). Comparisons across tapping conditions revealed that tapping resulted in higher ITC for both auditory ($p = 0.003$), and visual ($p = 0.006$) modalities compared to non-tapping, but

this effect was only seen in musicians (Auditory Tapping: $M = 0.563$, $SD = 0.241$; Auditory Non-Tapping: $M = 0.234$, $SD = 0.144$; $p = 0.007$). (Visual Tapping: $M = 0.569$, $SD = 0.204$; Visual Non-Tapping: $M = 0.357$, $SD = 0.154$; $p = 0.008$). (figures 4.4b & 5a)

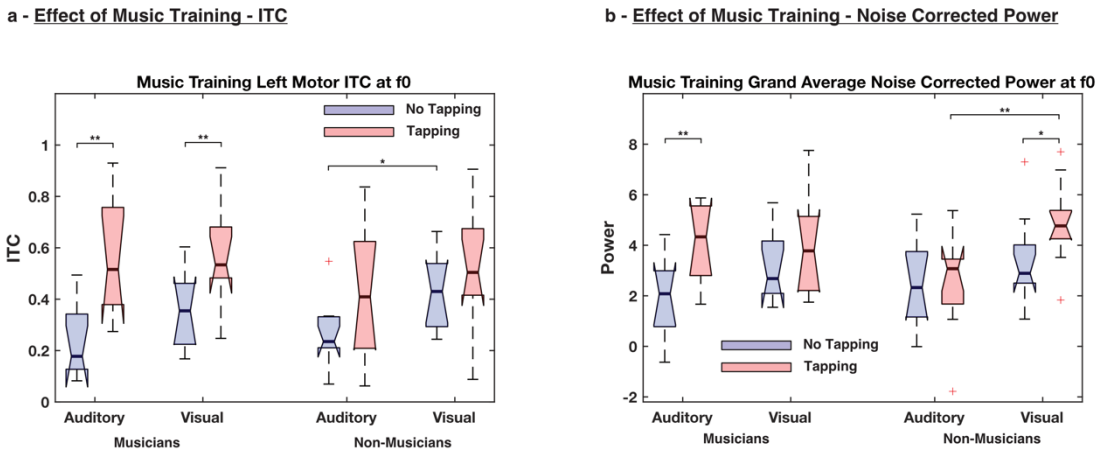

Fig 4.5. Differences between musicians and non-musicians in f0 ITC for the left motor components (a) and f0 noise-corrected grand-averaged power (b). The center line of each box in each box plot depicts the median and the notches reflect the 95% confidence interval. While no direct differences were seen between musicians and non-musicians, tapping in synchrony to auditory rhythms had a greater effect in f0 activity than compared to non-musicians as seen in ITC in the left motor components (a) and in the noise-corrected grand-averaged data (b)

4.4 Discussion

4.4.1 Summary of Results

In this experiment, we compared the effects of synchronizing to, or passively attending, auditory and visual rhythms on neural activations at the beat frequency and on mu rhythms. Our results show clear activation of the beat frequency for both auditory and visual rhythms across both ITC and noise-corrected power, suggesting both modalities can entrain rhythms at the beat frequency in neural populations (figure 4.3). We additionally show strong differential activation at the beat frequency and in mu power between tapping in synchrony to auditory and visual rhythms compared to passively attending the rhythms, where tapping in synchrony increases both power and phase-coherence at the beat frequency (figure 4.4), while decreasing mu power (figure 4.2). Surprisingly, we find evidence of stronger induced activation at the beat frequency from visual rhythms over auditory rhythms, most prominently in ITC measures, yet see no evidence of differential activation of mu rhythms across modalities. Although we do report greater auditory activity compared to visual activity in mu range for the grand averaged data, it is likely this result is due to increased alpha power over visual cortex specific to the auditory task (figure 4.2b). This would be expected given posterior alpha is known to decrease during tasks requiring visual attention (Fox & Snyder, 2011; Niedermeyer, 1997), such as in the visual conditions of this studly. Inspections of the

spectral topography plots of power at f0 indicate that f0 power is most modulated by tapping in the frontal-central regions for both modalities, while both visual conditions show relatively high f0 power posteriorly (figure 4.4c). While we make no direct statistical comparisons between the activity from the left-motor components and grand-averaged data, it does appear that power at the beat frequency is seen in the motor components clearly only when tapping, as opposed to in all cases in the grand averaged data (figures 4.3a & 4.3b). Yet when looking at the ITC at f0, there appears to be stronger activation for all conditions in the motor components compared to the grand averaged data (figures 4.3c & 4.3d). Finally, we find no main effects of music training in our measures, yet we do find that musicians tapping in synchrony to rhythms appears to have a stronger effect on f0 activity than compared to non-musicians, especially in the auditory modality (figure 4.5).

4.4.2 Mu Power

Mu rhythm activity is thought to increase during movement suppression (Pfurtscheller & Neuper, 1994; Pfurtscheller et al., 1997), and has been argued that it can serve as a marker for rhythmic timing processing (Ross et al., 2016a), based on the idea that the motor system is simulating the beat (Iversen & Patel, 2014; Ross et al., 2016b), and that the work of simulating the beat may require suppression to prevent movements related to beat simulation. Existing work made it unclear if attending rhythms would result in mu ERS or ERD however – one study has reported ERD (Wu et al., 2016).), yet another study suggests otherwise (Ross et al., 2016a). While this experiment cannot answer the question of whether rhythms increase mu activity directly as we had no quiet condition to test against, our results provide further insight into the role of mu activity.

It is well known that humans synchronize with greater precision and across a greater range of tempi to auditory rhythms than to visual rhythms (see Repp & Su, 2013 for review). One prominent explanation is that the auditory system is tightly tied into the motor system to use the motor system for auditory rhythmic timing processing (Iversen & Patel, 2014; Ross et al., 2016b), while more recent work has suggested that the visual system is able to do some rhythmic timing in house (Comstock & Balasubramaniam, 2018; Comstock et al., 2021). Under those conditions, and given the assumptions of beat stimulation, one would expect auditory rhythms to elicit stronger mu activity than visual rhythms, yet we find no difference. Further, if the motor system and auditory rhythm timing are tightly tied together, and that mu activity can serve as a marker of rhythmic processing, it could be expected that musical training would result in greater mu activity than compared to non-musicians. Yet, we find no significant effect on mu activity from music training and therefore cannot confirm that expectation.

These results can be interpreted in several ways. The strongest interpretation is as evidence against the idea of beat simulation within the motor cortex. Another possibility that cannot be dismissed is that isochronous rhythms used in this study did not modulate mu activity in the same way music would. This could be due to the isochronous rhythms simply not driving motor beat simulation in a way that would differentiate between auditory and visual rhythms. Additionally, given that motor imagery has been shown to reduce mu activity (McFarland et al., 2000), and exposing pianists to piano pieces that have played will result in mu ERD (Wu et al., 2016), it is possible that the simple

isochronous rhythms induced motor imagery for both auditory and visual rhythms, therefore counteracting any mu ERS due to inhibition of movement from beat simulation. A final consideration on the mu results is that mu activity arising from the primary motor cortex is known to be modulated by the premotor areas including SMA (Ulloa & Pineda, 2007). Given that the SMA has been implicated in rhythm processing (Iversen & Patel, 2014; Merchant & Honing, 2014; Ross et al., 2016b), and since this study did not isolate pre-motor or SMA activity, it may be pre-motor activity would show the differentiation we hypothesized between modalities.

4.4.3 Activity at f0

Numerous studies have shown neural activation at the beat frequency of a rhythm in power and phase coherence measures using a frequency tagging approach (Nozaradan et al., 2011, 2012a, 2012b, 2015; Doelling & Poeppel, 2015). Likewise, visual rhythms have been long known to entrain to flashing rhythms as (Vialatte et al., 2010).), although visual rhythms studies usually look at activity higher frequency ranges, e.g. 10 to 12 Hz, rather than at the lower frequencies used for SMS or auditory rhythm perception tasks. A recent study (Varlet et al 2020) has shown that audio-visual rhythms can elicit beta-coherence between EMG activity from a subject's non-moving finger and EEG activity over the cortical motor region that was stronger than elicited by audio rhythms alone, suggesting that information of the timing of the visual rhythms is present in the motor system, even when the subject is instructed to remain motionless. Counter to our hypothesis, the f0 activity localized to the left motor cortex in the current study show greater ITC for visual rhythms than auditory rhythms arising from the selected motor components, although we find no modality differences in the motor component data in mu activation or in power. In the grand-averaged data there is also evidence of greater f0 activity for visual rhythms in both ITC and in noise corrected power. This finding suggests that differences in SMS and rhythm perception capabilities between auditory and visual rhythms is not due greater entrainment ability of one modality over the other, but rather in how that entrained activity is utilized.

We consider it an interesting finding that the modality differences seen in left motor ITC were significant only in non-musicians, and only in the non-tapping conditions, which is similar to effects seen in the grand-average noise-corrected power data, where only non-musicians showed significant modality differences, but only in tapping conditions. Likewise, differences between tapping and non-tapping conditions were significant in left-motor ITC only in trained musicians, and significant for both modalities. While not conclusive, as we measured no main effect of music training, nor any significant differences between the musician and non-musician groups, these findings suggest music training allows musicians to entrain more equally to auditory and visual rhythms than non-musicians, while also benefitting more strongly from engaging the motor system during SMS than non-musicians. One curious result from the grand averaged noise corrected power is that tap condition differences were significant for musicians only for auditory rhythms, while significant for non-musicians only for visual rhythms. Inspection of the data (figure 4.5b) suggests that the boost to entrainment from tapping to auditory rhythms was greater than that experienced by non-musicians, which would be expected given the training musicians have in entraining to auditory rhythms.

Why non-musicians would show a difference across tapping conditions for visual rhythms while musicians do not show that difference is unclear, however.

4.4.4 Limitations and Future Directions

One major limitation of this study is in its use of isochronous rhythms, and interpreting the resultant frequency domain activity. There has been controversy over whether or not activity at the beat frequency of a rhythm represents neural entrainment to a rhythm, or if the activity at the beat frequency is essentially an artifact from applying an FFT to rhythmic stimulus to evoked potentials (Capilla et al., 2011; Novembre & Iannetti, 2018; Rajendran & Schnupp, 2019). One way around the issues is to use syncopated or metered stimuli that would produce little or no increase in frequency power at the frequency of interest (Lenc et al., 2019, Nozaradan et al., 2018). As this study was designed to use as simple stimuli as possible, one needs to take care to not over interpret the results. Indeed, it is possible that greater f0 activity seen in visual rhythms compared to auditory rhythms is simply due to the evoked potentials to visual stimuli being generally more pronounced than those evoked from similar auditory stimuli. However, this concern applies primarily only to the grand-averaged f0 ITC and noise-corrected power, as it is unlikely that the activity measured from the components isolated in the left motor cortex would contain sensory evoked artifacts as those components are not sourced in either auditory or visual regions.

Another concern for this study was that the musically trained participants had a wide range of experience, and none were professional musicians. Even so, an effect of music training on our makers of rhythm processing was apparent. We suspect that comparing professional musicians with non-musicians may produce much clearer results, as well as provide further insight into how music training may carryover timing processing from the auditory modality to the visual modality.

4.5 Conclusions

We showed that mu rhythm activity in response to passively attending and synchronizing to simple isochronous rhythms is not modulated by the modality of that rhythm. Further we find evidence that entrainment to visual rhythms may be stronger than auditory rhythms, even though humans are generally able to perceive and synchronize to auditory rhythms more precisely than to visual rhythms. This suggests that how the entrainment activity is utilized by the motor system is just as important as the entrainment activity itself. Finally, we see evidence that music training can alter measures of entrainment, although the exact nature of the interaction is not clear. These results suggest further investigation is needed into both the differences between auditory and visual rhythm processing mechanisms, and the effect of music training on those mechanisms.

Epilogue

The primary question motivating this dissertation was whether or not there is a common mechanism for auditory and visual rhythm timing. In chapter 1 we showed that previous research indicated activity related to visual timing has been found arising from the visual system, and suggested this may be evidence of a visual specific timing mechanism. In chapter 2 we showed evidence of the visual system reacting to timing errors in rhythmic visual flashes, suggesting that timing information is being processed within the visual system. Importantly, that timing activity did not correspond to a response-based error correction signal, nor improved error correction in tapping in the way equivalent auditory timing information did. This finding suggests the visual system and motor system are not effectively communicating rhythmic timing information as would be expected if the two systems were working in concert to process the timing of visual flashing rhythms.

Chapter 3 showed evidence of the prediction of the timing of flashes in the visual system in the beta-band. We interpret the beta-band modulation as attentional modulation of the sensory cortices to aid in the processing of imminent predicted events. As a similar pattern of activity in the beta band has been found emanating from the auditory cortex in response to auditory rhythms (Fujioka et al, 2009, 2015), the visual beta band activity does not by itself constitute clear evidence of visual system specific rhythm timing processing. Fujioka et al, (2015) proposed that the auditory beta modulation is driven due by interaction between the motor system and auditory system to modulate attention in the auditory cortex. Given the general lower precision of visual rhythm perception, it would be expected that visual system beta modulation would be less pronounced compared to auditory beta modulation. The striking strength and clarity of the visual beta modulation from posterior sources suggests that the visual system is perfectly capable of rhythm timing, but that rhythm timing is not able to be utilized in the way that auditory rhythm timing is. The additional results in the chapter showing modality specific timing activation across different regions of the brain provide further evidence in line with separate auditory and visual networks of timing activity.

In chapter 4 we show evidence of neural entrainment of visual rhythms within the motor system that is as strong, if not stronger than the entrainment induced by auditory rhythms. This finding was surprising considering the difficultly with which humans synchronize to visual flashing rhythms compared to comparable auditory rhythms. With that in mind, we suggest our findings indicate that visual rhythms are easily entrained and communicated to the motor system, yet the motor system is unable to utilize that entrainment in the same fashion that auditory induced neural entrainment is. This interpretation is bolstered by the finding that the visual system is able to phase lock with up to 100 Hz visual flashing rhythms (Williams et al., 2004), which is well outside the normal range of SMS (Repp & Su, 2013), and therefore well outside of the range likely to be driven by the motor system.

The evidence of modality specific rhythmic timing presented in these experiments leaves many unanswered questions. The biggest of which is why the visual system's entrainment of visual rhythms are not able to be properly utilized by the motor system? One important factor likely lies in the notion of modality appropriateness of the stimuli

that was briefly touched upon in chapter 1. Synchronization to rhythmic moving visual stimuli is improved over flashing stimuli of equivalent rhythm, likewise, synchronization to an auditory metronome is more precise than compared to a rhythmically equivalent frequency modulated siren (Hove et al., 2013b). In this case, as the synchronization capability was modulated by stimuli appropriateness, so was activity in the putamen, where greater activity corresponded to better synchronization and vise-versa. Another example of modality appropriateness can be seen in patients with Parkinson's disease, where exposure to auditory rhythms can improve patients gait more than visual flashing rhythms (Rochester et al., 2005; Arias and Cudeiro, 2008). Visual spatial rhythms, as in lines marked out on the floor, also improve the gait of Parkinson's patients, but the effect requires constant and dynamic updating of the stimuli (Azulay et al., 1999). When the lines are presented intermittently through strobe light effect, the improved gait largely goes away. These cases make it clear that the visual system interfaces with the motor system much more effectively with continuous timing information, in form of moving stimuli, than with discrete visual timing events, such as flashes. Likewise, the auditory system interfaces with the motor system more effectively with discrete timing events, such as a metronome, than with continuous timing events, such as a frequency modulated siren. In the cases where stimuli are modality appropriate, the sensory system and the motor system work together, with the motor system likely providing top-down timing prediction, and the sensory system providing bottom-up updates that correct for errors in timing. This experiment presented in chapter 2 expresses this process neatly, where errors induced into an auditory metronome resulted in a marked motor system response and updated prediction. In the visual case, there was a response to the timing error from the visual system, but the visual system was not able to effectively communicate that error to the motor system, resulting in no pronounced correction.

I postulate that the reason moving visual rhythms are more appropriate than flashing rhythms is due to visual-motor interaction being optimized for actively navigating the environment rather than extracting temporal information. The processing of timing information needed for updating motor actions is based on the continuous feedback from the visual system, allowing for dynamic corrections. Since discrete visual timing events, like flashing rhythms, are relatively rare in the environment, and much more so in our evolutionary past, there is no need for the kind of optimized timing systems seen in auditory rhythm timing. Yet a mechanistic explanation for this phenomenon is still missing.

In addition to a mechanistic explanation for the problem of how modality appropriateness effects rhythm timing, there are several questions that will need to be answered by future work. One question, mentioned earlier in chapter 1, is if there are multiple timing systems in the brain, how is one timing system chosen over another for a given timing event. Hass and Durstewitz (2016) suggest that the best timing mechanism would be determined in a Bayesian optimal manner, which is backed up by work showing that when multimodal timing information is present that the most optimal modality is utilized (Ernst and Banks, 2002). This would suggest that timing information is chosen from one modality at a time, however, there is evidence of increased neural entrainment when timing information is presented from multimodal auditory and visual rhythms compared to single modality rhythms (Nozaradan et al., 2012b; Varlet, et al.,

2020). The results from the experiment in chapter 4 suggest that neural entrainment of a rhythm is not enough however. One explanation for why this may be is presented in model of the role of the motor system in beat perception that suggests both phase and tempo need to be taken into account, and that confidence in beat tempo and phase are expressed by striatal dopamine levels in auditory-motor timing (Cannon & Patel, 2020). This model further postulates that the SMA is involved in the relative timing between auditory events that is updated at each event. As the auditory system is already utilizing the motor system for rhythm timing, it makes sense that SMS to auditory rhythms can be performed with the precision that it is. It also suggests that if the visual system can utilize the motor system for timing, SMS to visual rhythms would improve as well. The finding that moving visual rhythms improve SMS precision over flashing rhythms, yet don't show that level of improvement over flashing rhythms during pure rhythm perception tests (Silva & Castro, 2016) suggests it is possible for the visual system to use the motor-system for timing, but that it is not always the case. It is likely then, that confidence is lower for flashing visual rhythms compared to auditory rhythms, or moving visual rhythms, as the SMA is better served to processes the relative timing processing needed to compute phase.

The findings in this dissertation may have implications for several areas beyond just rhythm perception and SMS tasks. There has long been a debate about the nature of time perception itself, with some suggesting a single central mechanism for time perception, others suggesting multiple specialized mechanisms, and still others positing a distributed mechanism (Ivry & Spencer, 2004). A hybrid possibility has also been suggested in which there are overlapping networks involved in the processing of time perception and timing processing where the network is modulated based on modality and context of the timing task (Wiener et al., 2010, Wiener & Kanai, 2014). This framework posits the SMA and inferior frontal gyrus as central to all timing tasks, with sub-second timing involving sub-cortical structures, supra-second timing involving cortical structures, and the sensory cortices involved dependent on sensory modality of the timing. The experimental results indicating the visual rhythm processing within the visual system presented in this dissertation provide evidence supporting the idea of a hybrid distributed timing network.

Another area outside of SMS and rhythm perception to consider is that of language processing. The hierarchical structure of language has been shown to be reflected in the temporal aspects of language processing in the cortex (Ding et al., 2016, 2017). Presenting auditory recordings of sentences at a fixed rate where each syllable has a fixed results in increased evoked power at the syllable, phrase, and sentence level. Crucially, presenting similar recordings of nonsense syllables resulted in increased evoked power only at the syllable level. This hierarchical processing is similar to the hierarchical processing seen in the processing of metered rhythms (Nozaradan et al., 2011, 2012a), and fits well the notion that rhythm processing developed through vocal learning as presented in the ASAP hypothesis (Patel & Iversen, 2014). However, studies looking for evidence of hierarchical processing during the processing of written language have yet to presented. Likewise, studies investigating the visual systems ability to process metered rhythms are also currently lacking. If it is the case that the hierarchical processing evident while processing spoken language is due to language processing and

not simple auditory encoding, as suggested by the results from Ding et al., (2016, 2017), it could be expected that similar results would be found during the processing of written language.

While the work presented here provides evidence of modality specific rhythmic timing, and the speculation provided suggests a possible partial explanation, there are still experiments that should be done to strengthen the claim. For example, the experiment in chapter 3 showed beta activity rising in anticipation of a visual flash, but only a single rhythm was used. If beta activity is reflecting prediction, then an experiment using several rhythms of different tempi should result in the rate that beta rises to be modulated by the tempo of the rhythm. Another needed experiment is an error correction experiment using moving visual rhythms. If the visual system can utilize the motor system during an SMS task to moving rhythms, we should see error correction responses similar to those seen in the auditory error correction task both behaviorally and in neural responses. Using the same stimuli in purely perceptual experiment should provide different results however, where there should be a clear response to errors in the auditory rhythm, yet little response to errors in the moving visual rhythms. A further useful experiment would be to use a syncopated visual rhythm to measure visual neural entrainment against. Ideally, the stimuli should be designed so that a frequency analysis would reveal no power at the beat frequency, as that way any neural activity measured at the beat frequency could not be due the rhythmic transient evoked responses, and instead must be the result of neural entrainment.

One area where experiments would be useful to further uncover the mechanisms of rhythm timing is in the role of the SMA. As it seems the SMA plays a key role in how the motor system computes timing, it would be advantageous to isolate SMA activity in response to auditory and visual rhythm perception. An approach similar to how motor activity was isolated using mu rhythms in the fourth chapter of this dissertation may be useful to determine how the SMA is being activated during different types of visual rhythm perception tasks. This may be especially important as the SMA has been implicated in nearly all types of timing (Wiener et al., 2010). If the SMA is involved in all types of timing, it may be that both auditory and visual timing would elicit similar responses in SMA activity, which would provide evidence of overlapping timing networks.

One shortcoming of the experiments described so far is they lack causal explanatory power. Measuring neural activation during a rhythm timing task does not prove that activation is a necessary component of rhythm processing. Historically, this issue has been solved by studying lesion patients. For example, a study looking at the role of subcortical structures on rhythm processing involving two groups of patients: one with basal ganglia lesions, and the other with cerebellar lesions. In this study, cerebellar patients showed poorer rhythm tracking for fast rhythms, indicating the cerebellum is important for fast rhythm processing, while basal ganglia patients showed poorer rhythm tracking for complex rhythms, indicating the basal ganglia are important for processing complex and metered rhythms (Nozaradan et al., 2017). While lesion studies are useful, access to patients with lesions is not always practical, additionally, neural lesions are rarely in a clearly defined region or structure that allows for clear interpretation. A way around the issue is to use stimulation techniques such as transcranial magnetic

stimulation (TMS), which can be used to disrupt, or down-regulate cortical structures in the brain. For example, a study using TMS has been shown that the posterior parietal cortex plays a role in phase processing of auditory through down-regulating that area and measuring performance in a phase detection task (Ross, et al., 2018). A useful experiment to understand the difference in auditory and visual rhythm processing would be to use TMS to down-regulate motor structures and then measure neural entrainment using EEG in response to auditory and visual rhythms as was done in chapter 4. If the entrainment response is reduced after motor system down-regulation, it would provide clear evidence of a role for the motor system in rhythm processing.

The experiments I have just described may strengthen the claims made in this dissertation, but the mechanistic questions can likely only be solved through a combination of further empirical studies (including patient and animal studies) and modelling studies. I have attempted to lay out a few experiments that may provide a means to better understand the mechanisms involved, at least at the neural circuit level. Ultimately though, I believe that the mechanics of auditory and visual timing are likely more similar than not, even though I have shown evidence of modality specific timing. I must therefore conclude that full understanding of how visual rhythm processing works, will likely also involve full understanding of auditory rhythm processing, such that progress in one domain can be counted as progress in both.

References

Abbott, N. T., & Shahin, A. J. (2018). Cross-modal phonetic encoding facilitates the McGurk illusion and phonemic restoration. *Journal of neurophysiology*, *120*(6), 2988-3000.

Addyman, C., French, R. M., & Thomas, E. (2016). Computational models of interval timing. *Current Opinion in Behavioral Sciences*, *8*, 140-146.

Araneda, R., Renier, L., Ebner-Karestinos, D., Dricot, L., & De Volder, A. G. (2017). Hearing, feeling or seeing a beat recruits a supramodal network in the auditory dorsal stream. *European Journal of Neuroscience*, *45*(11), 1439-1450.

Arias, P., & Cudeiro, J. (2008). Effects of rhythmic sensory stimulation (auditory, visual) on gait in Parkinson's disease patients. *Experimental Brain Research*, *186*(4), 589-601.

Arnal, L. H., Doelling, K. B., & Poeppel, D. (2014). Delta–beta coupled oscillations underlie temporal prediction accuracy. *Cerebral Cortex*, *25*(9), 3077-3085.

Arnal, L. H., & Giraud, A. L. (2012). Cortical oscillations and sensory predictions. *Trends in cognitive sciences*, *16*(7), 390-398.

Arnal, L. H., Wyart, V., & Giraud, A. L. (2011). Transitions in neural oscillations reflect prediction errors generated in audiovisual speech. *Nature neuroscience*, *14*(6), 797.

Azulay, J. P., Mesure, S., Amblard, B., Blin, O., Sangla, I., & Pouget, J. (1999). Visual control of locomotion in Parkinson's disease. *Brain*, *122*(1), 111-120.

Balasubramaniam, R., Wing, A. M., & Daffertshofer, A. (2004). Keeping with the beat: movement trajectories contribute to movement timing. *Experimental Brain Research*, *159*(1), 129-134.

Bangert, M., & Altenmüller, E. O. (2003). Mapping perception to action in piano practice: a longitudinal DC-EEG study. *BMC neuroscience*, *4*(1), 1-14.

Bastos, A. M., Vezoli, J., Bosman, C. A., Schoffelen, J. M., Oostenveld, R., Dowdall, J. R., ... & Fries, P. (2015). Visual areas exert feedforward and feedback influences through distinct frequency channels. *Neuron*, *85*(2), 390-401.

Bauer, A. K. R., Bleichner, M. G., Jaeger, M., Thorne, J. D., & Debener, S. (2018). Dynamic phase alignment of ongoing auditory cortex oscillations. *Neuroimage*, *167*, 396-407.

Benjamini, Y., & Hochberg, Y. (1995). Controlling the false discovery rate: a practical and powerful approach to multiple testing. *Journal of the Royal statistical society: series B (Methodological)*, *57*(1), 289-300.

Bijsterbosch, J. D., Lee, K. H., Hunter, M. D., Tsoi, D. T., Lankappa, S., Wilkinson, I. D., ... & Woodruff, P. W. (2011). The role of the cerebellum in sub-and supraliminal error correction during sensorimotor synchronization: evidence from fMRI and TMS. *Journal of Cognitive Neuroscience*, *23*(5), 1100-1112.

Botvinick, M. M., Braver, T. S., Barch, D. M., Carter, C. S., & Cohen, J. D. (2001). Conflict monitoring and cognitive control. *Psychological review*, *108*(3), 624.

Botvinick, M. M., Cohen, J. D., & Carter, C. S. (2004). Conflict monitoring and anterior cingulate cortex: an update. *Trends in cognitive sciences*, *8*(12), 539-546.

Brown, S., & Jordania, J. (2013). Universals in the world's musics. *Psychology of Music*, *41*(2), 229-248.

Cameron, D. J., Pickett, K. A., Earhart, G. M., & Grahn, J. A. (2016). The effect of dopaminergic medication on beat-based auditory timing in Parkinson's disease. *Frontiers in neurology*, *7*.

Cannon, J. J., & Patel, A. D. (2020). How beat perception co-opts motor neurophysiology. *Trends in Cognitive Sciences*.

Capilla, A., Pazo-Alvarez, P., Darriba, A., Campo, P., & Gross, J. (2011). Steady-state visual evoked potentials can be explained by temporal superposition of transient event-related responses. *PloS one*, *6*(1), e14543.

Chang, C. Y., Hsu, S. H., Pion-Tonachini, L., & Jung, T. P. (2018, July). Evaluation of artifact subspace reconstruction for automatic EEG artifact removal. In *2018 40th Annual International Conference of the IEEE Engineering in Medicine and Biology Society (EMBC)* (pp. 1242-1245). IEEE.

Chen, J. L., Penhune, V. B., & Zatorre, R. J. (2008a). Listening to musical rhythms recruits motor regions of the brain. *Cerebral cortex*, *18*(12), 2844-2854.

Chen, J. L., Penhune, V. B., & Zatorre, R. J. (2008b). Moving on time: brain network for auditory-motor synchronization is modulated by rhythm complexity and musical training. *Journal of cognitive neuroscience*, *20*(2), 226-239.

Chen, Y., Repp, B. H., & Patel, A. D. (2002). Spectral decomposition of variability in synchronization and continuation tapping: Comparisons between auditory and visual pacing and feedback conditions. *Human movement science*, *21*(4), 515-532.

Chen, R., Yaseen, Z., Cohen, L. G., & Hallett, M. (1998). Time course of corticospinal excitability in reaction time and self-paced movements. *Annals of neurology*, *44*(3), 317-325.

Chen, J. L., Zatorre, R. J., & Penhune, V. B. (2006). Interactions between auditory and dorsal premotor cortex during synchronization to musical rhythms. *Neuroimage*, *32*(4), 1771-1781.

Collective, B. S. M., & Shaw, D. (2012, February). Makey Makey: improvising tangible and nature-based user interfaces. In *Proceedings of the sixth international conference on tangible, embedded and embodied interaction* (pp. 367-370). ACM.

Comstock, D., & Balasubramaniam, R (2017a). *Differences in Neural Correlates of Error Correction in Auditory and Visual Sensorimotor Synchronization*. Poster presented at the 24th Annual Cognitive Neuroscience Society Meeting.

Comstock, D., & Balasubramaniam, R. (2017b) *Beta-Band Response Synchronizes and Predicts Rhythmic Flashing Visual Stimuli*. Poster presented at the 47th Annual Society for Neuroscience Meeting.

Comstock, D.C. & Balasubramaniam, R. (2018). Neural responses to perturbations in visual
and auditory metronomes during sensorimotor synchronization. *Neuropsychologia* http://doi.org/10.1016/j.neuropsychologia.2018.05.013.

Comstock, D. C., Hove, M. J., & Balasubramaniam, R. (2018). Sensorimotor synchronization with auditory and visual modalities: behavioral and neural differences. *Frontiers in computational neuroscience*, *12*, 53.

Comstock, D. C., Ross, J. M., & Balasubramaniam, R. (2021). Modality-specific frequency band activity during neural entrainment to auditory and visual rhythms. *European Journal of Neuroscience, (in press)*

Cook, P., Rouse, A., Wilson, M., & Reichmuth, C. (2013). A California sea lion (Zalophus californianus) can keep the beat: motor entrainment to rhythmic auditory stimuli in a non vocal mimic. *Journal of Comparative Psychology*, *127*(4), 412.

Coull, J. T., Cheng, R. K., & Meck, W. H. (2011). Neuroanatomical and neurochemical substrates of timing. *Neuropsychopharmacology*, *36*(1), 3.

Coull, J. T., Vidal, F., & Burle, B. (2016). When to act, or not to act: that's the SMA's question. *Current Opinion in Behavioral Sciences*, *8*, 14-21.

Davie, C. A. (2008). A review of Parkinson's disease. *British medical bulletin*, *86*(1), 109-127.

Ding, N., Melloni, L., Yang, A., Wang, Y., Zhang, W., & Poeppel, D. (2017). Characterizing neural entrainment to hierarchical linguistic units using electroencephalography (EEG). *Frontiers in human neuroscience*, *11*, 481.

Ding, N., Melloni, L., Zhang, H., Tian, X., & Poeppel, D. (2016). Cortical tracking of hierarchical linguistic structures in connected speech. *Nature neuroscience*, *19*(1), 158-164.

Delorme, A., & Makeig, S. (2004). EEGLAB: an open source toolbox for analysis of single-trial EEG dynamics including independent component analysis. *Journal of neuroscience methods*, *134*(1), 9-21.

Delorme, A., Palmer, J., Onton, J., Oostenveld, R., & Makeig, S. (2012). Independent EEG sources are dipolar. *PloS one*, *7*(2), e30135.

Destoky, F., Philippe, M., Bertels, J., Verhasselt, M., Coquelet, N., Vander Ghinst, M., ... & Bourguignon, M. (2019). Comparing the potential of MEG and EEG to uncover brain tracking of speech temporal envelope. *Neuroimage, 184*, 201-213.

Doelling, K. B., & Poeppel, D. (2015). Cortical entrainment to music and its modulation by expertise. *Proceedings of the National Academy of Sciences*, *112*(45), E6233-E6242.

Doumas, M., Praamstra, P., & Wing, A. M. (2005). Low frequency rTMS effects on sensorimotor synchronization. *Experimental brain research*, *167*(2), 238-245.

Doyère, V., & El Massioui, N. (2016). A subcortical circuit for time and action: insights from animal research. *Current Opinion in Behavioral Sciences*, *8*, 147-152.

Endrass, T., Reuter, B., & Kathmann, N. (2007). ERP correlates of conscious error recognition: aware and unaware errors in an antisaccade task. *European Journal of Neuroscience*, *26*(6), 1714-1720.

Engel, A. K., & Fries, P. (2010). Beta-band oscillations—signalling the status quo?. *Current opinion in neurobiology*, *20*(2), 156-165.

Ernst, M. O., & Banks, M. S. (2002). Humans integrate visual and haptic information in a statistically optimal fashion. *Nature*, *415*(6870), 429.

Falkenstein, M., Hoormann, J., Christ, S., & Hohnsbein, J. (2000). ERP components on reaction errors and their functional significance: a tutorial. *Biological psychology*, *51*(2), 87-107.

Fitch, W. (2016). Dance, music, meter and groove: a forgotten partnership. *Frontiers in human neuroscience*, *10*, 64.

Ford, J. M., & Hillyard, S. A. (1981). Event-Related Potentials (ERPs) to Interruptions of a Steady Rhythm. *Psychophysiology*, *18*(3), 322-330.

Foxe, J. J., & Snyder, A. C. (2011). The role of alpha-band brain oscillations as a sensory suppression mechanism during selective attention. *Frontiers in psychology*, *2*, 154.

Fujioka, T., Ross, B., & Trainor, L. J. (2015). Beta-band oscillations represent auditory beat and its metrical hierarchy in perception and imagery. *Journal of neuroscience*, *35*(45), 15187-15198.

Fujioka, T., Trainor, L. J., Large, E. W., & Ross, B. (2009). Beta and gamma rhythms in human auditory cortex during musical beat processing. *Annals of the New York Academy of Sciences*, *1169*(1), 89-92.

Fujioka, T., Trainor, L. J., Large, E. W., & Ross, B. (2012). Internalized timing of isochronous sounds is represented in neuromagnetic beta oscillations. *Journal of Neuroscience*, *32*(5), 1791-1802.

Gan, L., Huang, Y., Zhou, L., Qian, C., & Wu, X. (2015). Synchronization to a bouncing ball with a realistic motion trajectory. *Scientific reports*, *5*, 11974.

Gelman, A., & Stern, H. (2006). The difference between "significant" and "not significant" is not itself statistically significant. *The American Statistician*, *60*(4), 328-331.

Grahn, J. A., & Brett, M. (2007). Rhythm and beat perception in motor areas of the brain. *Journal of cognitive neuroscience*, *19*(5), 893-906.

Grahn, J. A., & Brett, M. (2009). Impairment of beat-based rhythm discrimination in Parkinson's disease. *Cortex*, *45*(1), 54-61.

Grahn, J. A., Henry, M. J., & McAuley, J. D. (2011). FMRI investigation of cross-modal interactions in beat perception: audition primes vision, but not vice versa. *Neuroimage*, *54*(2), 1231-1243.

Grahn, J. A., & Rowe, J. B. (2009). Feeling the beat: premotor and striatal interactions in musicians and nonmusicians during beat perception. *Journal of Neuroscience*, *29*(23), 7540-7548.

Gordon, C. L., Cobb, P. R., & Balasubramaniam, R. (2018). Recruitment of the motor system during music listening: An ALE meta-analysis of fMRI data. *PloS one*, *13*(11), e0207213.

Grube, M., Cooper, F. E., Chinnery, P. F., & Griffiths, T. D. (2010). Dissociation of duration-based and beat-based auditory timing in cerebellar degeneration. *Proceedings of the National Academy of Sciences*, *107*(25), 11597-11601.

Grube, M., Lee, K. H., Griffiths, T. D., Barker, A. T., & Woodruff, P. W. (2010). Transcranial magnetic theta-burst stimulation of the human cerebellum distinguishes absolute, duration-based from relative, beat-based perception of subsecond time intervals. *Frontiers in Psychology*, *1*, 171.

Gruzelier, J. H., Holmes, P., Hirst, L., Bulpin, K., Rahman, S., Van Run, C., & Leach, J. (2014). Replication of elite music performance enhancement following alpha/theta neurofeedback and application to novice performance and improvisation with SMR benefits. *Biological psychology*, *95*, 96-107.

Gu, B. M., van Rijn, H., & Meck, W. H. (2015). Oscillatory multiplexing of neural population codes for interval timing and working memory. *Neuroscience & Biobehavioral Reviews*, *48*, 160-185.

Gupta, D. S., & Chen, L. (2016). Brain oscillations in perception, timing and action. *Current Opinion in Behavioral Sciences*, *8*, 161-166.

Haegens, S., & Golumbic, E. Z. (2018). Rhythmic facilitation of sensory processing: a critical review. *Neuroscience & Biobehavioral Reviews*, *86*, 150-165.

Hagen, E. H., & Bryant, G. A. (2003). Music and dance as a coalition signaling system. *Human nature*, *14*(1), 21-51.

Hass, J., & Durstewitz, D. (2016). Time at the center, or time at the side? Assessing current models of time perception. *Current Opinion in Behavioral Sciences*, *8*, 238-244.

Hyman, J. M., Ma, L., Balaguer-Ballester, E., Durstewitz, D., & Seamans, J. K. (2012). Contextual encoding by ensembles of medial prefrontal cortex neurons. *Proceedings of the National Academy of Sciences*, *109*(13), 5086-5091.

Hove, M. J., Balasubramaniam, R., & Keller, P. E. (2014). The time course of phase correction: A kinematic investigation of motor adjustment to timing perturbations during sensorimotor synchronization. *Journal of Experimental Psychology: Human Perception and Performance*, *40*(6), 2243.

Hove, M. J., Fairhurst, M. T., Kotz, S. A., & Keller, P. E. (2013b). Synchronizing with auditory and visual rhythms: an fMRI assessment of modality differences and modality appropriateness. *Neuroimage*, *67*, 313-321.

Hove, M. J., Iversen, J. R., Zhang, A., & Repp, B. H. (2013a). Synchronization with competing visual and auditory rhythms: bouncing ball meets metronome. *Psychological Research*, *77*(4), 388-398.

Hove, M. J., & Keller, P. E. (2010). Spatiotemporal relations and movement trajectories in visuomotor synchronization. *Music Perception: An Interdisciplinary Journal*, *28*(1), 15-26.

Hove, M. J., Marie, C., Bruce, I. C., & Trainor, L. J. (2014). Superior time perception for lower musical pitch explains why bass-ranged instruments lay down musical rhythms. *Proceedings of the National Academy of Sciences*, *111*(28), 10383-10388.

Hove, M. J., Spivey, M. J., & Krumhansl, C. L. (2010). Compatibility of motion facilitates visuomotor synchronization. *Journal of Experimental Psychology: Human Perception and Performance*, *36*(6), 1525.

Iversen, J. R. (2016). In the Beginning Was the Beat: Evolutionary Origins of Musical Rhythm in Humans. In The Cambridge Companion to Percussion, Russel Hartenberger (ed), Cambridge University Press.

Iversen, J. R., & Balasubramaniam, R. (2016). Synchronization and temporal processing. *Current Opinion in Behavioral Sciences*, *8*, 175-180.

Iversen, J. R., Patel, A. D., Nicodemus, B., & Emmorey, K. (2015). Synchronization to auditory and visual rhythms in hearing and deaf individuals. *Cognition*, *134*, 232-244.

Iversen, J. R., Repp, B. H., & Patel, A. D. (2009). Top-down control of rhythm perception modulates early auditory responses. *Annals of the New York Academy of Sciences*, *1169*(1), 58-

Ivry, R. B., & Spencer, R. M. (2004). The neural representation of time. *Current opinion in neurobiology*, *14*(2), 225-232.

Janata, P., Tomic, S. T., & Haberman, J. M. (2012). Sensorimotor coupling in music and the psychology of the groove. *Journal of Experimental Psychology: General*, *141*(1), 54.

Jäncke, L., Loose, R., Lutz, K., Specht, K., & Shah, N. J. (2000). Cortical activations during paced finger-tapping applying visual and auditory pacing stimuli. *Cognitive Brain Research*, *10*(1-2), 51-66.

Jang, J., Jones, M., Milne, E., Wilson, D., & Lee, K. H. (2016). Contingent negative variation (CNV) associated with sensorimotor timing error correction. *NeuroImage*, *127*, 58-66.

Jantzen, K. J., Ratcliff, B. R., & Jantzen, M. G. (2017). Cortical Networks for Correcting Errors in Sensorimotor Synchronization Depend on the Direction of Asynchrony. *Journal of motor behavior*, 1-14.

Jantzen, K. J., Steinberg, F. L., & Kelso, J. A. S. (2005). Functional MRI reveals the existence of modality and coordination-dependent timing networks. *Neuroimage*, *25*(4), 1031-1042.

Kavanagk, R. N., Darcey, T. M., Lehmann, D., & Fender, D. H. (1978). Evaluation of methods for three-dimensional localization of electrical sources in the human brain. *IEEE Transactions on Biomedical Engineering*, (5), 421-429.

Kilavik, B. E., Zaepffel, M., Brovelli, A., MacKay, W. A., & Riehle, A. (2013). The ups and downs of beta oscillations in sensorimotor cortex. *Experimental neurology*, *245*, 15-26.

Kopell, N., Ermentrout, G. B., Whittington, M. A., & Traub, R. D. (2000). Gamma rhythms and beta rhythms have different synchronization properties. *Proceedings of the National Academy of Sciences, 97*(4), 1867-1872.

Kotz, S. A., Brown, R. M., & Schwartze, M. (2016). Cortico-striatal circuits and the timing of action and perception. *Current Opinion in Behavioral Sciences*, *8*, 42-45.

Kotz, S. A., Ravignani, A., & Fitch, W. T. (2018). The Evolution of Rhythm Processing. Trends in Cognitive 848 Sciences.

Kraut, M. A., Arezzo, J. C., & Vaughan, H. G. (1985). Intracortical generators of the flash VEP in monkeys. *Electroencephalography and Clinical Neurophysiology/Evoked Potentials Section*, *62*(4), 300-312.

Laland, K., Wilkins, C., & Clayton, N. (2016). The evolution of dance. *Current Biology*, *26*(1), R5-R9.

Lange, K. (2013). The ups and downs of temporal orienting: a review of auditory temporal orienting studies and a model associating the heterogeneous findings on the auditory N1 with opposite effects of attention and prediction. *Frontiers in human neuroscience*, *7*.

Large, E. W., & Gray, P. M. (2015). Spontaneous tempo and rhythmic entrainment in a bonobo (Pan paniscus). *Journal of Comparative Psychology*, *129*(4), 317.

Large, E. W., & Snyder, J. S. (2009). Pulse and meter as neural resonance. *Annals of the New York Academy of Sciences*, *1169*(1), 46-57.

Lenc, T., Keller, P. E., Varlet, M., & Nozaradan, S. (2019). Reply to Rajendran and Schnupp: Frequency tagging is sensitive to the temporal structure of signals. *Proceedings of the National Academy of Sciences*, *116*(8), 2781-2782.

Levitin, D. J., Grahn, J. A., London, J. (2018) The psychology of music: Rhythm and movement. *Annual Review of Psychology, 69*:51-75.

Lopez-Calderon, J., & Luck, S. J. (2014). ERPLAB: an open-source toolbox for the analysis of event-related potentials. *Frontiers in human neuroscience*, *8*.

Lorås, H., Sigmundsson, H., Talcott, J. B., Öhberg, F., & Stensdotter, A. K. (2012). Timing continuous or discontinuous movements across effectors specified by different pacing modalities and intervals. *Experimental brain research*, *220*(3-4), 335-347.

Luck, S. J., & Kappenman, E. S. (Eds.). (2011). *The Oxford handbook of event-related potential components*. Oxford university press.

Lusk, N. A., Petter, E. A., MacDonald, C. J., & Meck, W. H. (2016). Cerebellar, hippocampal, and striatal time cells. *Current Opinion in Behavioral Sciences*, *8*, 186-192.

MacDonald, C. J., Lepage, K. Q., Eden, U. T., & Eichenbaum, H. (2011). Hippocampal "time cells" bridge the gap in memory for discontiguous events. *Neuron*, *71*(4), 737-749.

Makeig, S., Debener, S., Onton, J., & Delorme, A. (2004). Mining event-related brain dynamics. *Trends in cognitive sciences*, *8*(5), 204-210.

Manning, F., & Schutz, M. (2013). "Moving to the beat" improves timing perception. *Psychonomic bulletin & review*, *20*(6), 1133-1139.

Matell, M. S., & Meck, W. H. (2004). Cortico-striatal circuits and interval timing: coincidence detection of oscillatory processes. *Cognitive brain research*, *21*(2), 139-170.

McFarland, D. J., Miner, L. A., Vaughan, T. M., & Wolpaw, J. R. (2000). Mu and beta rhythm topographies during motor imagery and actual movements. *Brain topography*, *12*(3), 177-186.

Meijer, D., Te Woerd, E., & Praamstra, P. (2016). Timing of beta oscillatory synchronization and temporal prediction of upcoming stimuli. *NeuroImage*, *138*, 233-241.

Merchant, H., & De Lafuente, V. (2014). Introduction to the neurobiology of interval timing. *Neurobiology of interval timing*, 1-13.

Merchant, H., Grahn, J., Trainor, L., Rohrmeier, M., & Fitch, W. T. (2015). Finding the beat: A neural perspective across humans and non-human primates. *Philosophical Transactions of the Royal Society B: Biological Sciences, 370*(1664).

Merchant, H., & Honing, H. (2014). Are non-human primates capable of rhythmic entrainment? Evidence for the gradual audiomotor evolution hypothesis. *Frontiers in neuroscience*, *7*, 274.

Merchant H, Perez O, Zarco W, Gamez J. (2013) Interval tuning in the primate medial premotor cortex as a general timing mechanism. *J. Neurosci. 33*, 9082–9096.

Merchant, H., & Yarrow, K. (2016). How the motor system both encodes and influences our sense of time. *Current Opinion in Behavioral Sciences*, *8*, 22-27.

Merker, B., Morley, I., & Zuidema, W. (2015). Five fundamental constraints on theories of the origins of music. *Phil. Trans. R. Soc. B*, *370*(1664), 20140095.

Michalareas, G., Vezoli, J., Van Pelt, S., Schoffelen, J. M., Kennedy, H., & Fries, P. (2016). Alpha-beta and gamma rhythms subserve feedback and feedforward influences among human visual cortical areas. *Neuron*, *89*(2), 384-397.

Morillon, B., Hackett, T. A., Kajikawa, Y., & Schroeder, C. E. (2015). Predictive motor control of sensory dynamics in auditory active sensing. *Current Opinion in Neurobiology*, *31*, 230-238.

Morein-Zamir, S., Soto-Faraco, S., & Kingstone, A. (2003). Auditory capture of vision: examining temporal ventriloquism. *Cognitive Brain Research*, *17*(1), 154-163.

Mullen, T. R., Kothe, C. A., Chi, Y. M., Ojeda, A., Kerth, T., Makeig, S., ... & Cauwenberghs, G. (2015). Real-time neuroimaging and cognitive monitoring using wearable dry EEG. *IEEE Transactions on Biomedical Engineering*, *62*(11), 2553-2567.

Näätänen, R., & Winkler, I. (1999). The concept of auditory stimulus representation in cognitive neuroscience. *Psychological bulletin*, *125*(6), 826.

Nettl, B. (2015). *The study of ethnomusicology: Thirty-three discussions*. University of Illinois Press.

Ng, B. S. W., Schroeder, T., & Kayser, C. (2012). A precluding but not ensuring role of entrained low-frequency oscillations for auditory perception. *Journal of Neuroscience*, *32*(35), 12268-12276.

Niedermeyer, E. (1997). Alpha rhythms as physiological and abnormal phenomena. *International Journal of Psychophysiology*, *26*(1-3), 31-49.

Novembre, G., & Iannetti, G. D. (2018). Tagging the musical beat: Neural entrainment or event-related potentials?. *Proceedings of the National Academy of Sciences*, *115*(47), E11002-E11003.

Nozaradan, S., Keller, P. E., Rossion, B., & Mouraux, A. (2018). EEG frequency-tagging and input–output comparison in rhythm perception. *Brain topography*, *31*(2), 153-160.

Nozaradan, S., Peretz, I., Missal, M., & Mouraux, A. (2011). Tagging the neuronal entrainment to beat and meter. *Journal of Neuroscience*, *31*(28), 10234-10240.

Nozaradan, S., Peretz, I., & Mouraux, A. (2012a). Selective neuronal entrainment to the beat and meter embedded in a musical rhythm. *Journal of Neuroscience*, *32*(49), 17572-17581.

Nozaradan, S., Peretz, I., & Mouraux, A. (2012b). Steady-state evoked potentials as an index of multisensory temporal binding. *Neuroimage*, *60*(1), 21-28.

Nozaradan, S., Schwartze, M., Obermeier, C., & Kotz, S. A. (2017). Specific contributions of basal ganglia and cerebellum to the neural tracking of rhythm. *Cortex*, *95*, 156-168.

Nozaradan, S., Zerouali, Y., Peretz, I., & Mouraux, A. (2015). Capturing with EEG the neural entrainment and coupling underlying sensorimotor synchronization to the beat. *Cerebral Cortex*, *25*(3), 736-747.

Obleser, J., Eisner, F., & Kotz, S. A. (2008). Bilateral speech comprehension reflects differential sensitivity to spectral and temporal features. *Journal of neuroscience*, *28*(32), 8116-8123.

Okawa, H., Suefusa, K., & Tanaka, T. (2017). Neural Entrainment to Auditory Imagery of Rhythms. *Frontiers in human neuroscience*, *11*, 493.

Olvet, D. M., & Hajcak, G. (2008). The error-related negativity (ERN) and psychopathology: toward an endophenotype. *Clinical psychology review*, *28*(8), 1343-1354.

Onton, J., Westerfield, M., Townsend, J., & Makeig, S. (2006). Imaging human EEG dynamics using independent component analysis. Neuroscience & biobehavioral reviews, 30(6), 808-822.

Overbeek, T. J., Nieuwenhuis, S., & Ridderinkhof, K. R. (2005). Dissociable components of error processing: on the functional significance of the Pe vis-à-vis the ERN/Ne. *Journal of Psychophysiology*, *19*(4), 319-329.

Palmer, J. A., Kreutz-Delgado, K., & Makeig, S. (2012). AMICA: An adaptive mixture of independent component analyzers with shared components. *Swartz Center for Computatonal Neursoscience, University of California San Diego, Tech. Rep*.

Parise, C., & Spence, C. (2008). Synesthetic congruency modulates the temporal ventriloquism effect. *Neuroscience Letters*, *442*(3), 257-261.

Patel, A. D. (2006). Musical rhythm, linguistic rhythm, and human evolution. *Music Perception: An Interdisciplinary Journal*, *24*(1), 99-104.

Patel, A. D., & Iversen, J. R. (2014). The evolutionary neuroscience of musical beat perception: the Action Simulation for Auditory Prediction (ASAP) hypothesis. *Frontiers in systems neuroscience*, *8*, 57.

Patel, A. D., Iversen, J. R., Bregman, M. R., & Schulz, I. (2009). Experimental evidence for synchronization to a musical beat in a nonhuman animal. *Current biology*, *19*(10), 827-830.

Perception Research Systems. 2007. *Paradigm Stimulus Presentation,* Retrieved from http://www.paradigmexperiments.com

Pfurtscheller, G., & Da Silva, F. L. (1999). Event-related EEG/MEG synchronization and desynchronization: basic principles. *Clinical neurophysiology*, *110*(11), 1842-1857.

Pfurtscheller, G., & Neuper, C. (1994). Event-related synchronization of mu rhythm in the EEG over the cortical hand area in man. *Neuroscience letters*, *174*(1), 93-96.

Pfurtscheller, G., Neuper, C., Andrew, C., & Edlinger, G. (1997). Foot and hand area mu rhythms. *International Journal of Psychophysiology*, *26*(1-3), 121-135.

Piazza, C., Miyakoshi, M., Akalin-Acar, Z., Cantiani, C., Reni, G., Bianchi, A. M., & Makeig, S. (2016). An automated function for identifying eeg independent components representing bilateral source activity. In *XIV Mediterranean Conference on Medical and Biological Engineering and Computing 2016* (pp. 105-109). Springer, Cham.

Picazio, S., Veniero, D., Ponzo, V., Caltagirone, C., Gross, J., Thut, G., & Koch, G. (2014). Prefrontal control over motor cortex cycles at beta frequency during movement inhibition. *Current Biology*, *24*(24), 2940-2945.

Pion-Tonachini, L., Kreutz-Delgado, K., & Makeig, S. (2019). The ICLabel dataset of electroencephalographic (EEG) independent component (IC) features. *Data in brief*, *25*, 104101.

Phillips-Silver, J., & Trainor, L. J. (2005). Feeling the beat: movement influences infant rhythm perception. *Science*, *308*(5727), 1430-1430.

Phillips-Silver, J., & Trainor, L. J. (2007). Hearing what the body feels: Auditory encoding of rhythmic movement. *Cognition*, *105*(3), 533-546.

Phillips-Silver, J., & Trainor, L. J. (2008). Vestibular influence on auditory metrical interpretation. *Brain and cognition*, *67*(1), 94-102.

Praamstra, P., Turgeon, M., Hesse, C. W., Wing, A. M., & Perryer, L. (2003). Neurophysiological correlates of error correction in sensorimotor-synchronization. *Neuroimage*, *20*(2), 1283-1297.

Proksch, S., Comstock, D. C., Médé, B., Pabst, A., & Balasubramaniam, R. (2020). Motor and predictive processes in auditory beat and rhythm perception. *Frontiers in Human Neuroscience*, *14*, 375.

Provasi, J., Anderson, D. I., & Barbu-Roth, M. (2014). Rhythm perception, production, and synchronization during the perinatal period. *Frontiers in psychology*, *5*, 1048.

Rajendran, V. G., & Schnupp, J. W. (2019). Frequency tagging cannot measure neural tracking of beat or meter. *Proceedings of the National Academy of Sciences*, *116*(8), 2779-2780.

Rauschecker, J. P. (2017). Where, When, and How: are they all Sensorimotor? Towards a unified view of the dorsal pathway in vision and audition. *Cortex*.

Ravignani, A., & Cook, P. F. (2016). The evolutionary biology of dance without frills. *Current Biology*, *26*(19), R878-R879.

Ravignani, A., Dalla-Bella, S., Falk, S., and Kello, C. (2019). Rhythm in speech and animal vocalizations: a cross-species perspective: speech rhythm across species. *Ann. N. Y. Acad. Sci.* 1452, 79–98. doi: 10.1111/nyas.14166

Repp, B. H. (2000). Compensation for subliminal timing perturbations in perceptual-motor synchronization. *Psychological research*, *63*(2), 106-128.

Repp, B. H. (2001a). Phase correction, phase resetting, and phase shifts after subliminal timing perturbations in sensorimotor synchronization. *Journal of Experimental Psychology: Human Perception and Performance*, *27*(3), 600.

Repp, B. H. (2001b). Processes underlying adaptation to tempo changes in sensorimotor synchronization. *Human movement science*, *20*(3), 277-312.

Repp, B. H. (2003). Rate limits in sensorimotor synchronization with auditory and visual sequences: The synchronization threshold and the benefits and costs of interval subdivision. *Journal of motor behavior*, *35*(4), 355-370.

Repp, B. H. (2005). Sensorimotor synchronization: a review of the tapping literature. *Psychonomic bulletin & review*, *12*(6), 969-992.

Repp, B. H., & Keller, P. E. (2004). Adaptation to tempo changes in sensorimotor synchronization: Effects of intention, attention, and awareness. *The Quarterly Journal of Experimental Psychology Section A*, *57*(3), 499-521.

Repp, B. H., & Penel, A. (2004). Rhythmic movement is attracted more strongly to auditory than to visual rhythms. *Psychological research*, *68*(4), 252-270.

Repp, B. H., & Su, Y. H. (2013). Sensorimotor synchronization: a review of recent research (2006–2012). *Psychonomic bulletin & review*, *20*(3), 403-452.

Ridderinkhof, K. R., Ullsperger, M., Crone, E. A., & Nieuwenhuis, S. (2004). The role of the medial frontal cortex in cognitive control. *Science*, *306*(5695), 443-447.

Riecke, L., Sack, A. T., & Schroeder, C. E. (2015). Endogenous delta/theta sound-brain phase entrainment accelerates the buildup of auditory streaming. *Current Biology*, *25*(24), 3196-3201.

Rochester, L., Hetherington, V., Jones, D., Nieuwboer, A., Willems, A. M., Kwakkel, G., & Van Wegen, E. (2005). The effect of external rhythmic cues (auditory and visual) on walking during a functional task in homes of people with Parkinson's disease. *Archives of physical medicine and rehabilitation*, *86*(5), 999-1006.

Ross, J., Iversen, J., Makeig, S., & Balasubramaniam, R. Comstock, D. C. (2016a) An EEG examination of neural entrainment and action simulation during rhythm perception. *Poster presentation at the 14th International Conference for Music Perception and Cognition*, San Francisco, CA

Ross, J. M., Iversen, J. R., & Balasubramaniam, R. (2016b). Motor simulation theories of musical beat perception. *Neurocase*, *22*(6), 558-565.

Ross, J. M., Iversen, J. R., & Balasubramaniam, R. (2018). The Role of Posterior Parietal Cortex in Beat-based Timing Perception: A Continuous Theta Burst Stimulation Study. *Journal of cognitive neuroscience*, (Early Access), 1-10.

Ross, J. M., Warlaumont, A. S., Abney, D. H., Rigoli, L. M., & Balasubramaniam, R. (2016). Influence of musical groove on postural sway. *Journal of Experimental Psychology: Human Perception and Performance*, *42*(3), 308.

Rouse, A. A., Cook, P. F., Large, E. W., & Reichmuth, C. (2016). Beat keeping in a sea lion as coupled oscillation: implications for comparative understanding of human rhythm. *Frontiers in neuroscience*, *10*, 257.

Rüsseler, J., Altenmüller, E., Nager, W., Kohlmetz, C., & Münte, T. F. (2001). Event-related brain potentials to sound omissions differ in musicians and non-musicians. *Neuroscience letters*, *308*(1), 33-36.

Saleh, M., Reimer, J., Penn, R., Ojakangas, C. L., & Hatsopoulos, N. G. (2010). Fast and slow oscillations in human primary motor cortex predict oncoming behaviorally relevant cues. *Neuron*, *65*(4), 461-471.

Sarnthein, J., Petsche, H., Rappelsberger, P., Shaw, G. L., & Von Stein, A. (1998). Synchronization between prefrontal and posterior association cortex during human working memory. *Proceedings of the National Academy of Sciences*, *95*(12), 7092-7096.

Savage, P. E., Brown, S., Sakai, E., & Currie, T. E. (2015). Statistical universals reveal the structures and functions of human music. *Proceedings of the National Academy of Sciences*, *112*(29), 8987-8992.

Scherg, M. (1990). Fundamentals of dipole source potential analysis. *Auditory evoked magnetic fields and electric potentials. Advances in audiology*, *6*, 40-69.

Schroeder, C. E., & Lakatos, P. (2009). Low-frequency neuronal oscillations as instruments of sensory selection. *Trends in neurosciences*, *32*(1), 9-18.

Schubotz, R. I. (2007). Prediction of external events with our motor system: towards a new framework. *Trends in cognitive sciences*, *11*(5), 211-218.

Schubotz, R. I., Friederici, A. D., & Von Cramon, D. Y. (2000). Time perception and motor timing: a common cortical and subcortical basis revealed by fMRI. *Neuroimage*, *11*(1), 1-12.

Shuler, M. G. H. (2016). Timing in the visual cortex and its investigation. *Current opinion in behavioral sciences*, *8*, 73-77.

Silva, S., & Castro, S. L. (2016). Moving Stimuli Facilitate Synchronization But Not Temporal Perception. *Frontiers in psychology*, *7*, 1798.

Snyder, J. S., & Large, E. W. (2005). Gamma-band activity reflects the metric structure of rhythmic tone sequences. *Cognitive brain research*, *24*(1), 117-126.

Su, Y. H., & Pöppel, E. (2012). Body movement enhances the extraction of temporal structures in auditory sequences. *Psychological research*, *76*(3), 373-382.

Takeya, R., Kameda, M., Patel, A. D., & Tanaka, M. (2017). Predictive and tempo-flexible synchronization to a visual metronome in monkeys. *Scientific reports*, *7*(1), 6127.

Teki, S., Grube, M., Kumar, S., & Griffiths, T. D. (2011). Distinct neural substrates of duration-based and beat-based auditory timing. *Journal of Neuroscience*, *31*(10), 3805-3812.

Thaut, M. H., Miller, R. A., & Schauer, L. M. (1998). Multiple synchronization strategies in rhythmic sensorimotor tasks: phase vs period correction. *Biological cybernetics*, *79*(3), 241-250.

Todd, N. P., & Lee, C. S. (2015). The sensory-motor theory of rhythm and beat induction 20 years on: a new synthesis and future perspectives. *Frontiers in human neuroscience*, *9*, 444.

Tomassini, A., Ambrogioni, L., Medendorp, W. P., & Maris, E. (2017). Theta oscillations locked to intended actions rhythmically modulate perception. *Elife*, *6*, e25618.

Ulloa, E. R., & Pineda, J. A. (2007). Recognition of point-light biological motion: mu rhythms and mirror neuron activity. *Behavioural brain research*, *183*(2), 188-194.

Varlet, M., Nozaradan, S., Trainor, L., & Keller, P. E. (2020). Dynamic Modulation of Beta Band Cortico-Muscular Coupling Induced by Audio–Visual Rhythms. *Cerebral Cortex Communications, 1*(1), tgaa043.

Vialatte, F. B., Maurice, M., Dauwels, J., & Cichocki, A. (2010). Steady-state visually evoked potentials: focus on essential paradigms and future perspectives. *Progress in neurobiology*, *90*(4), 418-438.

Von Stein, A., & Sarnthein, J. (2000). Different frequencies for different scales of cortical integration: from local gamma to long range alpha/theta synchronization. *International journal of psychophysiology*, *38*(3), 301-313.

Vorberg, D., & Wing, A. (1996). Modeling variability and dependence in timing. *Handbook of perception and action*, *2*, 181-262.

Vroomen, J., Bertelson, P., & de Gelder, B. (2001). Directing spatial attention towards the illusory location of a ventriloquized sound. *Acta Psychologica*, *108*(1), 21-33.

Wang, J., Narain, D., Hosseini, E. A., & Jazayeri, M. (2018). Flexible timing by temporal scaling of cortical responses. *Nature neuroscience*, *21*(1), 102-110.

Wiener, M., & Kanai, R. (2016). Frequency tuning for temporal perception and prediction. *Current Opinion in Behavioral Sciences*, *8*, 1-6.

Wiener, M., Turkeltaub, P., & Coslett, H. B. (2010). The image of time: a voxel-wise meta-analysis. *Neuroimage*, *49*(2), 1728-1740.

Wing, A. M., and Kristofferson, A. (1973). The timing of interresponse intervals. Percept. Psychophys. 13, 455–460. doi: 10.3758/bf03205802

Williams, P. E., Mechler, F., Gordon, J., Shapley, R., & Hawken, M. J. (2004). Entrainment to video displays in primary visual cortex of macaque and humans. *Journal of Neuroscience*, *24*(38), 8278-8288.

Wilson, M., & Cook, P. F. (2016). Rhythmic entrainment: why humans want to, fireflies can't help it, pet birds try, and sea lions have to be bribed. *Psychonomic bulletin & review*, *23*(6), 1647-1659.

Wu, C. C., Hamm, J. P., Lim, V. K., & Kirk, I. J. (2016). Mu rhythm suppression demonstrates action representation in pianists during passive listening of piano melodies. *Experimental brain research*, *234*(8), 2133-2139.

Yeung, N., Botvinick, M. M., & Cohen, J. D. (2004). The neural basis of error detection: conflict monitoring and the error-related negativity. *Psychological review*, *111*(4), 931.

Zatorre, R. J., & Belin, P. (2001). Spectral and temporal processing in human auditory cortex. *Cerebral cortex*, *11*(10), 946-953.

Zatorre, R. J., Chen, J. L., & Penhune, V. B. (2007). When the brain plays music: auditory–motor interactions in music perception and production. *Nature reviews neuroscience*, *8*(7), 547.

Zatorre, R. J., Evans, A. C., Meyer, E., & Gjedde, A. (1992). Lateralization of phonetic and pitch discrimination in speech processing. *Science*, *256*(5058), 846-849.

Zhou, B., Yang, S., Mao, L., & Han, S. (2014). Visual feature processing in the early visual cortex affects duration perception. *Journal of Experimental Psychology: General*, *143*(5), 1893.

Appendix A - Supplemental Materials for Chapter 3

Figures:

Figures from each cluster are provided, separated by visual and auditory conditions. Each figure contains component dipole position figures; induced and evoked ERSP figures; induced, evoked and ITC time course activity in the beta band; and box plots showing peak times of induced, evoked, and ITC activity in the beta band; box plots showing peak power for normalized induced and evoked beta activity. In the ERSP plots a significant difference from baseline is indicated with dotted lines for $p < 0.01$ in the induced ERSP plots and $p < 0.001$ in the evoked ERSP plots. Standard error is indicated by shaded areas in induced, evoked, and ITC time course activity in beta band plots. Significant differences are denoted in the box plots (* = $p < 0.05$, ** = $p < 0.01$, *** = $p < 0.001$. Notches in the bars in the box plots indicate 95% confidence intervals, and median values are indicated with the black line.

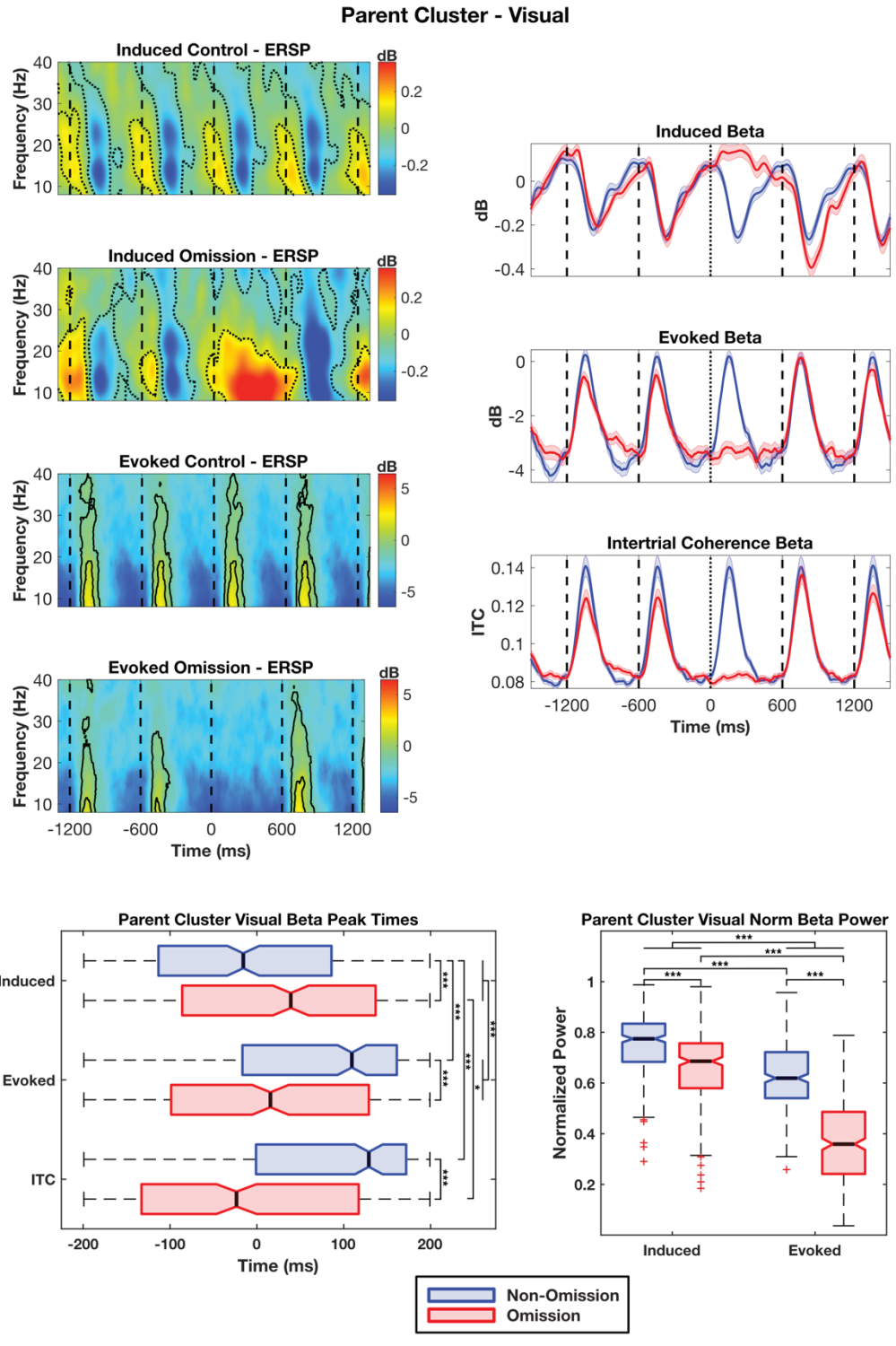
Parent Cluster - Visual
Induced Control - ERSP
Induced Omission - ERSP
Evoked Control - ERSP
Evoked Omission - ERSP
Frequency (Hz)
dB
Time (ms)
Induced Beta
Evoked Beta
Intertrial Coherence Beta
ITC
Parent Cluster Visual Beta Peak Times
Induced
Evoked
ITC
Parent Cluster Visual Norm Beta Power
Normalized Power
Non-Omission
Omission

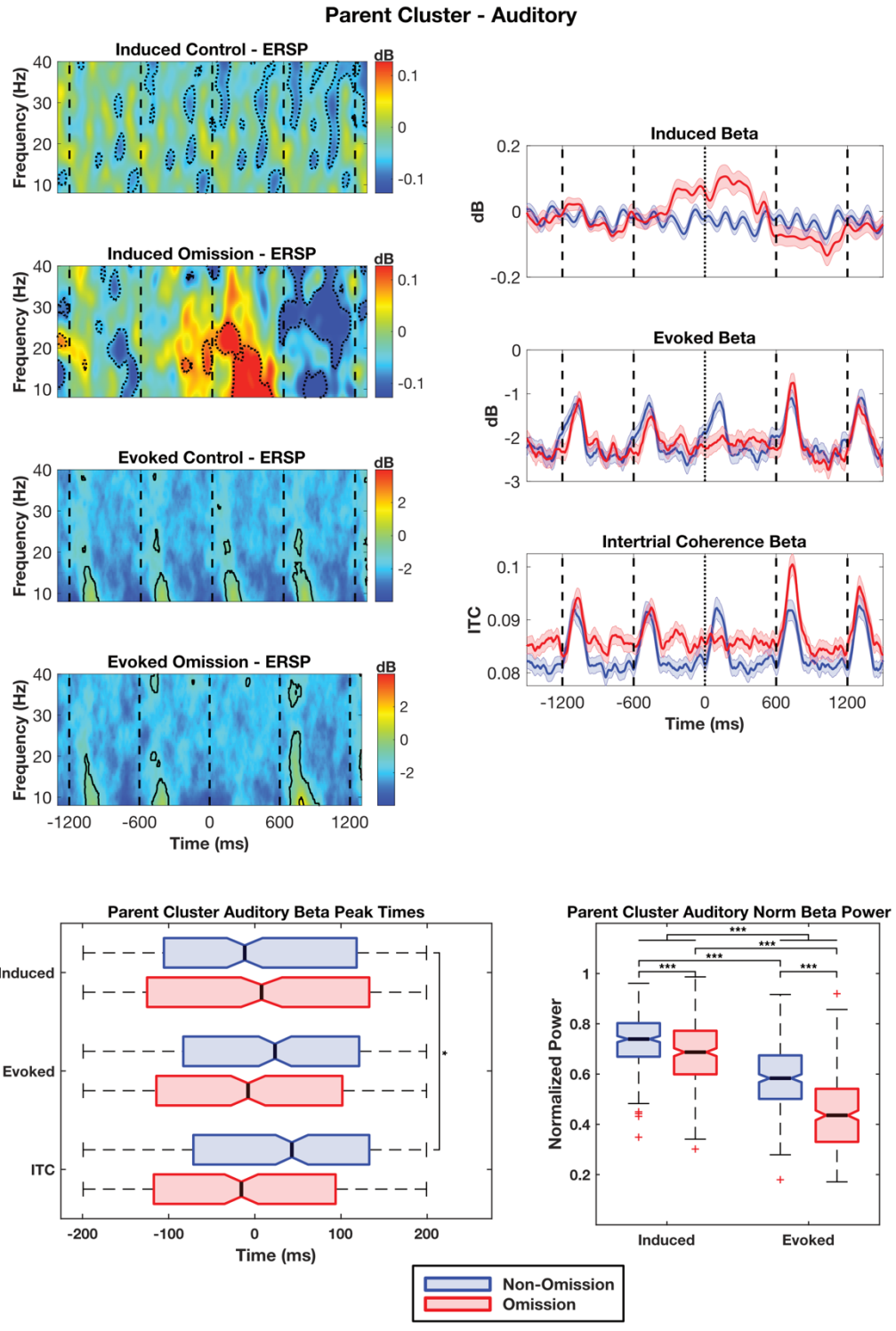
Parent Cluster - Auditory
Induced Control - ERSP
Induced Omission - ERSP
Evoked Control - ERSP
Evoked Omission - ERSP
Frequency (Hz)
dB
Time (ms)
Induced Beta
Evoked Beta
Intertrial Coherence Beta
ITC
Parent Cluster Auditory Beta Peak Times
Induced
Evoked
ITC
Parent Cluster Auditory Norm Beta Power
Normalized Power
Non-Omission
Omission

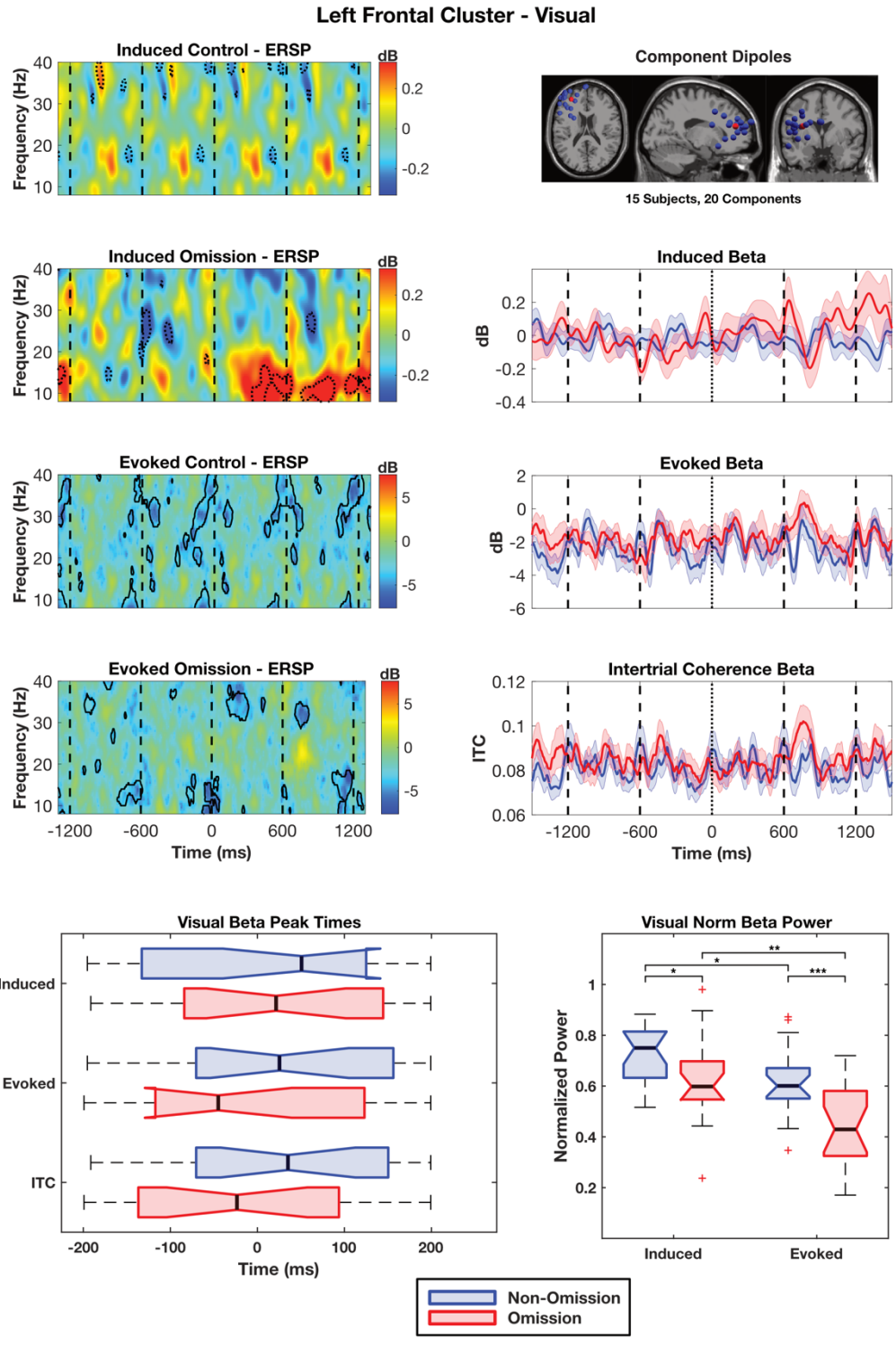
Left Frontal Cluster - Visual
Induced Control - ERSP
Component Dipoles
15 Subjects, 20 Components
Induced Omission - ERSP
Induced Beta
Evoked Control - ERSP
Evoked Beta
Evoked Omission - ERSP
Intertrial Coherence Beta
Frequency (Hz)
dB
ITC
Time (ms)
Visual Beta Peak Times
Induced
Evoked
ITC
Visual Norm Beta Power
Normalized Power
Non-Omission
Omission

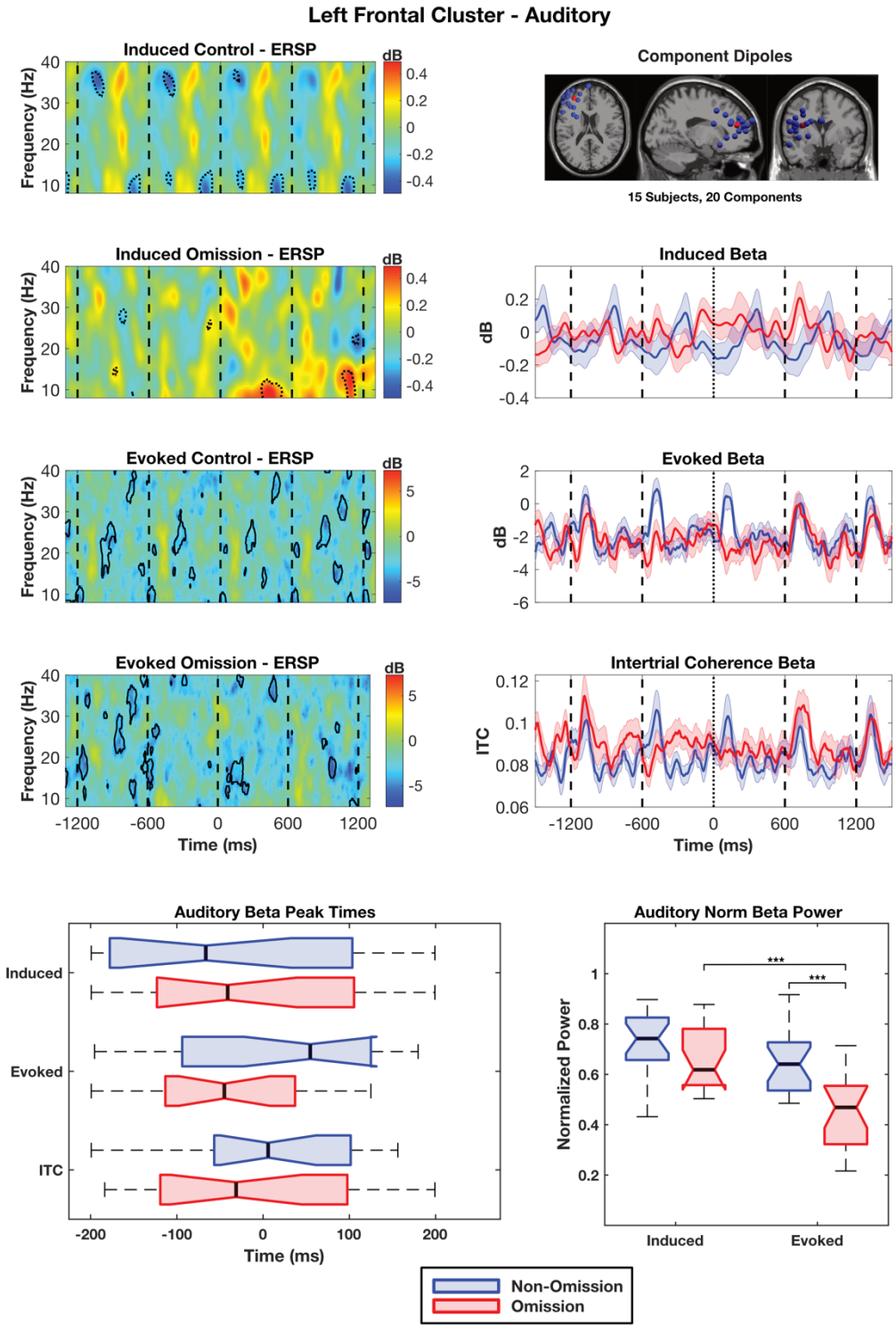
Left Frontal Cluster - Auditory
Induced Control - ERSP
Component Dipoles
15 Subjects, 20 Components
Induced Omission - ERSP
Induced Beta
Evoked Control - ERSP
Evoked Beta
Evoked Omission - ERSP
Intertrial Coherence Beta
Frequency (Hz)
dB
Time (ms)
ITC
Auditory Beta Peak Times
Induced
Evoked
Auditory Norm Beta Power
Normalized Power
***
Non-Omission
Omission

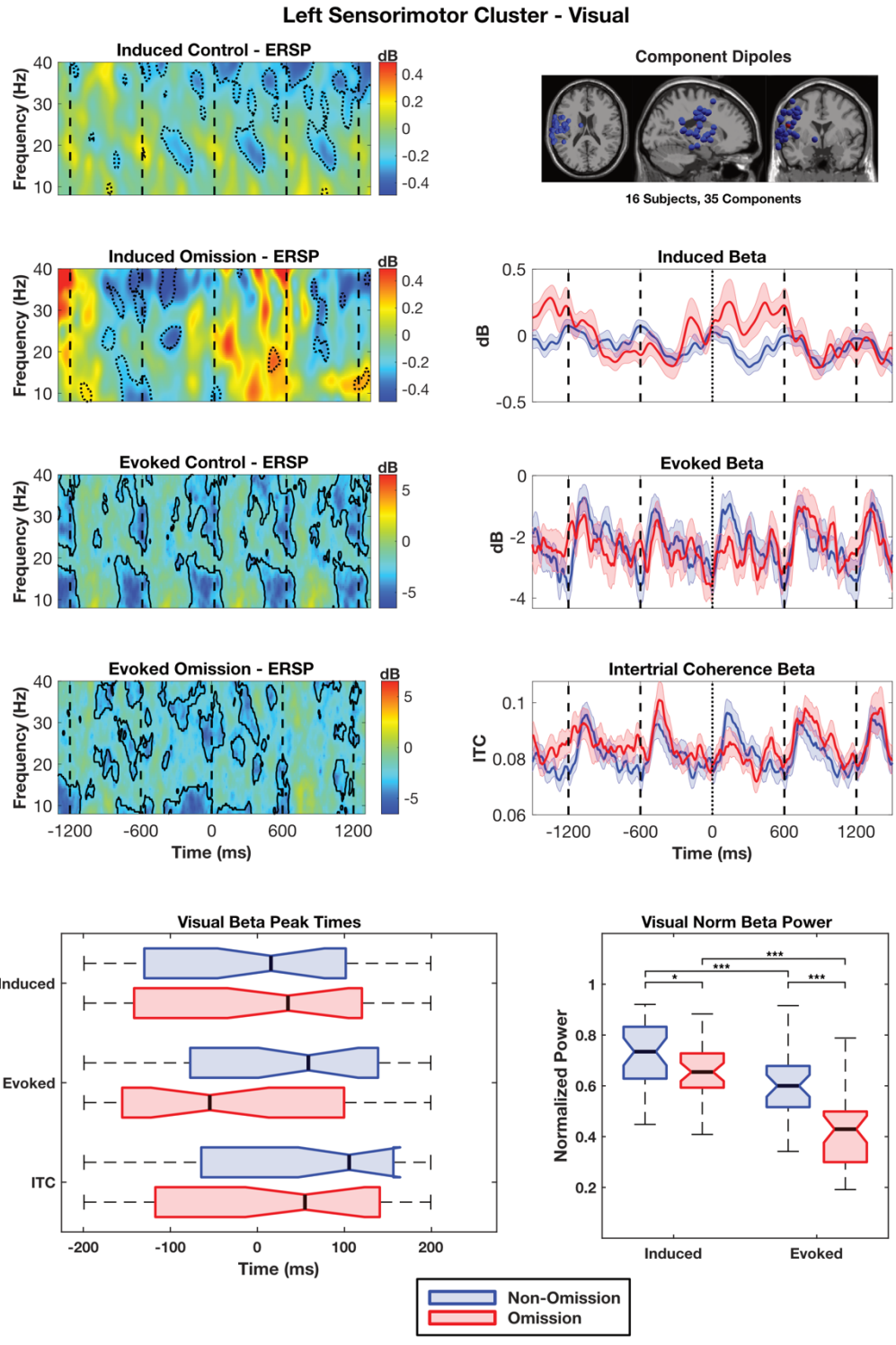
Left Sensorimotor Cluster - Visual
Induced Control - ERSP
Component Dipoles
16 Subjects, 35 Components
Induced Omission - ERSP
Induced Beta
Evoked Control - ERSP
Evoked Beta
Evoked Omission - ERSP
Intertrial Coherence Beta
Frequency (Hz)
dB
ITC
Time (ms)
Visual Beta Peak Times
Induced
Evoked
ITC
Visual Norm Beta Power
Normalized Power
Non-Omission
Omission

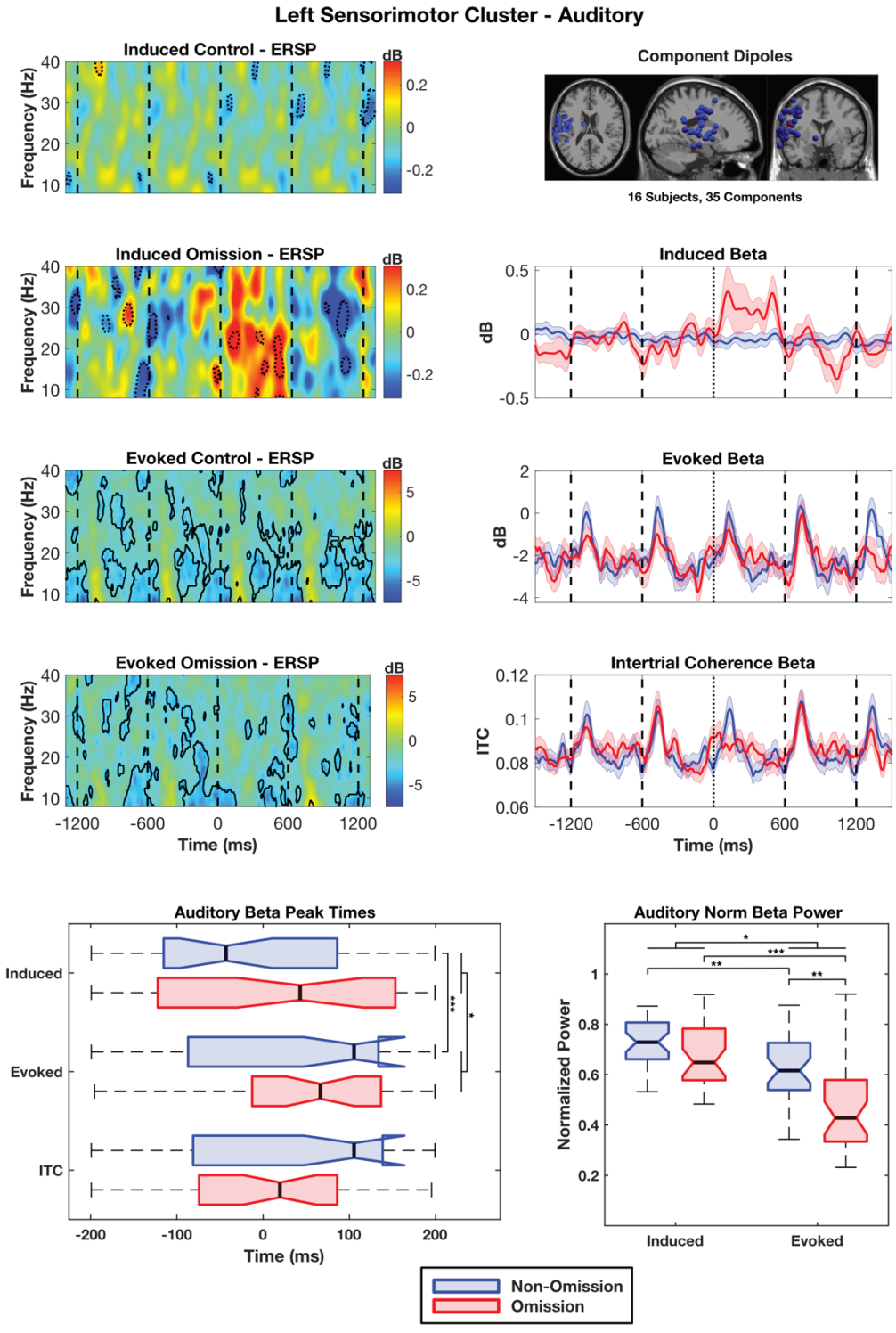
Left Sensorimotor Cluster - Auditory
Induced Control - ERSP
Component Dipoles
16 Subjects, 35 Components
Induced Omission - ERSP
Induced Beta
Evoked Control - ERSP
Evoked Beta
Evoked Omission - ERSP
Intertrial Coherence Beta
Frequency (Hz)
dB
ITC
Time (ms)
Auditory Beta Peak Times
Induced
Evoked
ITC
Auditory Norm Beta Power
Normalized Power
Non-Omission
Omission

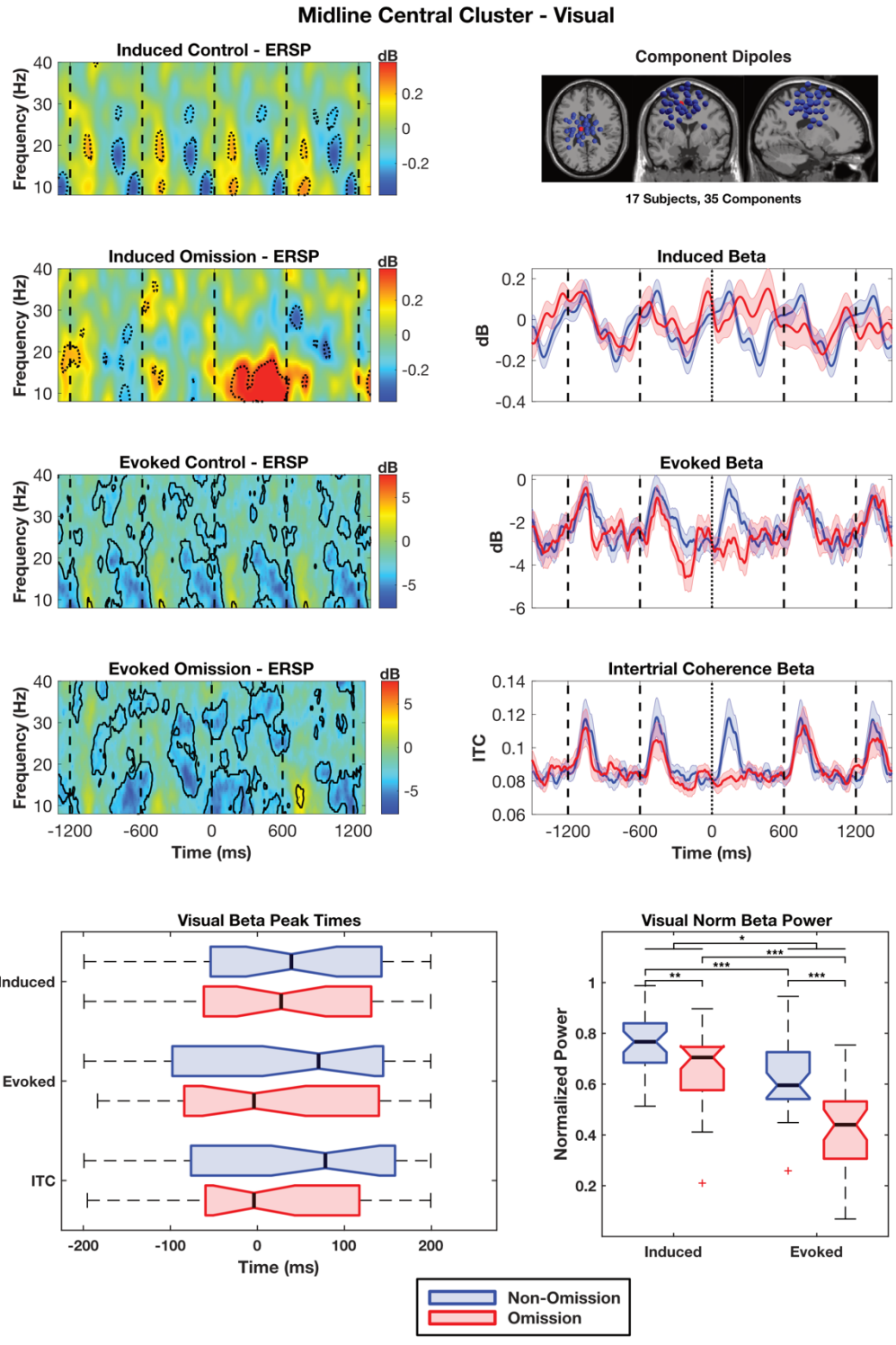
Midline Central Cluster - Visual
Induced Control - ERSP
Component Dipoles
17 Subjects, 35 Components
Induced Omission - ERSP
Induced Beta
Evoked Control - ERSP
Evoked Beta
Evoked Omission - ERSP
Intertrial Coherence Beta
Frequency (Hz)
dB
ITC
Time (ms)
Visual Beta Peak Times
Induced
Evoked
ITC
Visual Norm Beta Power
Normalized Power
Non-Omission
Omission

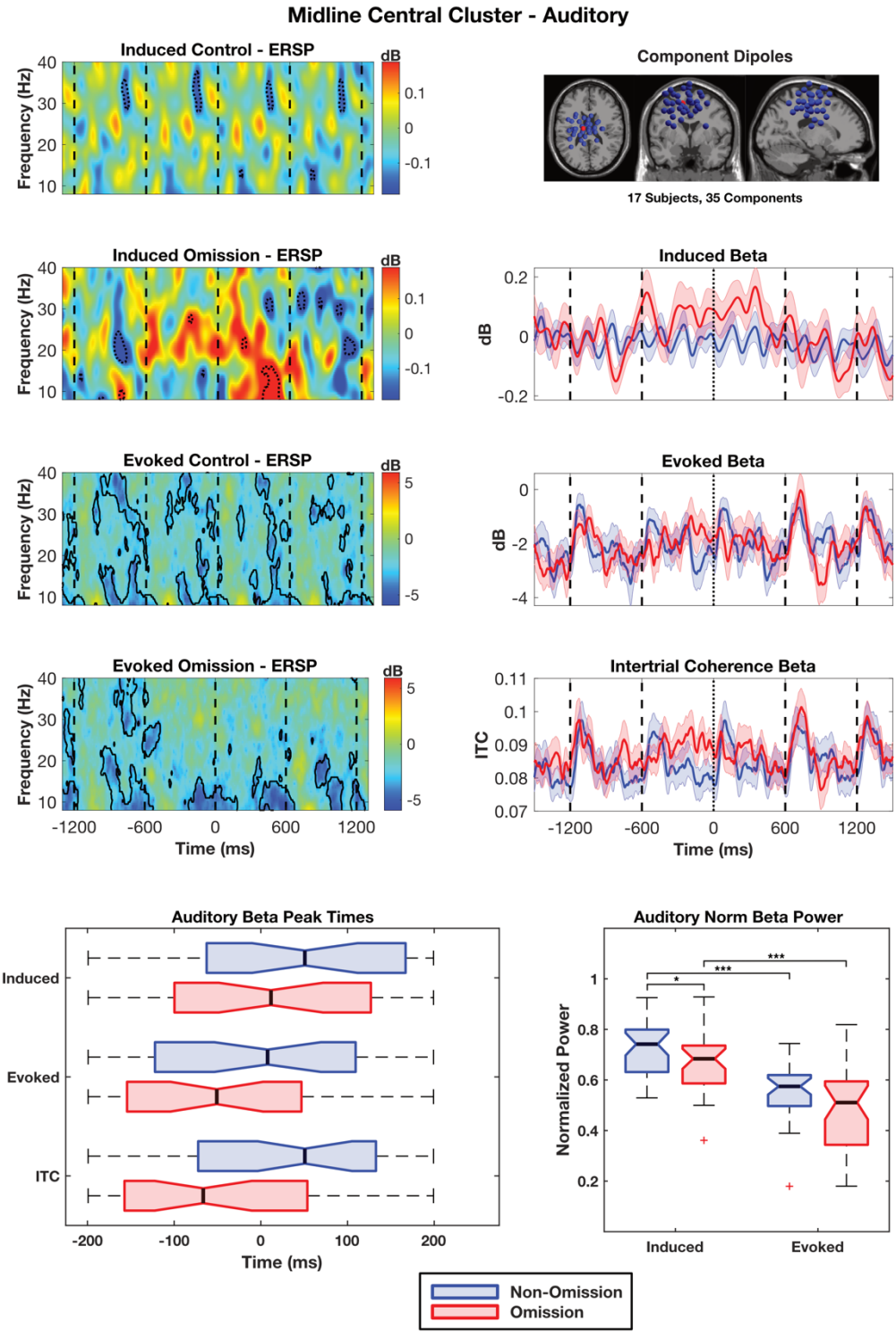
Midline Central Cluster - Auditory
Induced Control - ERSP
Component Dipoles
17 Subjects, 35 Components
Induced Omission - ERSP
Induced Beta
Evoked Control - ERSP
Evoked Beta
Evoked Omission - ERSP
Intertrial Coherence Beta
Frequency (Hz)
dB
Time (ms)
ITC
Auditory Beta Peak Times
Induced
Evoked
ITC
Auditory Norm Beta Power
Normalized Power
Non-Omission
Omission

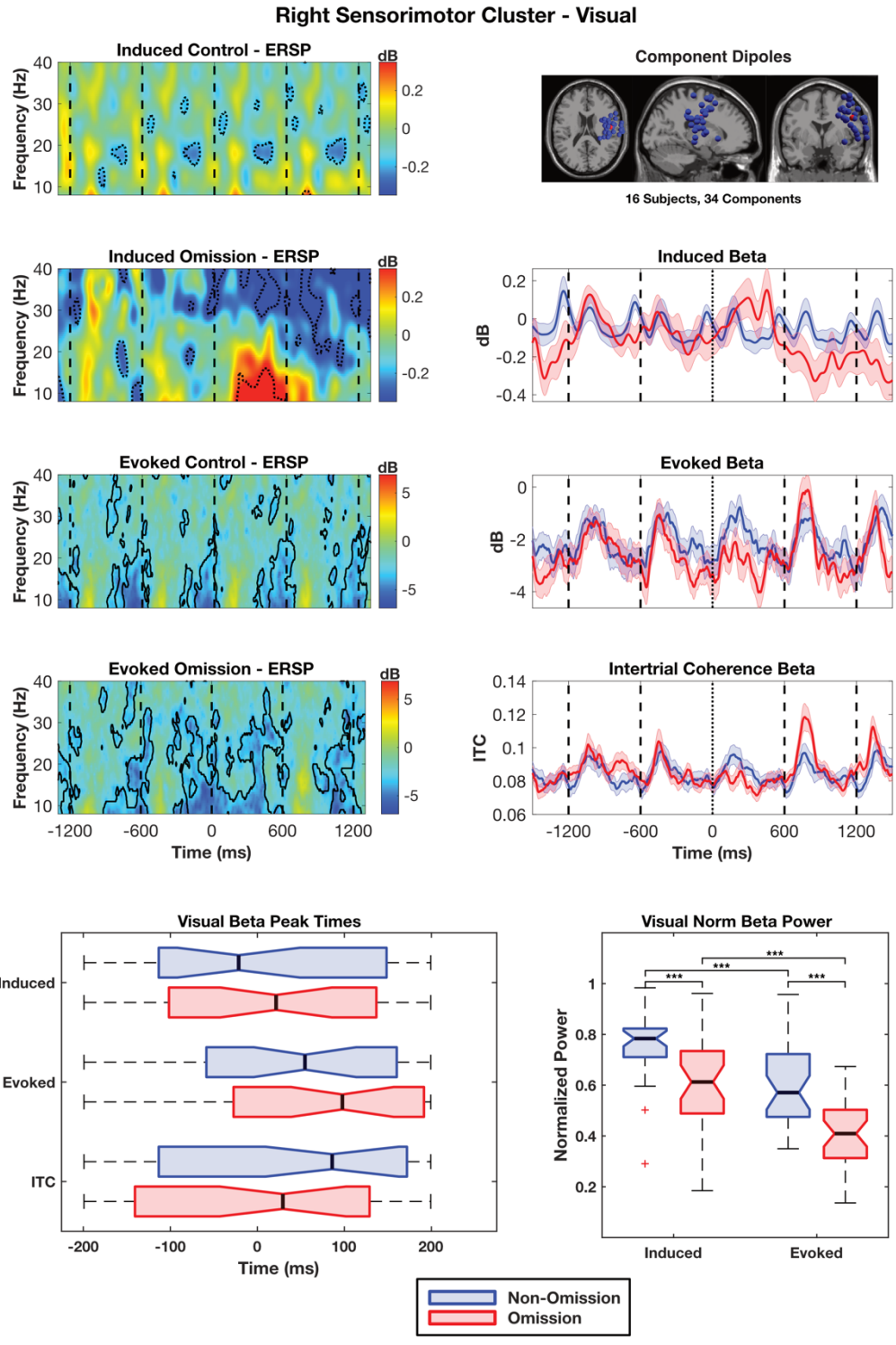
Right Sensorimotor Cluster - Visual
Induced Control - ERSP
Component Dipoles
16 Subjects, 34 Components
Induced Omission - ERSP
Induced Beta
Evoked Control - ERSP
Evoked Beta
Evoked Omission - ERSP
Intertrial Coherence Beta
Frequency (Hz)
dB
ITC
Time (ms)
Visual Beta Peak Times
Induced
Evoked
ITC
Visual Norm Beta Power
Normalized Power
Non-Omission
Omission

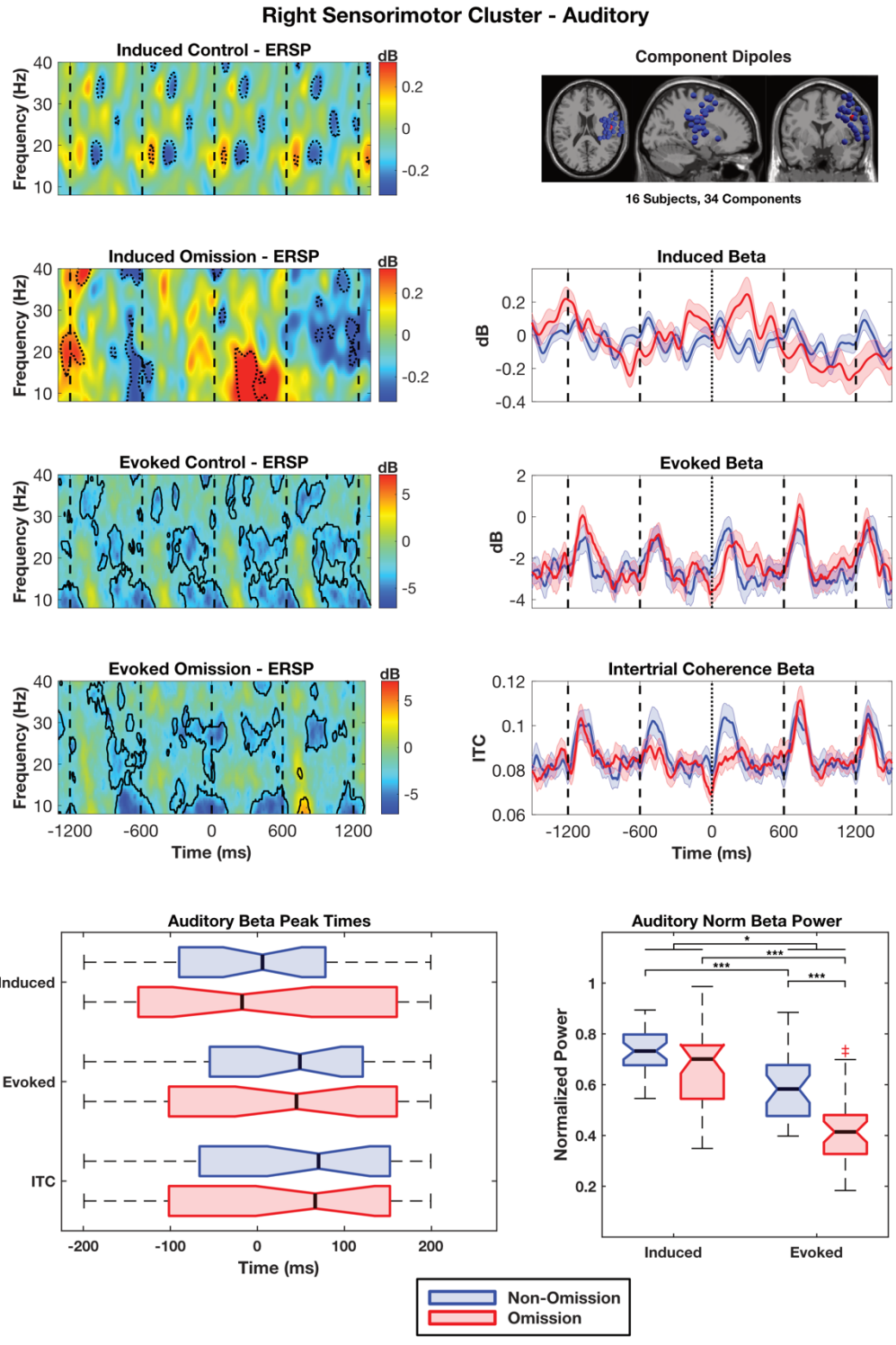
Right Sensorimotor Cluster - Auditory
Induced Control - ERSP
Component Dipoles
16 Subjects, 34 Components
Induced Omission - ERSP
Induced Beta
Evoked Control - ERSP
Evoked Beta
Evoked Omission - ERSP
Intertrial Coherence Beta
Frequency (Hz)
dB
Time (ms)
ITC
Auditory Beta Peak Times
Induced
Evoked
ITC
Auditory Norm Beta Power
Normalized Power
Non-Omission
Omission

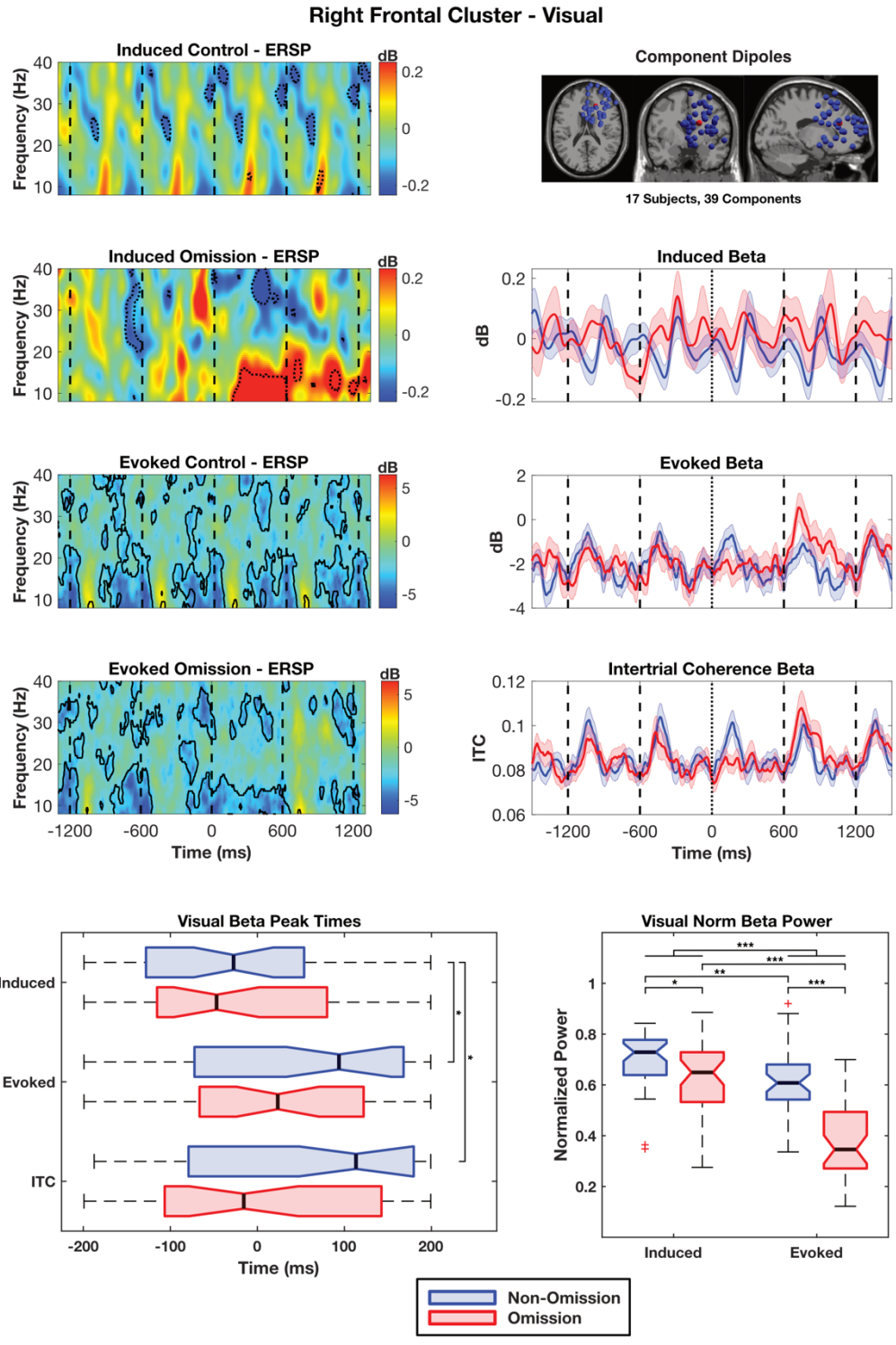
Right Frontal Cluster - Visual
Induced Control - ERSP
Frequency (Hz)
dB
Component Dipoles
17 Subjects, 39 Components
Induced Omission - ERSP
Induced Beta
Evoked Control - ERSP
Evoked Beta
Evoked Omission - ERSP
Intertrial Coherence Beta
ITC
Time (ms)
Visual Beta Peak Times
Induced
Evoked
ITC
Visual Norm Beta Power
Normalized Power
Non-Omission
Omission

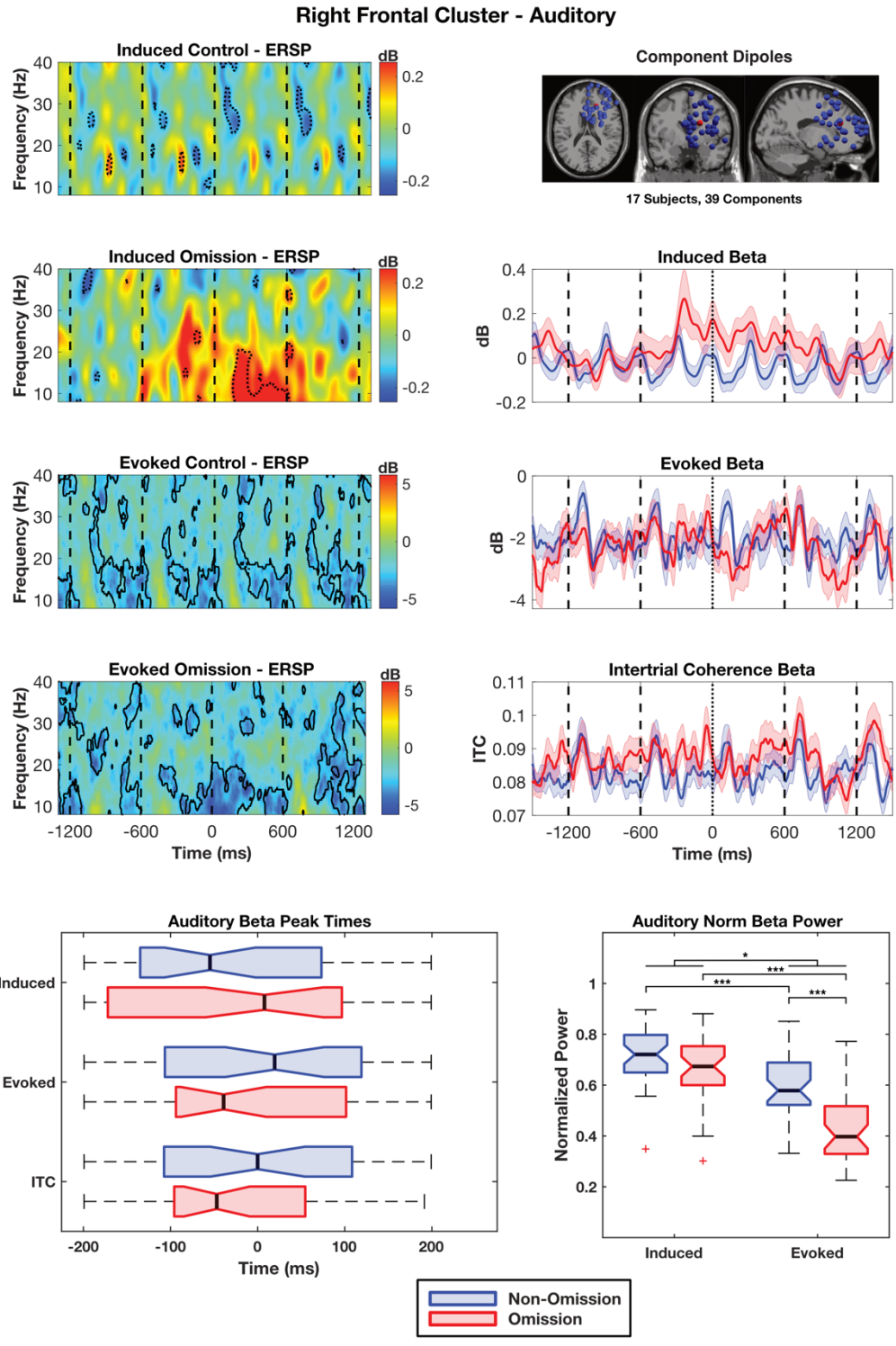
Right Frontal Cluster - Auditory
Induced Control - ERSP
Component Dipoles
17 Subjects, 39 Components
Induced Omission - ERSP
Induced Beta
Evoked Control - ERSP
Evoked Beta
Evoked Omission - ERSP
Intertrial Coherence Beta
Frequency (Hz)
dB
ITC
Time (ms)
Auditory Beta Peak Times
Induced
Evoked
ITC
Auditory Norm Beta Power
Normalized Power
Non-Omission
Omission

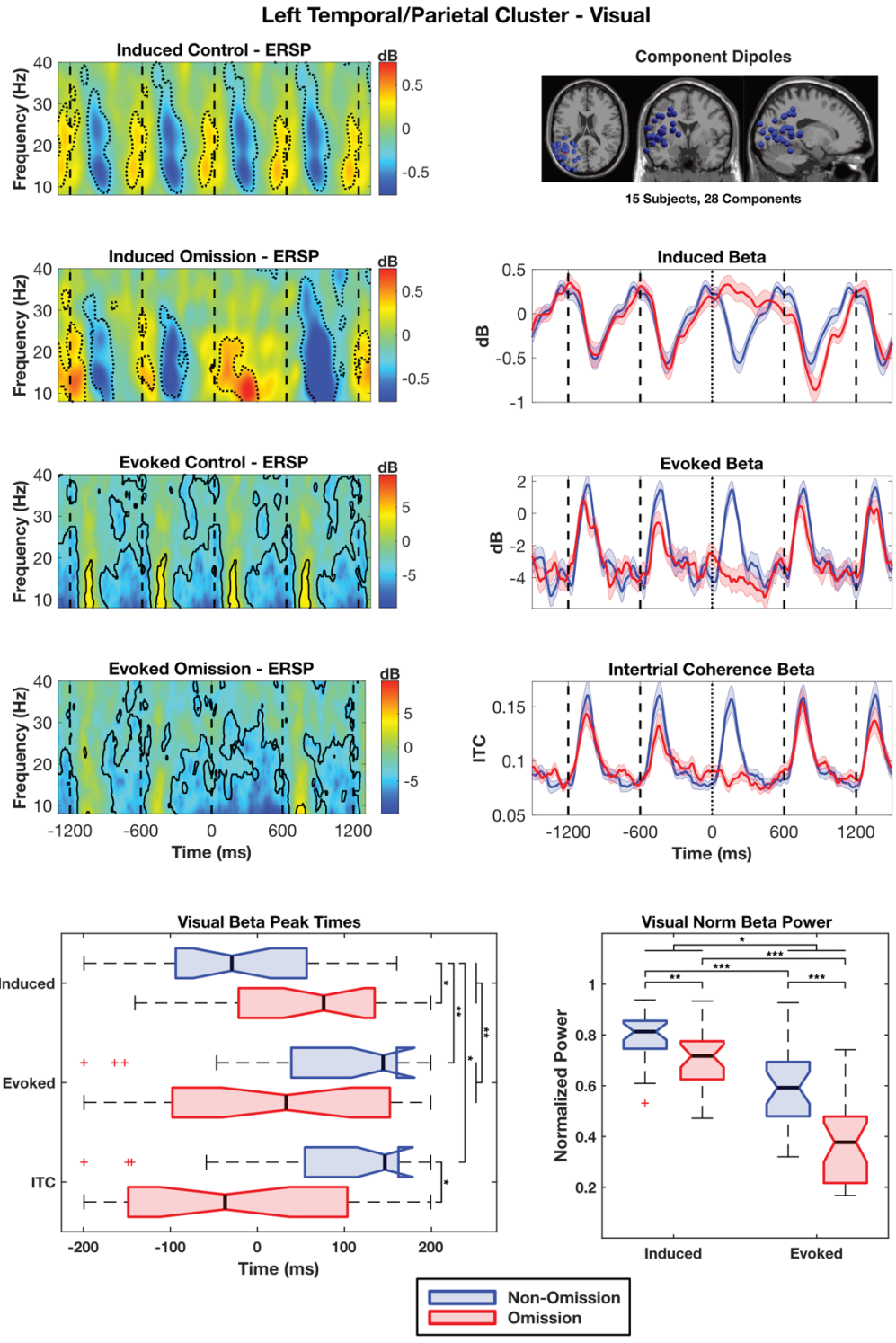
Left Temporal/Parietal Cluster - Visual
Induced Control - ERSP
Component Dipoles
15 Subjects, 28 Components
Induced Omission - ERSP
Induced Beta
Evoked Control - ERSP
Evoked Beta
Evoked Omission - ERSP
Intertrial Coherence Beta
Frequency (Hz)
dB
ITC
Time (ms)
Visual Beta Peak Times
Induced
Evoked
ITC
Visual Norm Beta Power
Normalized Power
Non-Omission
Omission

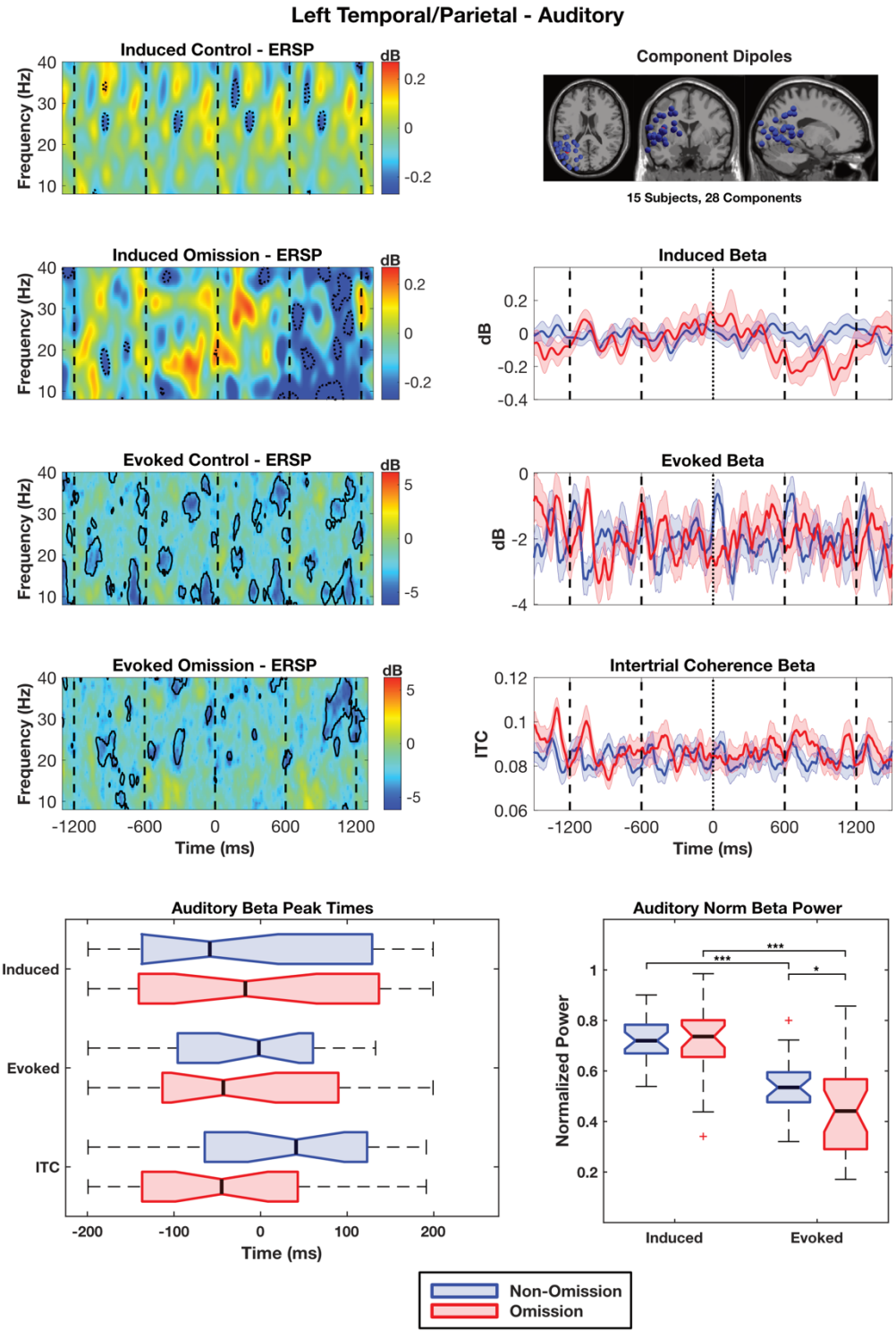
Left Temporal/Parietal - Auditory
Induced Control - ERSP
Component Dipoles
15 Subjects, 28 Components
Induced Omission - ERSP
Induced Beta
Evoked Control - ERSP
Evoked Beta
Evoked Omission - ERSP
Intertrial Coherence Beta
Frequency (Hz)
dB
Time (ms)
ITC
Auditory Beta Peak Times
Induced
Evoked
Auditory Norm Beta Power
Normalized Power
Non-Omission
Omission

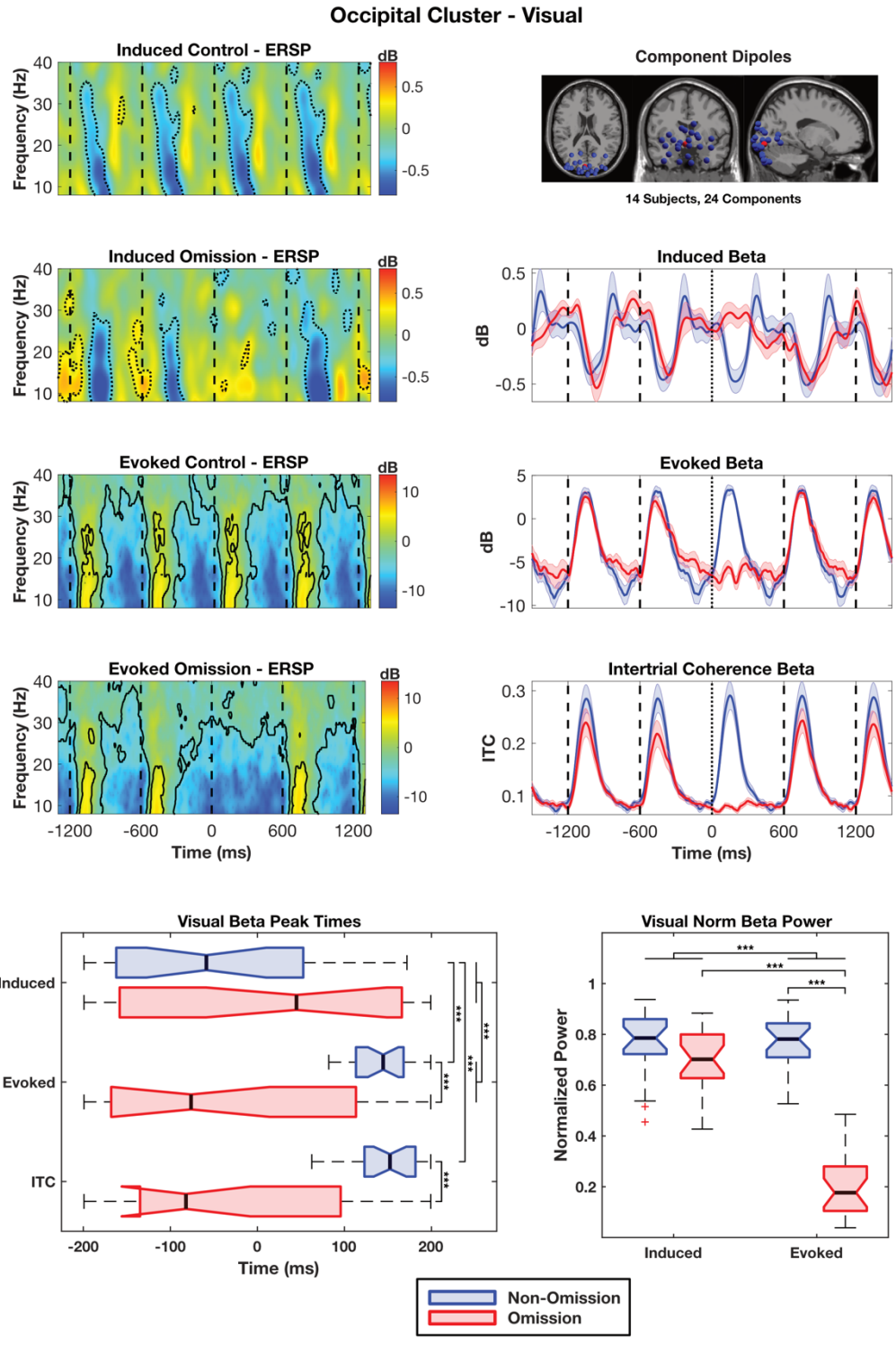
Occipital Cluster - Visual
Induced Control - ERSP
Component Dipoles
14 Subjects, 24 Components
Induced Omission - ERSP
Induced Beta
Evoked Control - ERSP
Evoked Beta
Evoked Omission - ERSP
Intertrial Coherence Beta
Frequency (Hz)
dB
Time (ms)
ITC
Visual Beta Peak Times
Visual Norm Beta Power
Induced
Evoked
Normalized Power
Non-Omission
Omission

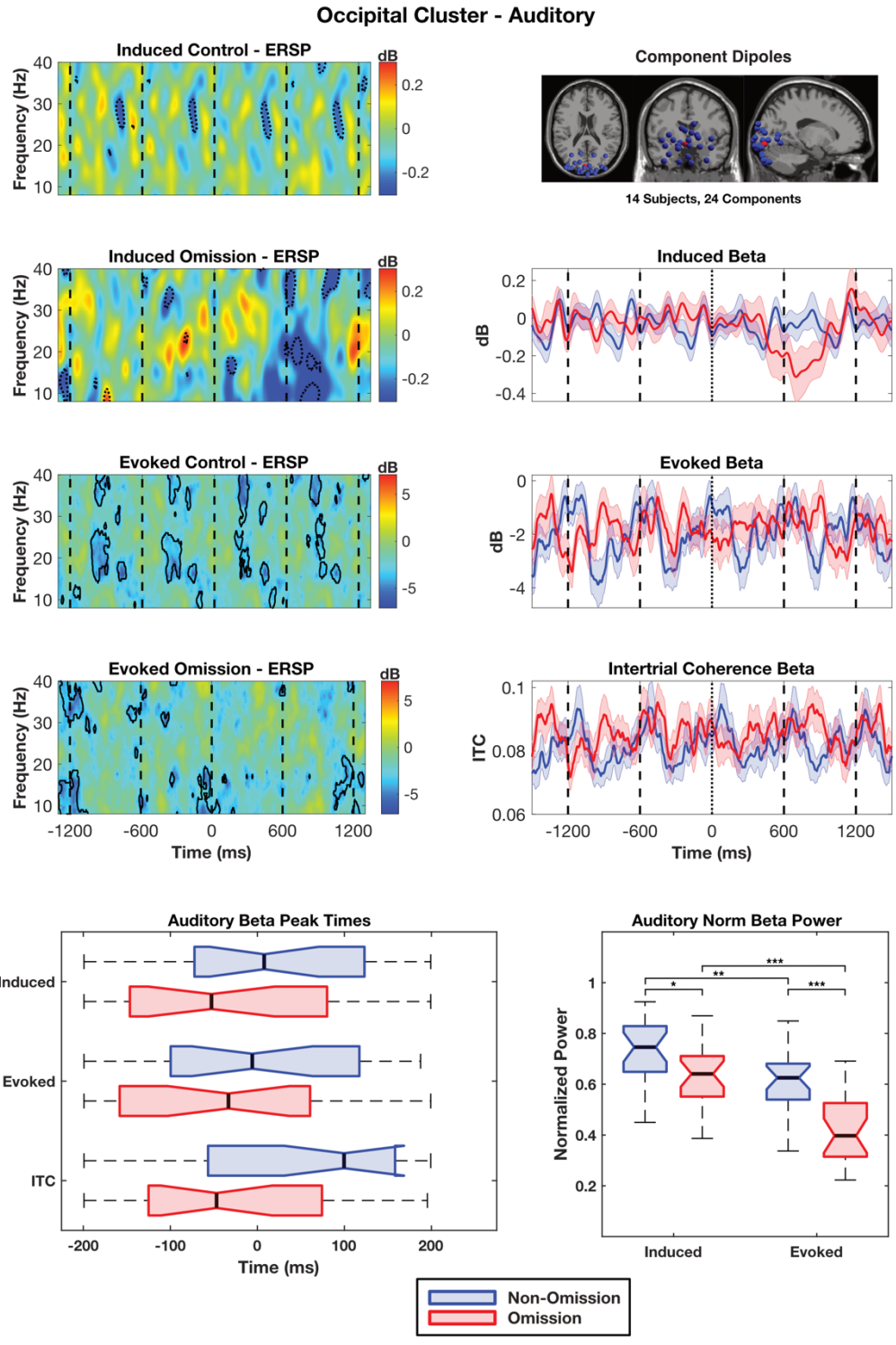
Occipital Cluster - Auditory
Induced Control - ERSP
Component Dipoles
14 Subjects, 24 Components
Induced Omission - ERSP
Induced Beta
Evoked Control - ERSP
Evoked Beta
Evoked Omission - ERSP
Intertrial Coherence Beta
Frequency (Hz)
dB
Time (ms)
ITC
Auditory Beta Peak Times
Induced
Evoked
ITC
Auditory Norm Beta Power
Normalized Power
Non-Omission
Omission

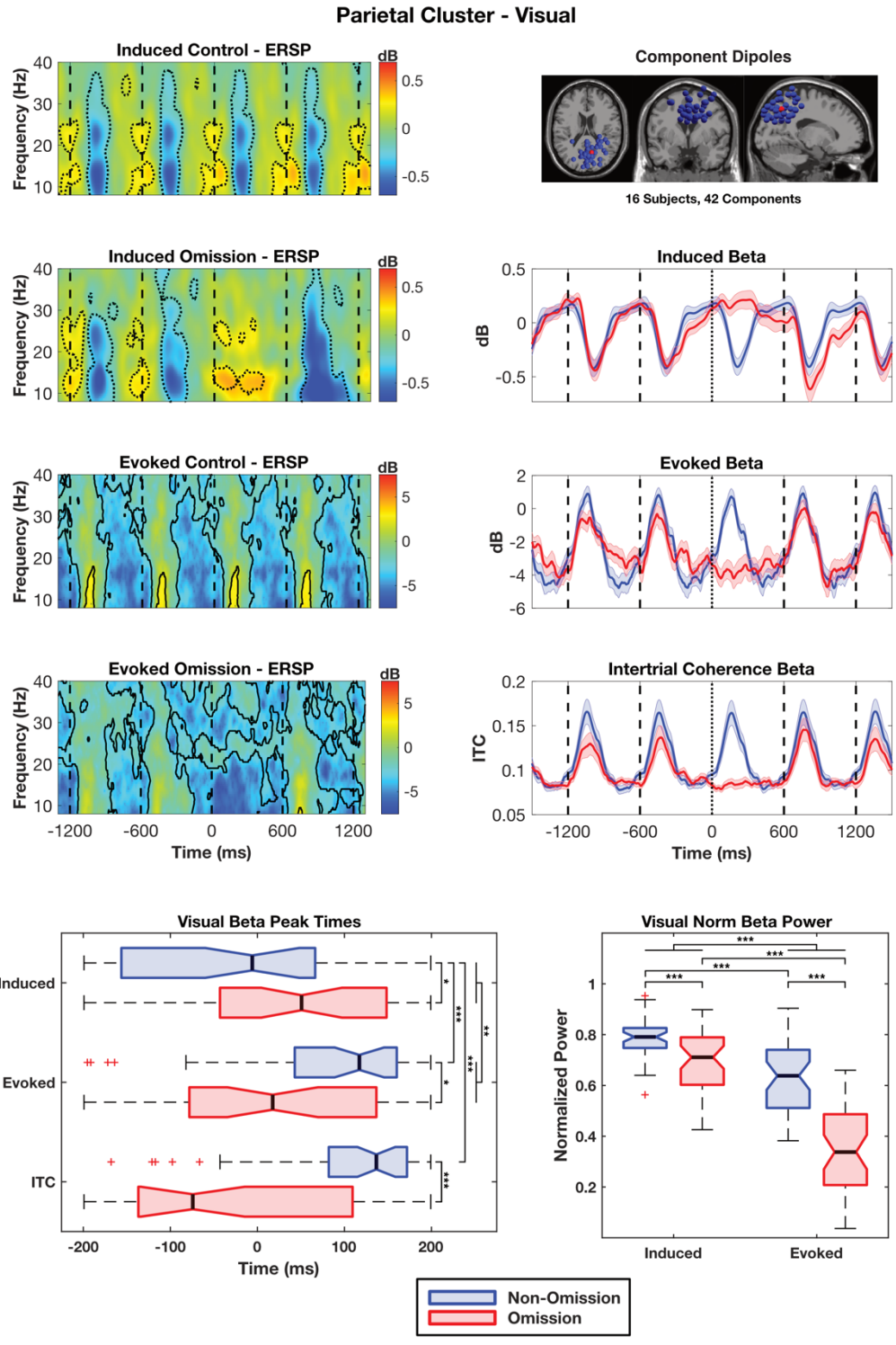
Parietal Cluster - Visual
Induced Control - ERSP
Component Dipoles
16 Subjects, 42 Components
Induced Omission - ERSP
Induced Beta
Evoked Control - ERSP
Evoked Beta
Evoked Omission - ERSP
Intertrial Coherence Beta
Frequency (Hz)
dB
ITC
Time (ms)
Visual Beta Peak Times
Visual Norm Beta Power
Induced
Evoked
Normalized Power
Non-Omission
Omission

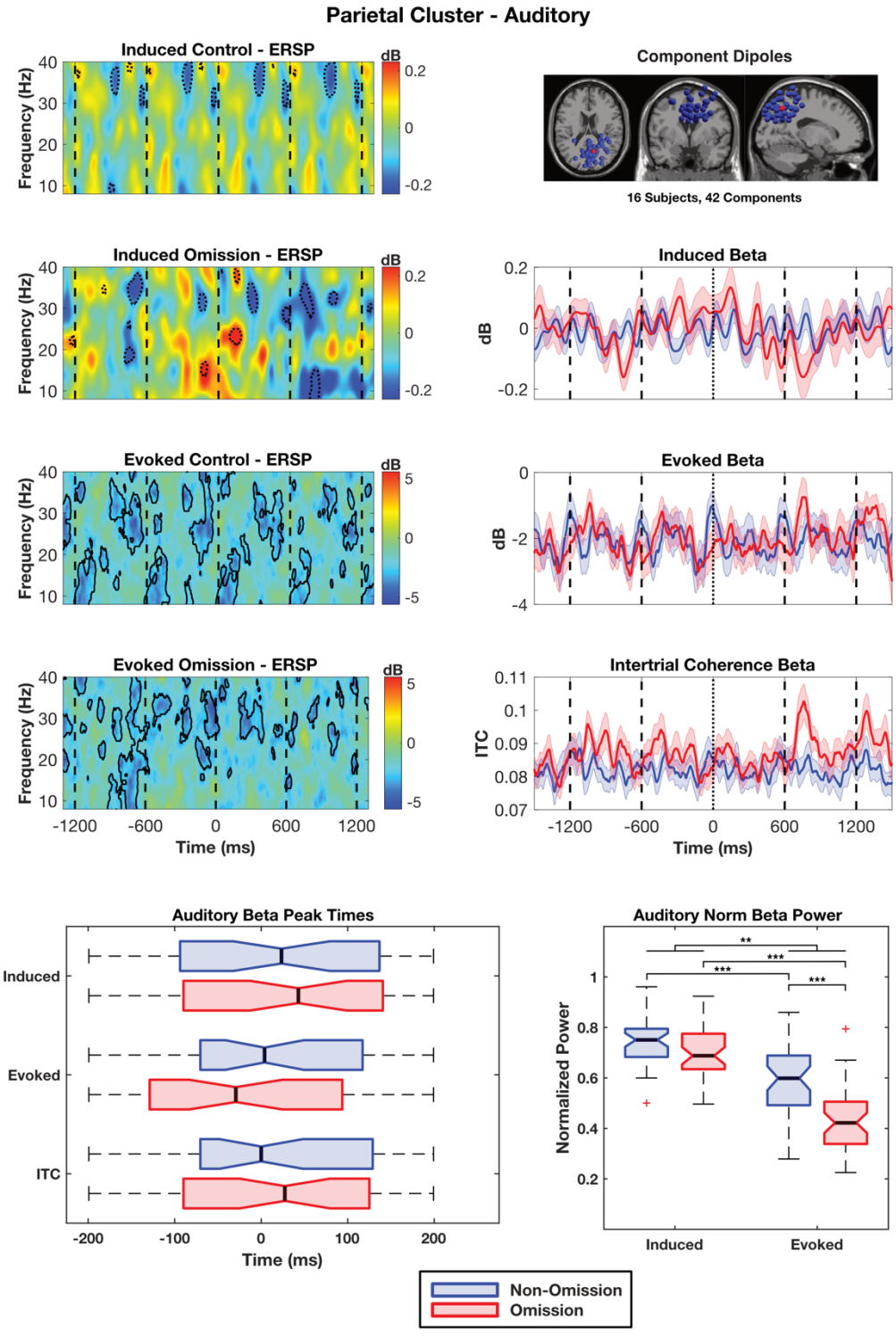
Parietal Cluster - Auditory
Induced Control - ERSP
Component Dipoles
16 Subjects, 42 Components
Induced Omission - ERSP
Induced Beta
Evoked Control - ERSP
Evoked Beta
Evoked Omission - ERSP
Intertrial Coherence Beta
Frequency (Hz)
dB
Time (ms)
ITC
Auditory Beta Peak Times
Induced
Evoked
Auditory Norm Beta Power
Normalized Power
Non-Omission
Omission

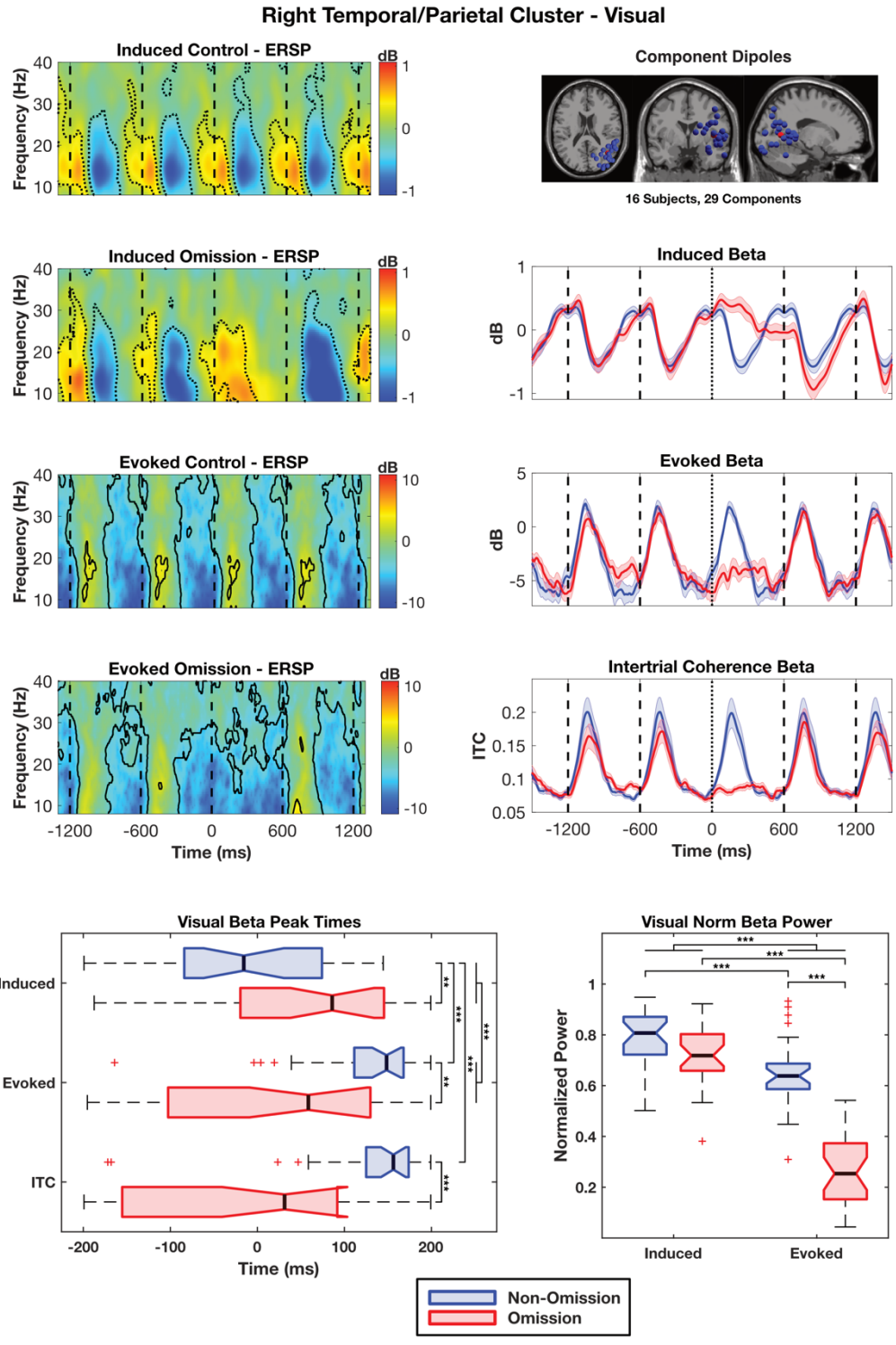
Right Temporal/Parietal Cluster - Visual
Induced Control - ERSP
Component Dipoles
16 Subjects, 29 Components
Induced Omission - ERSP
Induced Beta
Evoked Control - ERSP
Evoked Beta
Evoked Omission - ERSP
Intertrial Coherence Beta
Frequency (Hz)
dB
ITC
Time (ms)
Visual Beta Peak Times
Visual Norm Beta Power
Induced
Evoked
Normalized Power
Non-Omission
Omission

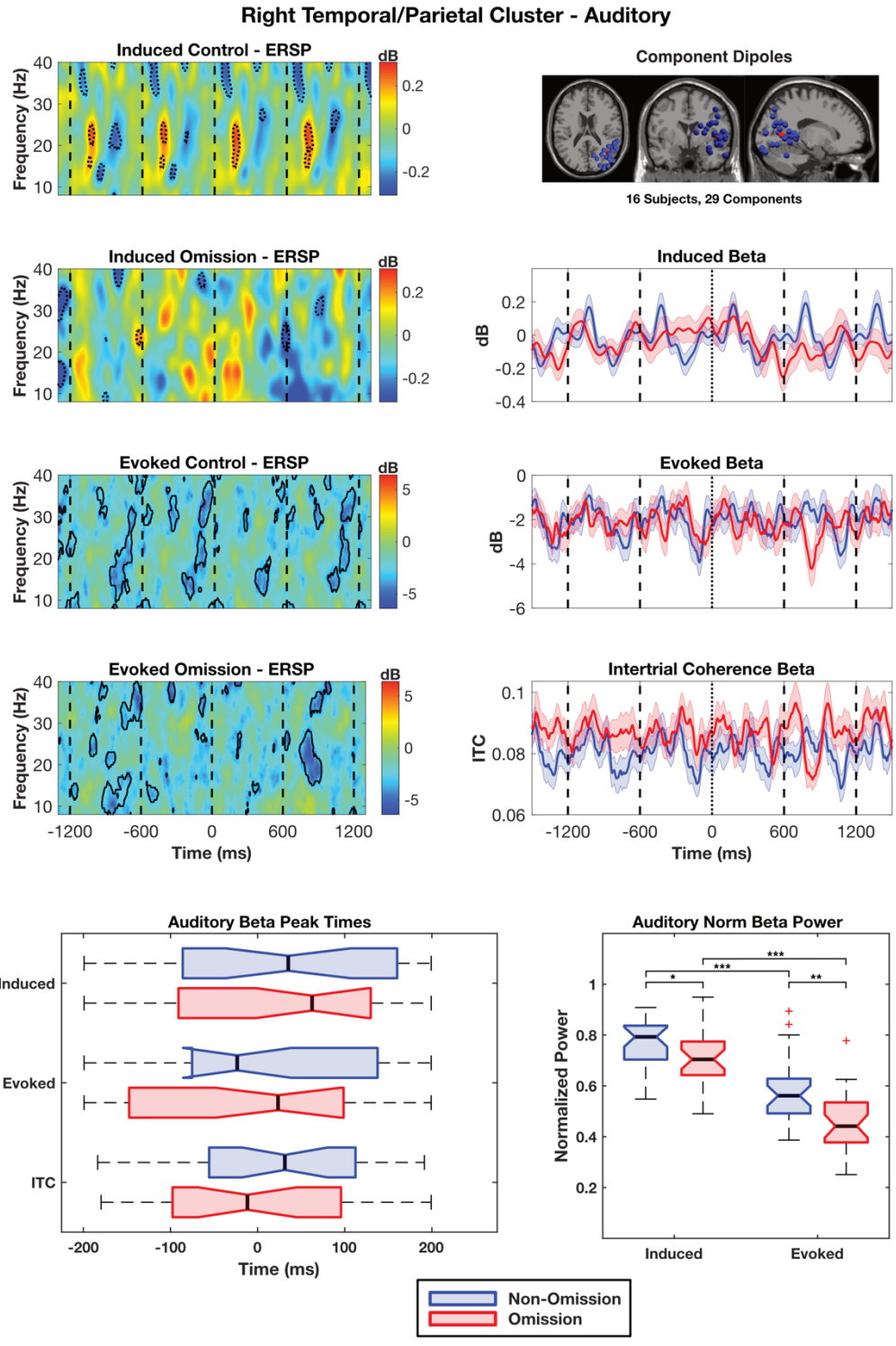
Right Temporal/Parietal Cluster - Auditory
Induced Control - ERSP
Component Dipoles
16 Subjects, 29 Components
Induced Omission - ERSP
Induced Beta
Evoked Control - ERSP
Evoked Beta
Evoked Omission - ERSP
Intertrial Coherence Beta
Frequency (Hz)
dB
Time (ms)
ITC
Auditory Beta Peak Times
Induced
Evoked
Auditory Norm Beta Power
Normalized Power
Non-Omission
Omission

Supplemental Table 1

Visual Condition		Slope Values								T-Tests							
		Control		Omission		Shuffled		Contrast		Control to Omission			Control to Shuffle		Omission to Shuffle		Contrast Test
Cluster	Slope Type	*mean*	*sd*	*mean*	*sd*	*mean*	*sd*	*mean*	*sd*	*df*	*ts*	*pv*	*ts*	*pv*	*ts*	*pv*	*ts*	*pv*
0 - Parent	Induced Trough	0.00236	0.00298	0.00249	0.00329	0.00000	0.00027	-0.00263	0.00648	288	-0.61	0.793	13.36	0.000	12.77	0.000	-6.89	0.000
	Induced Fixed	0.00071	0.00293	0.00085	0.00267	0.00001	0.00012	-0.00098	0.00494	288	-0.76	0.734	4.07	0.001	5.37	0.000	-3.38	0.004
	Evoked Trough	0.02022	0.03432	0.01675	0.03443	-0.00035	0.00353	-0.01362	0.07582	288	1.24	0.473	10.15	0.000	8.35	0.000	-3.05	0.018
	Evoked Fixed	-0.00164	0.01712	-0.00165	0.01738	-0.00006	0.00121	0.00160	0.03640	288	0.01	0.992	-1.57	0.327	-1.56	0.327	0.75	0.723
1 - L. Frontal	Induced Trough	0.00176	0.00237	0.00232	0.00282	0.00003	0.00016	-0.00285	0.00580	19	-0.74	0.734	3.22	0.018	3.63	0.008	-2.20	0.113
	Induced Fixed	-0.00042	0.00214	0.00072	0.00258	0.00002	0.00010	-0.00184	0.00497	19	-1.79	0.224	-0.90	0.682	1.21	0.486	-1.65	0.265
	Evoked Trough	0.02721	0.03375	0.02426	0.03271	0.00013	0.00244	-0.02118	0.06897	19	0.30	0.919	3.58	0.016	3.30	0.025	-1.37	0.426
	Evoked Fixed	0.00028	0.02031	0.00010	0.01942	0.00058	0.00132	0.00066	0.04499	19	0.03	0.988	-0.07	0.982	-0.11	0.981	0.07	0.982
2 - L. Motor	Induced Trough	0.00223	0.00273	0.00208	0.00404	-0.00004	0.00027	-0.00197	0.00769	34	0.22	0.956	4.93	0.000	3.19	0.013	-1.52	0.305
	Induced Fixed	0.00064	0.00194	0.00034	0.00224	-0.00001	0.00012	-0.00005	0.00481	34	0.61	0.796	1.99	0.141	0.93	0.668	-0.06	0.981
	Evoked Trough	0.01093	0.02892	0.01295	0.03644	-0.00039	0.00266	-0.01536	0.07383	34	-0.28	0.930	2.35	0.098	2.21	0.123	-1.23	0.481
	Evoked Fixed	-0.00279	0.01855	-0.00403	0.01696	-0.00014	0.00122	0.00512	0.03637	34	0.31	0.919	-0.85	0.655	-1.35	0.426	0.83	0.663
3 - Midline Central	Induced Trough	0.00264	0.00322	0.00262	0.00276	-0.00001	0.00021	-0.00262	0.00548	34	0.02	0.983	4.77	0.000	5.55	0.000	-2.83	0.027
	Induced Fixed	0.00068	0.00172	0.00083	0.00179	-0.00001	0.00012	-0.00099	0.00370	34	-0.39	0.868	2.34	0.076	2.77	0.030	-1.59	0.275
	Evoked Trough	0.01541	0.03024	0.01949	0.02755	0.00024	0.00357	-0.02333	0.06416	34	-0.58	0.807	2.87	0.038	4.04	0.003	-2.15	0.136
	Evoked Fixed	-0.00192	0.01502	0.00696	0.01813	-0.00010	0.00149	-0.01593	0.03532	34	-2.58	0.063	-0.72	0.727	2.32	0.101	-2.67	0.057
4 - R. Sensorimotor	Induced Trough	0.00287	0.00258	0.00202	0.00361	-0.00001	0.00021	-0.00117	0.00678	33	1.36	0.386	6.32	0.000	3.25	0.012	-1.01	0.627
	Induced Fixed	0.00056	0.00178	0.00002	0.00261	-0.00002	0.00010	0.00049	0.00563	33	0.96	0.652	1.90	0.169	0.10	0.981	0.51	0.840
	Evoked Trough	0.01235	0.03069	0.01420	0.02874	-0.00007	0.00317	-0.01612	0.05886	33	-0.30	0.919	2.30	0.102	2.76	0.050	-1.60	0.327
	Evoked Fixed	-0.00202	0.01948	-0.00172	0.01492	-0.00042	0.00114	0.00099	0.03162	33	-0.08	0.982	-0.48	0.841	-0.51	0.834	0.18	0.966
5 - R. Frontal	Induced Trough	0.00172	0.00277	0.00287	0.00369	-0.00003	0.00027	-0.00404	0.00735	38	-1.71	0.231	3.85	0.003	4.92	0.000	-3.44	0.007
	Induced Fixed	-0.00038	0.00241	-0.00017	0.00270	0.00000	0.00009	-0.00003	0.00526	38	-0.42	0.856	-1.00	0.630	-0.40	0.866	-0.04	0.981
	Evoked Trough	0.02279	0.03437	0.02175	0.03641	-0.00089	0.00377	-0.02160	0.08159	38	0.13	0.981	4.26	0.002	3.87	0.004	-1.65	0.317
	Evoked Fixed	0.00101	0.01758	0.00141	0.01853	0.00029	0.00118	-0.00152	0.03530	38	-0.12	0.981	0.25	0.935	0.38	0.897	-0.27	0.930
6 - L. Temporal/Parietal	Induced Trough	0.00237	0.00272	0.00338	0.00313	-0.00003	0.00017	-0.00441	0.00590	27	-1.62	0.265	4.58	0.001	5.56	0.000	-3.96	0.003
	Induced Fixed	0.00204	0.00254	0.00198	0.00270	-0.00001	0.00016	-0.00193	0.00468	27	0.13	0.968	4.17	0.002	3.75	0.004	-2.18	0.109
	Evoked Trough	0.01410	0.02736	0.01828	0.03417	0.00078	0.00354	-0.02167	0.07846	27	-0.47	0.846	2.62	0.063	2.67	0.058	-1.46	0.391
	Evoked Fixed	-0.00331	0.01625	0.00029	0.01569	0.00013	0.00141	-0.00375	0.03196	27	-0.97	0.614	-1.11	0.556	0.05	0.987	-0.62	0.785
7 - Occipital	Induced Trough	0.00200	0.00391	0.00123	0.00198	0.00021	0.00066	-0.00025	0.00613	23	0.85	0.685	2.52	0.058	2.23	0.104	-0.20	0.967
	Induced Fixed	-0.00062	0.00550	0.00031	0.00275	0.00001	0.00015	-0.00123	0.00683	23	-0.83	0.693	-0.57	0.806	0.53	0.832	-0.88	0.682
	Evoked Trough	0.02794	0.03953	0.00800	0.03610	-0.00029	0.00424	0.01165	0.07653	23	1.99	0.193	3.45	0.016	1.11	0.556	0.75	0.723
	Evoked Fixed	-0.00715	0.01160	-0.00947	0.01941	0.00022	0.00163	0.01199	0.04036	23	0.51	0.834	-3.09	0.031	-2.40	0.098	1.46	0.394
8 - Parietal	Induced Trough	0.00213	0.00261	0.00255	0.00336	-0.00003	0.00022	-0.00300	0.00658	41	-0.73	0.734	5.41	0.000	4.99	0.000	-2.95	0.019
	Induced Fixed	0.00096	0.00223	0.00135	0.00248	0.00001	0.00011	-0.00173	0.00379	41	-1.33	0.392	2.81	0.027	3.51	0.005	-2.95	0.019
	Evoked Trough	0.03244	0.03901	0.02068	0.03485	-0.00060	0.00409	-0.00952	0.08396	41	1.37	0.426	5.39	0.000	3.98	0.003	-0.73	0.723
	Evoked Fixed	0.00274	0.01507	-0.00207	0.01362	-0.00004	0.00122	0.00685	0.03282	41	1.47	0.380	1.24	0.479	-0.95	0.617	1.35	0.426
9 - R. Temporal/Parietal	Induced Trough	0.00371	0.00372	0.00323	0.00308	0.00006	0.00023	-0.00269	0.00549	28	0.74	0.734	5.21	0.000	5.46	0.000	-2.63	0.043
	Induced Fixed	0.00294	0.00389	0.00268	0.00306	0.00002	0.00018	-0.00240	0.00476	28	0.47	0.847	4.05	0.002	4.61	0.001	-2.72	0.037
	Evoked Trough	0.02333	0.03895	0.00933	0.04078	-0.00041	0.00423	0.00426	0.08653	28	1.39	0.422	3.24	0.022	1.32	0.442	0.27	0.930
	Evoked Fixed	-0.00335	0.01871	-0.00879	0.01773	0.00009	0.00131	0.01431	0.04105	28	1.10	0.556	-0.98	0.614	-2.68	0.058	1.88	0.231

Visual Slope statistics for each cluster for induced and evoked slopes. Contrast values are calculated as the control slope + the shuffle slope – (2 * omission slope). The contrast test compares the contrast values to zero. Degrees of freedom were the same for each of four t-tests on the same row. P-values displayed are FDR corrected.

Supplemental Table 2

Auditory Condition

		Slope Values								T-Tests							
		Control		Omission		Shuffled		Contrast		Control to Omission			Control to Shuffle		Omission to Shuffle		Contrast Test
Cluster	Slope Type	*mean*	*sd*	*mean*	*sd*	*mean*	*sd*	*mean*	*sd*	*df*	*ts*	*pv*	*ts*	*pv*	*ts*	*pv*	*ts*	*pv*
0 - Parent	Induced Trough	0.00186	0.00308	0.00202	0.00335	0.00001	0.00021	-0.00216	0.00701	288	-0.62	0.793	10.20	0.000	10.13	0.000	-5.24	0.000
	Induced Fixed	0.00008	0.00189	0.00009	0.00209	0.00001	0.00009	-0.00009	0.00476	288	-0.04	0.981	0.67	0.761	0.67	0.761	-0.32	0.901
	Evoked Trough	0.02290	0.03363	0.02033	0.03322	-0.00004	0.00306	-0.01780	0.07456	288	0.92	0.618	11.51	0.000	10.40	0.000	-4.06	0.001
	Evoked Fixed	0.00109	0.01779	-0.00055	0.01848	0.00015	0.00117	0.00233	0.04133	288	1.07	0.556	0.90	0.628	-0.64	0.769	0.96	0.614
1 - L. Frontal	Induced Trough	0.00105	0.00424	0.00163	0.00232	0.00007	0.00040	-0.00214	0.00555	19	-0.58	0.806	0.96	0.655	2.93	0.029	-1.73	0.240
	Induced Fixed	-0.00084	0.00277	0.00097	0.00238	-0.00001	0.00012	-0.00279	0.00590	19	-2.05	0.141	-1.35	0.397	1.86	0.197	-2.12	0.129
	Evoked Trough	0.00927	0.02620	0.02828	0.03242	-0.00014	0.00185	-0.04742	0.07493	19	-1.86	0.250	1.66	0.324	3.92	0.008	-2.83	0.054
	Evoked Fixed	0.00341	0.01589	0.00328	0.01881	-0.00030	0.00084	-0.00345	0.04142	19	0.02	0.988	1.03	0.593	0.86	0.655	-0.37	0.897
2 - L. Sensorimotor	Induced Trough	0.00150	0.00270	0.00189	0.00444	-0.00002	0.00019	-0.00230	0.00862	34	-0.50	0.841	3.30	0.011	2.53	0.050	-1.58	0.277
	Induced Fixed	-0.00001	0.00169	0.00006	0.00223	0.00000	0.00007	-0.00012	0.00510	34	-0.12	0.969	-0.04	0.981	0.14	0.968	-0.13	0.968
	Evoked Trough	0.01107	0.02256	0.03143	0.03536	0.00001	0.00242	-0.05177	0.07661	34	-2.74	0.050	2.92	0.035	5.25	0.000	-4.00	0.004
	Evoked Fixed	0.00308	0.01653	0.00411	0.01442	-0.00015	0.00110	-0.00529	0.03070	34	-0.30	0.919	1.15	0.537	1.77	0.267	-1.02	0.593
3 - Midline Central	Induced Trough	0.00183	0.00354	0.00215	0.00391	0.00003	0.00020	-0.00244	0.00714	34	-0.46	0.847	3.02	0.019	3.17	0.014	-2.02	0.137
	Induced Fixed	-0.00005	0.00140	-0.00009	0.00231	0.00001	0.00009	0.00015	0.00481	34	0.09	0.981	-0.28	0.929	-0.27	0.929	0.18	0.968
	Evoked Trough	0.02864	0.03863	0.01893	0.03400	0.00083	0.00297	-0.00839	0.07216	34	1.24	0.481	4.25	0.002	3.09	0.025	-0.69	0.747
	Evoked Fixed	-0.00319	0.01843	0.00039	0.01859	0.00027	0.00103	-0.00369	0.03589	34	-0.97	0.614	-1.09	0.556	0.04	0.988	-0.61	0.785
4 - R. Sensorimotor	Induced Trough	0.00186	0.00293	0.00118	0.00256	0.00003	0.00022	-0.00047	0.00592	33	1.02	0.625	3.72	0.004	2.62	0.042	-0.46	0.847
	Induced Fixed	0.00027	0.00203	0.00038	0.00156	-0.00002	0.00010	-0.00051	0.00403	33	-0.23	0.952	0.83	0.689	1.48	0.323	-0.74	0.734
	Evoked Trough	0.01731	0.02658	0.00938	0.02251	0.00013	0.00285	-0.00133	0.05211	33	1.31	0.442	3.67	0.008	2.43	0.087	-0.15	0.977
	Evoked Fixed	0.00160	0.01797	-0.00053	0.01891	0.00002	0.00127	0.00268	0.04903	33	0.39	0.896	0.51	0.834	-0.17	0.972	0.32	0.919
5 - R. Frontal	Induced Trough	0.00286	0.00353	0.00231	0.00389	-0.00011	0.00029	-0.00187	0.00837	38	0.66	0.771	5.11	0.000	3.94	0.002	-1.39	0.366
	Induced Fixed	-0.00017	0.00179	-0.00039	0.00242	0.00000	0.00010	0.00060	0.00534	38	0.42	0.856	-0.59	0.803	-0.98	0.641	0.70	0.757
	Evoked Trough	0.02024	0.03283	0.02181	0.02620	0.00065	0.00294	-0.02273	0.06200	38	-0.23	0.945	3.77	0.005	5.01	0.000	-2.29	0.102
	Evoked Fixed	0.00120	0.01681	0.00024	0.02091	-0.00011	0.00136	0.00061	0.04832	38	0.20	0.961	0.49	0.840	0.11	0.981	0.08	0.982
6 - L. Temporal/Parietal	Induced Trough	0.00191	0.00314	0.00238	0.00320	0.00004	0.00026	-0.00281	0.00710	27	-0.56	0.811	3.12	0.017	3.79	0.004	-2.10	0.126
	Induced Fixed	0.00022	0.00192	0.00023	0.00171	-0.00001	0.00009	-0.00025	0.00380	27	-0.02	0.983	0.63	0.793	0.75	0.734	-0.35	0.883
	Evoked Trough	0.01678	0.02840	0.02216	0.04056	-0.00078	0.00331	-0.02832	0.09018	27	-0.53	0.833	3.18	0.025	3.02	0.032	-1.66	0.317
	Evoked Fixed	-0.00053	0.01547	-0.00088	0.02210	-0.00023	0.00125	0.00100	0.04488	27	0.07	0.982	-0.10	0.981	-0.16	0.974	0.12	0.981
7 - Occipital	Induced Trough	0.00152	0.00239	0.00186	0.00296	0.00001	0.00023	-0.00219	0.00627	23	-0.46	0.847	3.18	0.017	2.95	0.026	-1.71	0.240
	Induced Fixed	0.00039	0.00205	-0.00015	0.00192	0.00002	0.00009	0.00071	0.00400	23	1.03	0.625	0.87	0.682	-0.44	0.851	0.87	0.682
	Evoked Trough	0.03113	0.03413	0.01391	0.03010	-0.00045	0.00305	0.00287	0.06284	23	2.03	0.182	4.47	0.002	2.41	0.098	0.22	0.949
	Evoked Fixed	0.00661	0.01898	-0.00177	0.01523	0.00032	0.00130	0.01047	0.03336	23	1.83	0.250	1.60	0.327	-0.66	0.768	1.54	0.362
8 - Parietal	Induced Trough	0.00135	0.00211	0.00210	0.00304	0.00003	0.00017	-0.00283	0.00622	41	-1.39	0.366	3.94	0.002	4.41	0.001	-2.94	0.019
	Induced Fixed	0.00012	0.00167	-0.00003	0.00187	-0.00001	0.00007	0.00017	0.00428	41	0.37	0.879	0.51	0.840	-0.06	0.981	0.26	0.938
	Evoked Trough	0.03394	0.04097	0.02020	0.03605	-0.00032	0.00310	-0.00678	0.08332	41	1.63	0.321	5.46	0.000	3.67	0.006	-0.53	0.833
	Evoked Fixed	0.00076	0.01546	-0.00282	0.01891	-0.00031	0.00095	0.00609	0.04178	41	0.92	0.621	0.45	0.858	-0.86	0.655	0.94	0.617
9 - R. Temporal/Parietal	Induced Trough	0.00258	0.00313	0.00270	0.00285	0.00002	0.00027	-0.00280	0.00678	28	-0.14	0.968	4.45	0.001	5.08	0.000	-2.22	0.101
	Induced Fixed	0.00057	0.00188	0.00021	0.00227	0.00000	0.00010	0.00016	0.00534	28	0.60	0.798	1.64	0.264	0.48	0.847	0.17	0.968
	Evoked Trough	0.03172	0.03733	0.01840	0.03940	-0.00034	0.00345	-0.00542	0.08205	28	1.43	0.398	4.66	0.001	2.56	0.069	-0.36	0.900
	Evoked Fixed	-0.00203	0.02424	-0.00699	0.01736	-0.00015	0.00132	0.01180	0.04222	28	0.90	0.833	-0.42	0.881	-2.12	0.148	1.51	0.371

Auditory Slope statistics for each cluster for induced and evoked slopes. Contrast values are calculated as the control slope + the shuffle slope – (2 * omission slope). The contrast test compares the contrast values to zero. Degrees of freedom were the same for each of four t-tests on the same row. P-values displayed are FDR corrected.

Supplemental Table 3

Visual Condition		Beta Peak Times (ms)						T-Tests								
		Control		Omission		Difference		Control to Omission				Induced to Evoked				Induced to Evoked Diffs
Clusters		*mean*	*sd*	*mean*	*sd*	*mean*	*sd*		*df*	*ts*	*pv*		*ts*	*pv*		*ts*	*pv*
0 - Parent	Induced	-12.95	120.03	28.74	129.27	-41.68	158.43	Induced	288	-4.47	0.000	Control	8.06	0.000		7.04	0.000
	Evoked	68.49	122.18	11.04	133.51	57.44	180.00	Evoked	288	5.43	0.000	Omission	-1.67	0.164			
1 - L. Frontal	Induced	11.33	137.98	21.48	138.89	-10.16	176.41	Induced	19	-0.26	0.877	Control	0.52	0.719		0.33	0.829
	Evoked	32.42	136.58	24.61	129.28	7.81	202.87	Evoked	19	0.17	0.933	Omission	0.08	0.963			
2 - L. Sensorimotor	Induced	-9.04	113.42	18.64	132.01	-27.68	164.27	Induced	34	-1.00	0.446	Control	1.66	0.177		1.86	0.128
	Evoked	40.63	127.36	-13.39	141.92	54.02	206.50	Evoked	34	1.55	0.210	Omission	-1.08	0.407			
3 - Midline Central	Induced	26.90	120.76	38.95	123.48	-12.05	158.26	Induced	34	-0.45	0.764	Control	-0.07	0.972		0.76	0.575
	Evoked	25.00	137.51	4.69	126.78	20.31	197.28	Evoked	34	0.61	0.670	Omission	-1.21	0.345			
4 - R. Sensorimotor	Induced	9.08	139.99	34.70	142.83	-25.62	144.20	Induced	33	-1.04	0.429	Control	1.55	0.210		1.00	0.443
	Evoked	56.41	127.25	46.65	127.69	9.77	141.52	Evoked	33	0.40	0.788	Omission	0.36	0.814			
5 - R. Frontal	Induced	-26.44	121.61	-0.40	126.78	-26.04	182.90	Induced	38	-0.89	0.497	Control	2.90	0.015		0.94	0.472
	Evoked	49.88	130.10	41.97	119.78	7.91	144.18	Evoked	38	0.34	0.821	Omission	1.50	0.227			
6 - L. Temporal/Parietal	Induced	-30.83	105.95	53.57	101.39	-84.40	144.69	Induced	27	-3.09	0.012	Control	3.24	0.008		3.69	0.003
	Evoked	77.57	130.09	-0.28	136.29	77.85	178.64	Evoked	27	2.31	0.060	Omission	-2.04	0.098			
7 - Occipital	Induced	-48.67	117.54	10.74	154.53	-59.41	148.07	Induced	23	-1.97	0.114	Control	7.35	0.000		4.90	0.000
	Evoked	127.93	71.77	-62.83	133.05	190.76	160.65	Evoked	23	5.82	0.000	Omission	-1.79	0.152			
8 - Parietal	Induced	-35.53	116.88	34.78	122.51	-70.31	161.65	Induced	41	-2.82	0.017	Control	4.95	0.000		4.06	0.001
	Evoked	92.82	106.72	25.11	138.61	67.71	171.43	Evoked	41	2.56	0.032	Omission	-0.35	0.818			
9 - R. Temporal/Parietal	Induced	-14.82	94.91	63.44	120.89	-78.26	123.60	Induced	28	-3.41	0.005	Control	5.61	0.000		6.09	0.000
	Evoked	121.77	79.30	-2.16	132.40	123.92	165.21	Evoked	28	4.04	0.001	Omission	-1.98	0.107			

Visual peak times for beta activity within +/- 200 ms of event or omission onset. Difference values are calculated as the difference between control and omission times. Control to omission tests comparisons are made for both induced and evoked activity. Induced to evoked test comparisons are made for both control and omission conditions. Induced to evoke difference tests are made between the difference values calculated. Degrees of freedom were the same for each of the t-tests on the same row. P-values displayed are FDR corrected.

Supplemental Table 4

Visual Condition		Normalized Beta Peak Power						T-Tests									
		Control		Omission		Difference		Control to Omission				Induced to Evoked				Induced to Evoked Diffs	
Clusters		*mean*	*sd*	*mean*	*sd*	*mean*	*sd*		*df*	*ts*	*pv*		*ts*	*pv*		*ts*	*pv*
0 - Parent	Induced	0.75	0.12	0.66	0.14	0.09	0.16	Induced	288	9.58	0.000	Control	-13.00	0.000		11.24	0.000
	Evoked	0.63	0.14	0.37	0.16	0.26	0.22	Evoked	288	20.04	0.000	Omission	-23.99	0.000			
1 - L. Frontal	Induced	0.72	0.12	0.62	0.16	0.10	0.17	Induced	19	2.52	0.045	Control	-2.88	0.023		1.60	0.206
	Evoked	0.61	0.13	0.43	0.16	0.18	0.16	Evoked	19	5.10	0.000	Omission	-4.57	0.001			
2 - L. Sensorimotor	Induced	0.72	0.13	0.65	0.11	0.07	0.16	Induced	34	2.47	0.041	Control	-4.79	0.000		2.36	0.050
	Evoked	0.59	0.11	0.43	0.16	0.16	0.19	Evoked	34	5.05	0.000	Omission	-7.93	0.000			
3 - Midline Central	Induced	0.76	0.11	0.66	0.13	0.10	0.16	Induced	34	3.69	0.002	Control	-4.80	0.000		2.46	0.042
	Evoked	0.63	0.14	0.42	0.15	0.21	0.23	Evoked	34	5.46	0.000	Omission	-6.37	0.000			
4 - R. Sensorimotor	Induced	0.75	0.13	0.61	0.16	0.15	0.16	Induced	33	5.32	0.000	Control	-5.64	0.000		1.40	0.267
	Evoked	0.60	0.16	0.40	0.13	0.20	0.17	Evoked	33	6.58	0.000	Omission	-6.84	0.000			
5 - R. Frontal	Induced	0.70	0.11	0.63	0.13	0.07	0.16	Induced	38	2.92	0.014	Control	-3.59	0.003		4.33	0.000
	Evoked	0.62	0.12	0.38	0.15	0.24	0.17	Evoked	38	8.65	0.000	Omission	-7.21	0.000			
6 - L. Temporal/Parietal	Induced	0.80	0.10	0.71	0.11	0.09	0.13	Induced	27	3.51	0.004	Control	-6.73	0.000		3.12	0.011
	Evoked	0.61	0.15	0.38	0.16	0.23	0.24	Evoked	27	5.16	0.000	Omission	-10.23	0.000			
7 - Occipital	Induced	0.76	0.13	0.69	0.13	0.07	0.17	Induced	23	2.05	0.099	Control	0.23	0.896		10.98	0.000
	Evoked	0.77	0.11	0.21	0.12	0.56	0.17	Evoked	23	15.91	0.000	Omission	-12.89	0.000			
8 - Parietal	Induced	0.79	0.09	0.69	0.12	0.10	0.15	Induced	41	4.34	0.000	Control	-6.30	0.000		4.38	0.000
	Evoked	0.63	0.14	0.35	0.17	0.28	0.23	Evoked	41	7.89	0.000	Omission	-10.70	0.000			
9 - R. Temporal/Parietal	Induced	0.79	0.11	0.72	0.13	0.06	0.16	Induced	28	2.03	0.099	Control	-5.60	0.000		8.47	0.000
	Evoked	0.65	0.14	0.26	0.14	0.38	0.18	Evoked	28	11.24	0.000	Omission	-14.50	0.000			

Normalized visual peak power for beta activity within +/- 200 ms of event or omission onset. Difference values are calculated as the difference between control and omission times. Control to omission tests comparisons are made for both induced and evoked activity. Induced to evoked test comparisons are made for both control and omission conditions. Induced to evoke difference tests are made between the difference values calculated. Degrees of freedom were the same for each of the t-tests on the same row. P-values displayed are FDR corrected.

Supplemental Table 5

Auditory Condition

Beta Peak Times (ms)

T-Tests

Clusters		Control		Omission		Difference		Control to Omission				Induced to Evoked			Induced to Evoked Diffs	
		mean	*sd*	*mean*	*sd*	*mean*	*sd*		*df*	*ts*	*pv*		*ts*	*pv*	*ts*	*pv*
0 - Parent	Induced	0.35	129.60	6.69	135.51	-6.34	182.30	Induced	288	-0.59	0.673	Control	0.95	0.462	1.28	0.304
	Evoked	10.64	122.49	-2.23	131.29	12.87	180.39	Evoked	288	1.21	0.336	Omission	-0.83	0.526		
1 - L. Frontal	Induced	-22.66	138.47	-19.92	136.10	-2.73	150.11	Induced	19	-0.08	0.963	Control	1.06	0.426	1.18	0.361
	Evoked	19.53	128.98	-28.91	109.66	48.44	136.99	Evoked	19	1.58	0.210	Omission	-0.21	0.907		
2 - L. Sensorimotor	Induced	-23.44	122.23	21.99	138.62	-45.42	151.10	Induced	34	-1.78	0.149	Control	3.27	0.006	2.39	0.047
	Evoked	64.96	124.59	29.58	111.35	35.38	167.02	Evoked	34	1.25	0.327	Omission	0.26	0.874		
3 - Midline Central	Induced	32.48	125.39	21.21	129.25	11.27	168.54	Induced	34	0.40	0.788	Control	-1.37	0.275	0.06	0.977
	Evoked	-11.61	129.08	-25.45	134.35	13.84	207.28	Evoked	34	0.39	0.788	Omission	-1.58	0.205		
4 - R. Sensorimotor	Induced	3.56	118.85	-6.89	151.20	10.45	200.26	Induced	33	0.30	0.847	Control	0.89	0.497	-0.93	0.478
	Evoked	30.91	114.84	59.28	125.09	-28.38	137.01	Evoked	33	-1.21	0.346	Omission	2.19	0.071		
5 - R. Frontal	Induced	-33.75	129.61	-7.21	141.50	-26.54	175.88	Induced	38	-0.94	0.470	Control	0.71	0.601	1.41	0.262
	Evoked	-10.42	122.37	-37.86	122.95	27.44	188.62	Evoked	38	0.91	0.485	Omission	-1.15	0.366		
6 - L. Temporal/Parietal	Induced	-16.74	146.03	-2.23	132.29	-14.51	198.83	Induced	27	-0.39	0.794	Control	0.10	0.952	0.46	0.764
	Evoked	-13.39	102.33	-22.32	121.03	8.93	172.75	Evoked	27	0.27	0.871	Omission	-0.60	0.673		
7 - Occipital	Induced	10.58	129.73	-30.44	125.69	41.02	193.50	Induced	23	1.04	0.430	Control	-0.12	0.951	-0.44	0.768
	Evoked	6.18	120.31	-10.42	150.06	16.60	192.28	Evoked	23	0.42	0.776	Omission	0.48	0.746		
8 - Parietal	Induced	20.00	128.40	24.65	132.50	-4.65	190.80	Induced	41	-0.16	0.934	Control	-0.75	0.581	0.14	0.943
	Evoked	1.58	119.70	0.84	141.81	0.74	186.44	Evoked	41	0.03	0.992	Omission	-0.84	0.525		
9 - R. Temporal/Parietal	Induced	29.90	135.02	29.36	131.53	0.54	215.35	Induced	28	0.01	0.992	Control	-0.56	0.700	0.15	0.934
	Evoked	7.41	135.23	-2.29	141.55	9.70	220.58	Evoked	28	0.24	0.890	Omission	-0.84	0.526		

Auditory peak times for beta activity within +/- 200 ms of event or omission onset. Difference values are calculated as the difference between control and omission times. Control to omission tests comparisons are made for both induced and evoked activity. Induced to evoked test comparisons are made for both control and omission conditions. Induced to evoke difference tests are made between the difference values calculated. Degrees of freedom were the same for each of the t-tests on the same row. P-values displayed are FDR corrected.

Supplemental Table 6

Auditory Condition

Clusters		Normalized Beta Peak Power						T-Tests									
		Control		Omission		Difference		Control to Omission				Induced to Evoked			Induced to Evoked Diffs		
		mean	*sd*	*mean*	*sd*	*mean*	*sd*		*df*	*ts*	*pv*		*ts*	*pv*	*ts*	*pv*
0 - Parent	Induced	0.73	0.10	0.68	0.12	0.05	0.16	Induced	288	5.72	0.000	Control	-15.65	0.000	6.51	0.000
	Evoked	0.59	0.13	0.44	0.15	0.15	0.19	Evoked	288	13.24	0.000	Omission	-20.27	0.000		
1 - L. Frontal	Induced	0.72	0.13	0.66	0.12	0.07	0.18	Induced	19	1.61	0.206	Control	-1.73	0.170	2.42	0.053
	Evoked	0.65	0.12	0.44	0.13	0.21	0.19	Evoked	19	4.85	0.000	Omission	-6.38	0.000		
2 - L. Motor	Induced	0.72	0.09	0.68	0.13	0.04	0.14	Induced	34	1.92	0.117	Control	-4.17	0.001	2.41	0.046
	Evoked	0.62	0.14	0.46	0.17	0.16	0.22	Evoked	34	4.19	0.001	Omission	-5.98	0.000		
3 - Midline Central	Induced	0.73	0.10	0.66	0.12	0.06	0.16	Induced	34	2.45	0.042	Control	-6.62	0.000	0.05	0.977
	Evoked	0.56	0.11	0.49	0.16	0.07	0.17	Evoked	34	2.31	0.056	Omission	-4.57	0.000		
4 - R. Motor	Induced	0.72	0.09	0.67	0.14	0.06	0.18	Induced	33	1.81	0.141	Control	-5.43	0.000	2.44	0.044
	Evoked	0.59	0.13	0.41	0.14	0.18	0.20	Evoked	33	5.31	0.000	Omission	-6.78	0.000		
5 - R. Frontal	Induced	0.72	0.11	0.66	0.13	0.05	0.16	Induced	38	2.07	0.087	Control	-4.70	0.000	2.90	0.015
	Evoked	0.60	0.11	0.43	0.15	0.17	0.21	Evoked	38	5.22	0.000	Omission	-7.47	0.000		
6 - L. Temporal/Parietal	Induced	0.72	0.09	0.72	0.14	0.00	0.17	Induced	27	0.15	0.934	Control	-7.18	0.000	2.24	0.068
	Evoked	0.54	0.11	0.43	0.17	0.11	0.21	Evoked	27	2.77	0.023	Omission	-7.22	0.000		
7 - Occipital	Induced	0.73	0.13	0.63	0.12	0.10	0.18	Induced	23	2.75	0.026	Control	-3.44	0.006	1.72	0.170
	Evoked	0.61	0.11	0.42	0.14	0.19	0.13	Evoked	23	7.17	0.000	Omission	-5.64	0.000		
8 - Parietal	Induced	0.74	0.09	0.70	0.11	0.04	0.13	Induced	41	2.15	0.075	Control	-7.05	0.000	3.47	0.003
	Evoked	0.59	0.14	0.44	0.13	0.16	0.18	Evoked	41	5.73	0.000	Omission	-9.79	0.000		
9 - R. Temporal/Parietal	Induced	0.77	0.09	0.70	0.11	0.07	0.13	Induced	28	2.72	0.025	Control	-7.57	0.000	1.40	0.270
	Evoked	0.58	0.13	0.45	0.12	0.13	0.20	Evoked	28	3.56	0.004	Omission	-7.18	0.000		

Normalized auditory peak power for beta activity within +/- 200 ms of event or omission onset. Difference values are calculated as the difference between control and omission times. Control to omission tests comparisons are made for both induced and evoked activity. Induced to evoked test comparisons are made for both control and omission conditions. Induced to evoke difference tests are made between the difference values calculated. Degrees of freedom were the same for each of the t-tests on the same row. P-values displayed are FDR corrected

Supplemental Table 7

Visual Baselines

Clusters		Control *mean*	*sd*	Omission *mean*	*sd*	T-Tests *df*	*ts*	*pv*
0 - Parent	Induced	0.56	4.12	0.95	4.29	288	-4.52	0.000
	Evoked	-18.89	5.22	-18.76	5.13	288	-0.97	0.541
1 - L. Frontal	Induced	-0.21	3.82	1.02	3.71	19	-3.10	0.024
	Evoked	-21.19	3.90	-20.05	3.97	19	-2.83	0.042
2 - L. Motor	Induced	-0.03	3.93	0.35	3.69	34	-1.27	0.378
	Evoked	-20.96	3.93	-20.29	4.35	34	-1.33	0.378
3 - Midline Central	Induced	-1.01	4.85	-0.80	5.09	34	-1.56	0.313
	Evoked	-21.12	5.70	-20.88	6.27	34	-0.66	0.729
4 - R. Motor	Induced	0.67	3.57	0.79	3.86	33	-0.43	0.798
	Evoked	-20.09	4.23	-19.51	4.39	33	-1.74	0.243
5 - R. Frontal	Induced	-0.39	4.41	0.59	4.61	38	-3.11	0.022
	Evoked	-21.10	5.16	-20.38	4.78	38	-1.68	0.256
6 - L. Temporal/Parietal	Induced	1.99	3.67	1.92	4.31	27	0.25	0.833
	Evoked	-17.16	4.34	-17.09	4.40	27	-0.18	0.873
7 - Occipital	Induced	1.07	3.68	1.20	3.75	23	-0.54	0.767
	Evoked	-14.43	4.36	-15.77	5.27	23	3.62	0.012
8 - Parietal	Induced	0.99	4.51	1.44	4.76	41	-3.79	0.008
	Evoked	-17.26	5.36	-17.81	5.47	41	2.03	0.142
9 - R. Temporal/Parietal	Induced	2.24	3.26	2.39	3.72	28	-0.66	0.729
	Evoked	-15.59	4.39	-15.97	3.92	28	0.97	0.541

Tests for differences in baselines for the visual modality for both induced and evoked activity for each cluster. Baseline values are from the beta band and extracted from the time-frequency calculations used to calculate beta peak power. P-values displayed are FDR corrected.

Supplemental Table 8

Auditory Baselines

Clusters		Control *mean*	Control *sd*	Omission *mean*	Omission *sd*	T-Tests *df*	T-Tests *ts*	T-Tests *pv*
0 - Parent	Induced	0.65	4.36	0.98	4.17	288	-3.42	0.008
	Evoked	-20.29	4.46	-19.56	4.25	288	-4.67	0.000
1 - L. Frontal	Induced	-0.09	3.57	1.22	3.53	19	-2.63	0.058
	Evoked	-21.08	3.86	-19.01	4.25	19	-3.14	0.024
2 - L. Motor	Induced	-0.03	3.99	0.85	3.45	34	-2.13	0.128
	Evoked	-20.77	4.01	-19.69	3.42	34	-2.04	0.142
3 - Midline Central	Induced	-0.87	5.16	-0.76	5.18	34	-0.96	0.541
	Evoked	-21.61	5.11	-21.27	4.78	34	-0.94	0.541
4 - R. Motor	Induced	0.52	4.02	0.59	3.61	33	-0.28	0.833
	Evoked	-19.72	3.88	-20.00	4.00	33	0.68	0.729
5 - R. Frontal	Induced	-0.35	4.59	0.61	4.64	38	-3.04	0.022
	Evoked	-21.21	4.55	-19.74	4.78	38	-3.31	0.015
6 - L. Temporal/Parietal	Induced	1.90	4.00	1.81	3.89	27	0.41	0.798
	Evoked	-19.07	4.56	-18.92	4.18	27	-0.35	0.812
7 - Occipital	Induced	0.68	3.47	0.80	3.40	23	-0.40	0.798
	Evoked	-20.91	4.38	-20.17	3.95	23	-1.33	0.378
8 - Parietal	Induced	1.41	4.77	1.53	4.74	41	-1.30	0.378
	Evoked	-19.68	4.76	-19.00	4.57	41	-1.89	0.182
9 - R. Temporal/Parietal	Induced	2.74	3.92	2.36	3.65	28	1.38	0.378
	Evoked	-18.61	4.26	-18.12	3.56	28	-0.96	0.541

Tests for differences in baselines for the auditory modality for both induced and evoked activity for each cluster. Baseline values are from the beta band and extracted from the time-frequency calculations used to calculate beta peak power. P-values displayed are FDR corrected.